DESIGN OF A FRANGIBLE COMPOSITE COVER FOR MISSILE LAUNCH TUBE

A THESIS SUBMITTED TO
THE GRADUATE SCHOOL OF NATURAL AND APPLIED SCIENCES
OF
MIDDLE EAST TECHNICAL UNIVERSITY

BY

OZAN AKKAŞ

IN PARTIAL FULFILLMENT OF THE REQUIREMENTS
FOR
THE DEGREE OF MASTER OF SCIENCE
IN
MECHANICAL ENGINEERING

JUNE 2018

Approval of the thesis:

DESIGN OF A FRANGIBLE COMPOSITE COVER FOR MISSILE LAUNCH TUBE

submitted by **OZAN AKKAŞ** in partial fulfillment of the requirements for the degree of **Master of Science in Mechanical Engineering, Middle East Technical University** by,

Prof. Dr. Halil Kalıpçılar _____
Dean, Graduate School of **Natural and Applied Sciences**

Prof. Dr. M. A. Sahir Arıkan _____
Head of Department, **Mechanical Engineering**

Prof. Dr. R. Orhan Yıldırım _____
Supervisor, **Mechanical Engineering Dept., METU**

Examining Committee Members

Prof. Dr. Metin Akkök _____
Mechanical Engineering Dept., METU

Prof. Dr. R. Orhan Yıldırım _____
Mechanical Engineering Dept., METU

Dr. Inst. Orkun Özşahin _____
Mechanical Engineering Dept., METU

Dr. Inst. Ulaş Yaman _____
Mechanical Engineering Dept., METU

Dr. Inst. Ekin Özgirgin Yapıcı _____
Mechanical Engineering Dept., Çankaya University

Date: 22.06.2018

I hereby declare that all information in this document has been obtained and presented in accordance with academic rules and ethical conduct. I also declare that, as required by these rules and conduct, I have fully cited and referenced all material and results that are not original to this work.

Name, Last name : Ozan AKKAŞ

Signature :

ABSTRACT

DESIGN OF A FRANGIBLE COMPOSITE COVER FOR MISSILE LAUNCH TUBE

Akkaş, Ozan

M.S., Department of Mechanical Engineering

Supervisor: Prof. Dr. R. Orhan Yıldırım

June 2018, 156 Pages

In this thesis study, launch tube covers are investigated and a frangible cover is designed by using composite materials. Requirements which are derived from system level requirements are taken into consideration during the design phase.

Suitable composite manufacturing method and materials are selected after literature survey. Load levels are determined by using experimental and analytical approaches. Material constants and limits are obtained from literature and coupon tests. Design parameters of the cover are chosen and determined by using finite element analysis.

After conducting sizing of the cover by using finite element analysis, detailed design is completed. After that, a mold is produced in order to be used for resin transfer molding and cover prototypes are manufactured.

A burst test set-up is designed and covers are tested in order to obtain inner and outer burst pressures. Experimental results are compatible with analytical results. Then the cover is used in firing test and desired results are observed.

Keywords: Frangible Cover, Fly-Through Cover, Fragile Cover, Composite Pod Cover, Missile Launch Tube, Resin Transfer Molding,

ÖZ

KIRILABİLEN KOMPOZİT LANÇER KAPAĞI TASARIMI

Akkaş, Ozan

Yüksek Lisans, Makina Mühendisliği Bölümü

Tez Yöneticisi: Prof. Dr. R. Orhan Yıldırım

Haziran 2018, 156 Sayfa

Bu tez çalışması kapsamında fırlatma tüpü kapakları incelenmiş ve kompozit malzemeler kullanan bir kırılgan kapak tasarımı yapılmıştır. Tasarım sürecinde, sistem seviyesi gereksinimlerden türetilen gereksinimler gözetilmiştir.

Literatür taraması sonrası uygun kompozit üretim yöntemi ve malzemeler seçilmiştir. Yük seviyeleri deneysel ve analitik yaklaşımlar kullanılarak belirlenmiştir. Malzeme sabitleri ve limitlerinin tespit edilmesi için literatur bilgisi ve kupon testler kullanılmıştır. Kapak tasarımında kullanılacak parametreler seçilmiş ve sonlu elemanlar analizi yapılarak belirlenmiştir.

Sonlu elemanlar analizleri ile ölçülendirme sonrasında kapağın detay tasarımı tamamlanmıştır. Daha sonra, reçine transfer metodu üretim yöntemine uygun bir kalıp tasarlanmış ve kapak prototipleri üretilmiştir.

Bir test düzeneği tasarlanmış, iç ve dış patlama basınçlarının belirlenmesi için kapaklar test edilmiştir. Deneysel sonuçlarla analiz sonuçları tutarlıdır. Daha sonra, kapak atışlı testte kullanılmış ve beklenen sonuçlar gözlemlenmiştir.

Anahtar Kelimeler: Kırılgan Kapak, Kırılabilen Kapak, Senkronize Açılan Kapak, Kompozit Pod Kapağı, Fırlatma Tüpü Kapağı, Reçine Transfer Metodu

to my family…

ACKNOWLEDGEMENTS

I would like to express my sincere appreciation to my supervisor Prof. Raif Orhan Yıldırım for his invaluable supervision, guidance and support.

This thesis is a SAYP project which is conducted with Undersecretariat for Defence Industries of Turkey, METU and ROKETSAN Agreement. Support of Undersecretariat for Defence Industries, METU and ROKETSAN is highly appreciated.

I would like to offer my special thanks to my manager Mrs. Aslı Akgöz Bingöl for her ineffable support, guidance and vision. I am also grateful to my director Mr. Anıl Ünal for his encouragements.

TABLE OF CONTENTS

LIST OF TABLES

TABLES

LIST OF FIGURES

FIGURES

LIST OF SYMBOLS AND ABBREVIATIONS

SYMBOLS AND ABBREVIATIONS

a	Surface Fit Equation Parameter 1 (Confidential)
ASTM	American Society for Testing and Materials
ASY	Asymmetry
atm	Atmosphere (pressure)
b	Surface Fit Equation Parameter 2 (Confidential)
c	Surface Fit Equation Parameter 3 (Confidential)
CAAM	Common Anti-Air Modular Missile
CFD	Computational Fluid Dynamics
CMC	Ceramic Matrix Composite
CTE	Coefficient of Thermal Expansion
d	Multiplying Factor for Dimension Value (Confidential)
DH	Height of Dome
DT	Thickness of Dome
e	Natural log base (2.71828)
E	Elastic Modulus
EMC	Electro-magnetic compatibility
EMI	Electro-magnetic interference

etc	et cetera
F	Multiplying Factor for Force Value (Confidential)
FEA	Finite Element Analysis
FWD	Forward
GB	Giga Byte
GHz	Giga Hertz
GPa	Giga Pascal
HM	High Modulus
Hz	Hertz
IM	Intermediate Modulus
i.e.	that is
kHz	Kilo Hertz
L	Multiplying Factor for Dimension Value (Confidential)
LS	Length of Coupon
LC	Load Cell
LR	Length of Resin
m	Meter
m/s	Meter per Second
MK	Mark

MMC	Metal Matrix Composite
MMT	Modified Mohr Theory
MPa	Mega Pascal
ms	Millisecond
N	Newton
n	Factor of Safety
NH	Height of Notch
NL	Length of Notch
^{o}C	Centigrade Degree
P	Multiplying Factor for Pressure Value (Confidential)
P_1	Pressure (for 5L distance)
P_2	Pressure (for 18L distance)
$P_{Applied}$	Applied Pressure
P_{Burst}	Burst Pressure
PMC	Polymer Matrix Composite
RAM	Random Access Memory
RGM	Sub-marine launch guided missile
RTM	Resin Transfer Molding

S, Max. Principal	Maximum Principal Stress
S, Min. Principal	Minimum Principal Stress
SMC	Sheet Molding Compound
SSM	Surface-to-Surface Missile
S_{UC}	Compressive Strength
S_{UT}	Tensile Strength
t	Multiplying Factor for Time Value (Confidential)
tc	Thickness of Coupon
t0	Start Time
TECABS	Technologies for Carbon Fiber Reinforced Modular Automotive Body Structures
U, Magnitude	Total Deformation
UAV	Unmanned Air Vehicle
UHM	Ultra High Modulus
V	Multiplying Factor for Mach Number Value (Confidential)
VLS	Vertical Launching System
VOC	Volatile Organic Compound

W	Width of Coupon
ε_f	Failure Strain
σ_A	Principal Stress Component (Maximum)
σ_B	Principal Stress Component (Minimum)
υ	Poisson's Ratio

CHAPTER 1

INTRODUCTION

1.1 Introduction

After the invention of gunpowder, it had been started to be used for different purposes. In the early stages, fireworks are produced with this material and used for entertainment purposes.

Afterward, it has been started to be used for the development of bombs and rockets due to the necessity of defense or attack. "Rocket" is a general term that describes a system which delivers a payload to a specific target by means of rocket propulsion. From early stages of the invention, rocket science has been developed and during this period different rocket systems have been produced. These developments include different aspects, namely; range, accuracy, precision, payload capacity, reliability, guidance, smartness, maneuverability, life, cost, easiness of operation, transportation and storage. Nowadays, due to the logistics and tactical reasons, rockets are generally fired by means of launch tubes. At the most of the rocket systems, launch tubes are used for not only launching but also transportation and storage. When the lifecycle of a munition is considered, its life has a long duration of storage and one or more cycle of transportation, before launching.

The launch tube is used as a transportation container during transportation, and it is used as a storage container during storage. Due to the special requirements of subcomponents of the munition or to increase the life of the munition, a rocket has

to be isolated from the environment. For these purposes, inside volume of a launch tube is a closed chamber and generally, it is filled with inert gas. In order to provide and sustain the isolation, the tube must have covers at front and aft sides. Photographs of two sample covers are given in Figure 1.

Basically, these covers provide protection by means of isolating the inside volume of the tube from the environment. Typically, they are gas-tight and they seal the inert gas inside the tube. Also, they prevent moisture permeability into the tube. Most of the rocket systems have multiple launch tubes. In these systems, a high pressure is applied to the cover of the adjacent tube when a rocket is fired. The cover should resist this pressure. Additionally, pod covers shall provide electromagnetic shielding if EMI/EMC protection is required. Moreover, the cover shall be opened at the incident of the firing of the rocket and it should not interact with the rocket. Typical lifecycle of a typical pod cover is explained in Figure 2.

Figure 1: Test Launch of Arrow 3 Missile (Left) [1], RGM-84 Harpoon SSM was Launched from an Mk-16 (Right) [2]

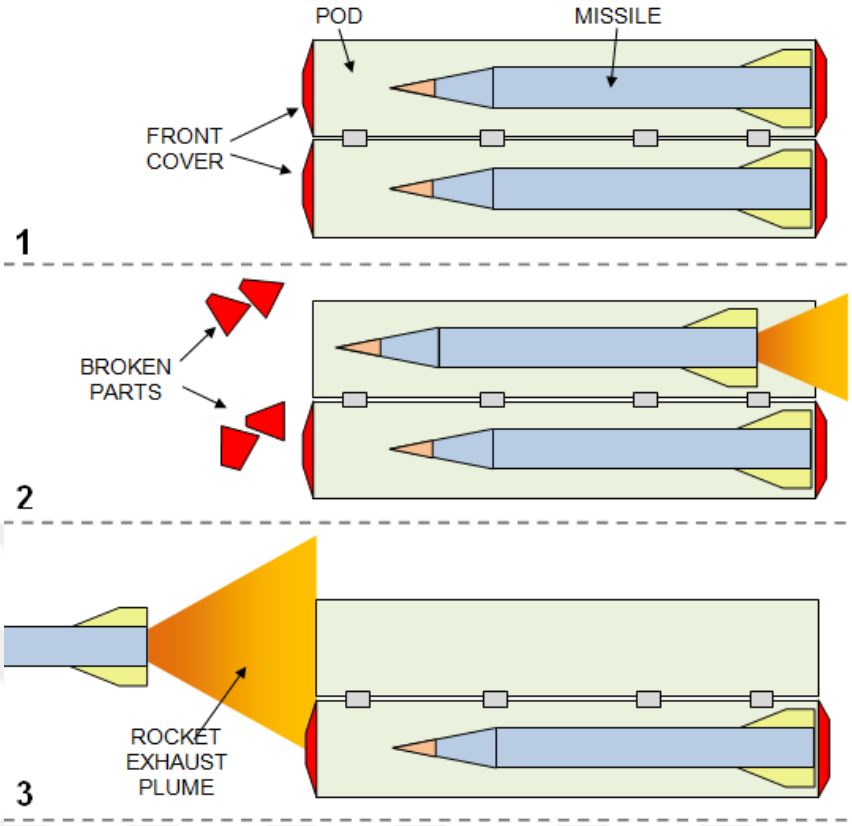

Figure 2: Lifecycle of a Typical Pod Cover

1.2 Aim of the Study

Pod covers are one of the main elements of missile launch systems. They can directly affect the success of the weapon. Especially in new weapon system concepts pod covers are preferred to be used due to their logistics and operational advantages. Therefore usage of a pod cover is becoming inevitable. This is one of the reasons that make this study significant.

Their role in the system is critical. For example, malfunction of the pod cover can make the missile scrap, obstruct the operation or even it can risk the safety of staff's life. Examples of the accidents exist in the literature.

Pod covers take a role in every phase of the lifecycle of the system. They take the role from the beginning of the production, through the transportation, storage, periodic maintenance and operation phases. Therefore; it can be said that they not only have important functions but also have duties in all phases of the system's lifecycle.

Design of pod cover requires knowledge of different disciplines, such as solid mechanics, fluid dynamics, material engineering, system engineering, etc. As a result, it can be said that design process is challenging. Contradictory requirements (resistive to outer load, weak to inner load) make the design more challenging, especially for frangible pod covers. Another reason can be difficulties in load measurement. Chaotic nature of a missile launch makes measurement difficult and cost of launching a missile is relatively high when compared with the cost of the whole cover design process.

Literature information about this subject is limited. The only information can be taken from patents or articles of Chinese institutions which give very shallow information. As far as the studies related to missile launch tube cover is considered there is no published work in Turkey. Lack of literature information about the subject in national as well as in international levels necessitates a detailed research to be carried out to find a reasonable solution to the problem.

In order to increase the level of technological readiness, this study is supported by Undersecretary of Defense Industry. The demand for domestic inventive studies is also one of the reasons that make this study important.

Main reasons that motivate this study are briefly explained. At the end of the study, it is expected to gain information and fill the gap in the area of the pod cover design.

The main objective of this study is to gain systematic information about the technology of frangible pod covers. It is aimed to investigate a proper design,

manufacturing, and verification of the cover. Another aim is to adopt a composite manufacturing methodology and composite materials in the design.

Moreover, it is aimed to gain information about the aspects of the pod cover design and related technologies. Therefore, following items shall be gained at the end of the study.

- Literature information about pod covers
- Information about the historical development of pod covers
- Research about similar systems
- Definition and analysis of pod cover requirements
- Approach to the design process of a pod cover
- Knowledge about the technology of composite materials and manufacturing methods
- Implementation of composite material technologies into the pod cover design
- Develop a methodology for the design process of frangible pod cover
- Testing and verification of the cover

CHAPTER 2

LITERATURE SURVEY

2.1 Missile Launch Tube Covers

In the literature, this type of covers are referred by different terms. Frangible cover, fragile cover, fly-through cover are some of the examples. The term "cover" is also referred by closure, cap, lid, hatch, opening, diaphragm in different sources.

In order to provide objectives of the cover, different design solutions found in the literature, are considered. They are examined in 6 groups according to their working principles and structural design.

Cover types that will be examined in the following sections are:

- Covers Activated by Mechanism
- Hard Covers
- Diaphragm Type Covers
- Foam Type Covers
- Covers Containing Pyrotechnic
- Other Type Covers

The covers that cannot be categorized as a group or that possess specifications of more than one category are reviewed in Other Types category.

Covers can also be investigated in terms of other specifications. These specifications mostly arise from the requirement of the weapon systems. For example, in most of the naval systems, the cover is not destructed and it is closed after firing. In those systems, the cover is closed in order to prevent the enemy to identify the amount of munition that the ship is equipped with. Thus, this feature necessitates such a specification. Interaction with the cover is another specification that can be categorized. The interaction can be absent or available for different systems. Other specifications that can be investigated for launch tube covers are listed below:

- Type of activation
    1. Automatic Activation
    2. Manuel Activation
- Effect that activates the cover
    3. Impact of the munition
    4. Pressure of the rocket engine
    5. Actuation of the mechanism
- Opening situation
    1. Shattering
    2. Rupturing
    3. Monolithic
- Usage of the cover
    1. Single-use
    2. Permanent-use
- Type of Structure
    1. Monolithic structure
    2. Segmentary
- Interaction with munition
    1. Available
    2. Absent

- Platform
    1. Land
    2. Air
    3. Naval
    4. Subsea
- Closing after firing
    1. Available
    2. Absent

2.1.1 Covers Activated by Mechanism

This type is the widest section of cover types. General view of this type of covers is given in Figure 3. First examples of launch tubes have been multi-use (they can be used for more than one launch). Moreover, most of them have metallic front doors and mechanisms in order to open them. They contain spring, piston, hinge mechanisms and they are opened manually before the launch.

At the beginning of the invention of this type of covers, mechanisms were very primitive and they were prone to failure. This is the main disadvantage of this type of covers. When the mechanism fails, the rocket can hit the cover and create dangerous situations. In the past, this type of catastrophic results was observed [3]. In order to prevent this type of problems, poke-yoke methods are used and precaution systems are added. By the help of this system, firing is not allowed when the cover is not opened. Although safety problems were solved, malfunction of the weapon system had still existed. Frequent malfunctions, maintenance effort and cost, low reliability had been triggered the invention of the other types of covers and different mechanism.

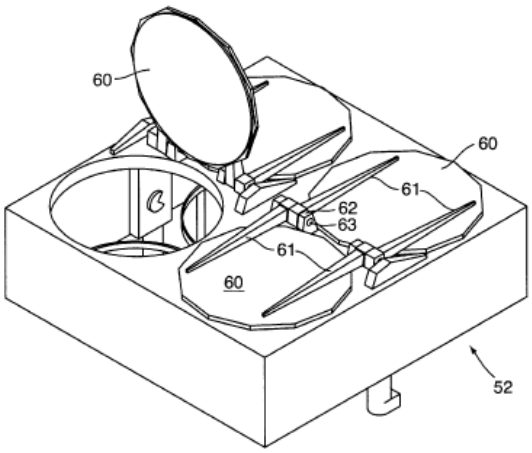

Figure 3: Example of a Cover That Uses Mechanism [4]

When the mechanism type and other type of covers are considered, it can be seen that reliability, autonomy, and performance are the main aspects that inventors are dealing with. For instance; in the combat, manual operation of the cover is not desired due to time consumption. In order to solve this problem, self-activated cover mechanisms are developed. These covers can be opened automatically before the rocket launch by using pressure pulse exiting from the nozzle of the rocket engine [5] (Figure 4.a), or by adding a trigger section to the sequence of the firing process that actuates mechanism to open [4, 6] (Figure 4.d), or mechanical contact between the cover and rocket [7] (Figure 4.b).

The mechanisms that are activated with the pressure level which is set to a specific value lower than the maximum gauge pressure obtained inside the tube during firing. This is the main working principle of the pressure activated cover mechanism (Figure 4.c) [8]. All of the pressure activated cover mechanisms are specifically calibrated to a necessary pressure value.

In order to eliminate the necessity of pressure setting, a different mechanism that can be activated with pressure pulse is developed [9]. In that system, the mechanism is sensitive to pressure increasing rate. When sudden pressure increase occurs, it opens the cover. If the pressure increase rate is slow the cover is insensitive.

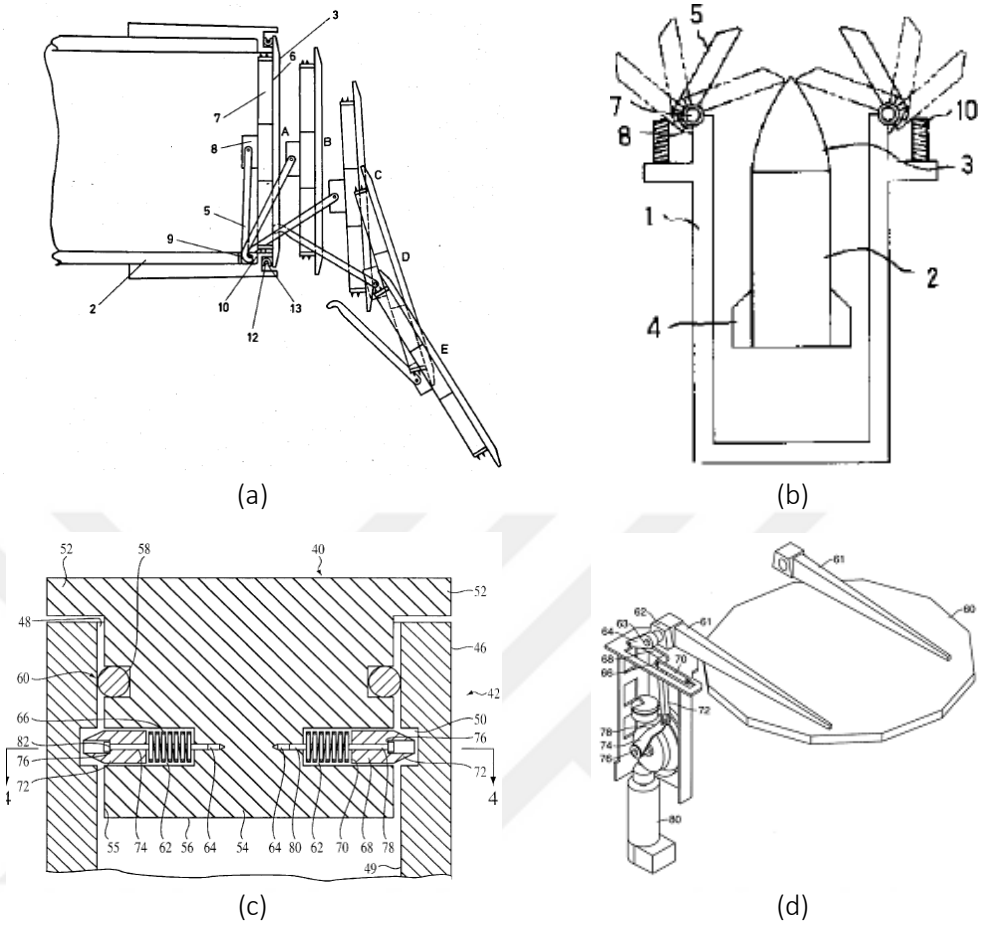

Figure 4: Schematics of Four Cover Examples that Have Different Mechanism [5, 7, 8, 4]

In some systems, it is necessary to close the cover after the launch of the munition. This requirement arises from tactical reasons. In such systems, the cover is suddenly opened, and it stays open during the launch of the missile, then it is closed. This feature can be gained by using mechanism type covers. In those systems, the pressure of rocket engine [10], spring tension [7], or two-way working actuators can be used (Figure 5) [11].

In some specific circumstances, usage of mechanism type covers is inevitable. On the other hand, their tendency to fail, complexity, relatively high cost, maintenance issues are important drawbacks.

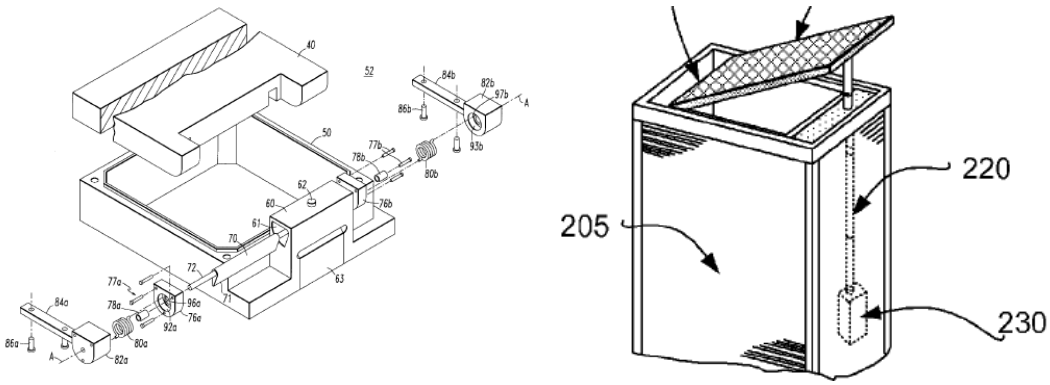

Figure 5: Two Cover Examples that Have Mechanism [10, 11]

These types of covers which are activated by mechanism are prone to fail, require maintaining, and their cost is relatively high. Incidentally, the resetting process of the primitive mechanisms between two launches is time-consuming and maintaining cost is, also, relatively high. Because of these negative aspects of the mechanisms, the idea of single-use hard cover appears to be a solution to the problems of mechanism type covers have.

Photographs of two sample covers are given in Figure 6.

Figure 6: Photographs of Hatch Cover Systems of Babur Missile [12] (Left) and Common Anti-air Modular Missile (CAMM) launching from Lockheed Martin's MK 41 Vertical Launching System (VLS) [13] (Right)

2.1.2 Hard Covers

Hard cover types are for single-use and after the launch, the new one is assembled to the system for the next launch if the launch tube is not of a single-use. They are capable of being broken with the contact of rocket's nose cone or inside pressure at the instant of firing.

Hard type covers have been used in a rocket cell closure system since 1971. The first hard cover comprises a polyurethane-based plastic plate, metal frame at the periphery in order to fix the cover at the launcher interface (Figure 7) [3]. In this cover design, rocket's nose cone or other aerodynamic surfaces, such as wings, can be damaged if they hit the cover. Remaining debris can be another reason that can damage the rocket or make the interaction between the rocket and system.

In order to reduce the effect of interaction between rocket and cover, dissimilar material combinations are used. This design approach provides a cover that avoids disadvantages of the fracture behavior. In this design philosophy; brittle and frangible materials (i.e. Tempered glass) are used to guarantee easy fragmentation of the cover assembly. In addition; resilient materials such as foam or rubber are used to reduce the impact on the frangible layer and prevent damage to the rocket body. In some systems, rippable vapor barrier films are used in order to eliminate the water permeability and aluminum foils to prevent EMI, as well [14].

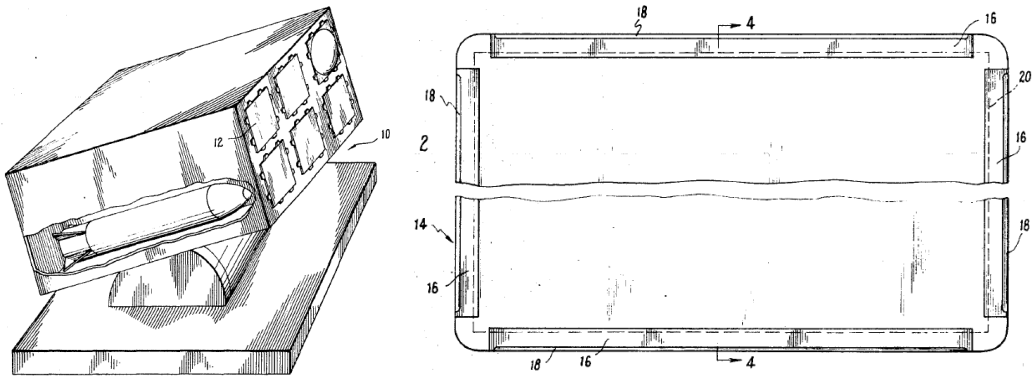

Figure 7: General (Left) and Front View (Right) of a Hard Cover Example [3]

In the literature, it is stated that hard cover that has a combination of different material layers, such as; tempered glass and impact resistant foam, satisfies more environmental requirements when compared with other types. Examples of these environmental effects are; exposure to water, icing, electromagnetic interference, variations in humidity, temperature extremes, hail impact, debris from the adjacent tube, etc. [15].

In some systems, the interaction between the rocket and the cover is not allowed. In these systems, the cover is capable of being broken and blown off of the launch tube without any contact with the rocket's nose cone. This capability is achieved by means of material mechanics. Thus, cover has different resistance and behavior to inner and outer effects [16].

Another hard cover that minimizes cover-rocket interaction has a subassembly that can easily break the rigid plate (Figure 8). In that design, rocket's nose cone contacts the subassembly that is consisting of a sharp edge which applies point load to the plate of cover assembly [17].

Photographs of two sample covers are given in Figure 9.

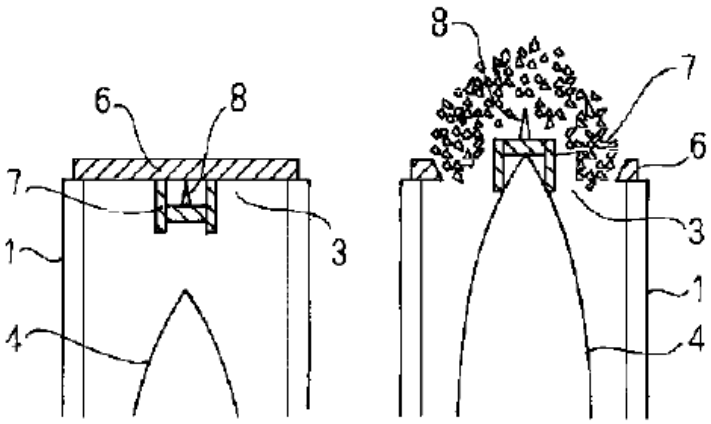

Figure 8: Working Principle of a Hard Cover which is broken by Missile's Nose [17]

Figure 9: Launch of Sea Skua [18] (Left) and Marte mk2 Missile [19] (Right)

2.1.3 Diaphragm Type Covers

Another cover type is diaphragm type. In this type of covers, basically, a flexible diaphragm (or membrane) is stretched and fixed to the opening of the launch tube by means of a rigid frame. The motivation of this cover type is to reduce the rocket-cover interaction and damage effects as seen in the prior hard type covers. Also, it is designed to apply a minimum resistance force to the munition during exit [20].

The diaphragm can resist the uniform pressure load, but it fails easily when a concentrated load is applied to a small area.

In order to obtain effective diaphragm covers, layers of the diaphragms are arranged and scored, as seen in Figure 10.a. Thus, rupture can be initiated at the center of the diaphragm and followed to the tear line which is determined by scored path. [20]

Further studies reveal that similar rupture behavior can be obtained by arranging the layup angles of the fabric laminates. This approach eases the manufacturing, reduces the cost and increases repeatability and reliability of the cover with eliminating the manual scoring process. This cover can be seen in Figure 10.b [21].

In another design, this philosophy is applied to a square shaped cover. In that design, a flexible material is used. Slices which are seen in Figure 10.c are fixed by using a fragile material at the center. When nose cone of the rocket hit the center part of the assembly, connections of the flexible slices are broken. Then flexible slices allow the rocket to exit and the apertures between the slices allow rocket fins to exit without any interaction [22]. Photographs of two sample covers are given in Figure 11.

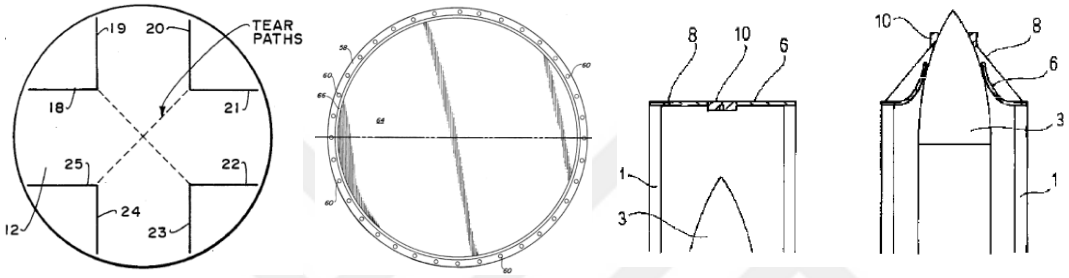

(a) (b) (c)

Figure 10: Front Views of Different Diaphragm Covers (a) with Tear Paths [20] and (b) without Tear Paths [21], and (c) Section View of a Cover Ruptured by Missile Nose [22]

Figure 11: Photographs of Harpoon [2] (Left) and Patriot Missile [23] (Right)

2.1.4 Foam Type Covers

Foam type is another cover type. Typically, this type of covers comprises lightweight foam material and they generally have dome-shaped geometry in order to distribute the outer loads.

In a foam cover design which is explained in a US patent, the cover assembly consists dome-shaped foam segments and a part at the aperture of the segments as seen in Figure 12. In the patent, it is claimed that, this approach has numerous advantages. For example, this design does not affect the rocket exit. Moreover, foam segments do not interfere with rockets aerodynamic control surfaces. Also, the segments are small and lightweight and they do not create surface damage. In this cover design, in order to obtain a barrier to water or other effects, the cover is coated with a special coating. Furthermore, resistance to environmental effects of foam material is improved [24].

On the contrary, weakness of this cover types in terms of protection levels is stated in some sources. It is stated that they cannot provide sufficient environmental protection and they can be broken even during the assembly [14]. However, the foam material is also used as supplementary material in other cover types. For example, impact resistant foam is used in hard covers that comprise tempered glasses [15]. Photograph of a foam type cover example can be seen in Figure 13.

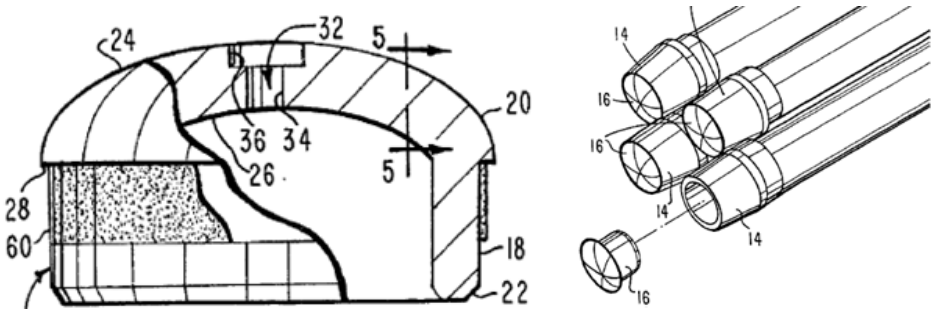

Figure 12: Section View (Left) and Assembly View (Right) of a Foam Type Cover [24]

Figure 13: Photographs of Seasparrow Missile [25]

2.1.5 Covers Containing Pyrotechnics

Pyrotechnics, in other words, explosives, have been used in different applications that require quick response, such as automotive airbags or emergency window opening mechanism of fighter aircraft [26]. Pyrotechnics have been used in launch tube cover systems for more than fifty years [27].

In a cover design example, which dates back to 1959, pyro bolt (explosive bolt) is used to activate the opening mechanism of the cover. In that system, once the pyro bolts are fired, the cap part is released. Then, the spring which is seen in Figure 14, operates to pull the cap to open position [27].

In another cover design, the explosive cord is used. In that design, a cord that has a shaped charge is mounted on dome-shaped geometry. The cord is arranged on a predetermined pattern, as seen in Figure 15.a. When the explosive is detonated, cap part of the cover is divided into two parts and allows the rocket to exit as seen in Figure 15.b [28].

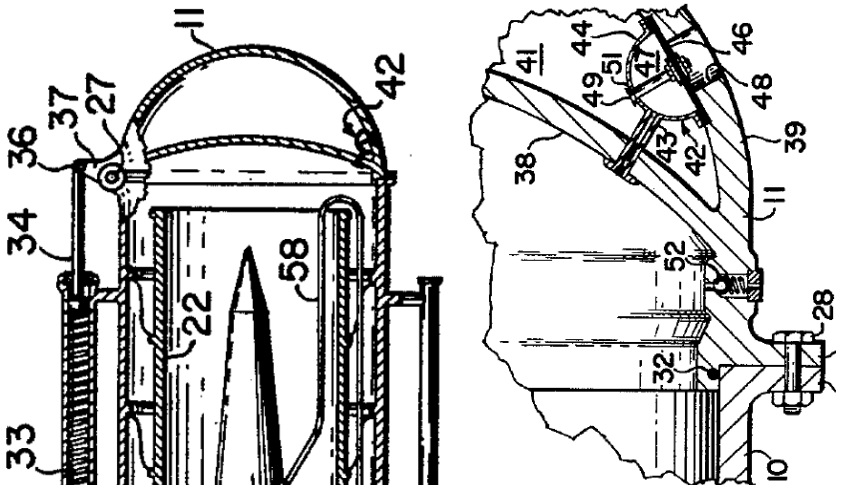

(a) (b)

Figure 14: Side View (Left) and Detailed View (Right) of a Pyrotechnic Type Cover Example [27]

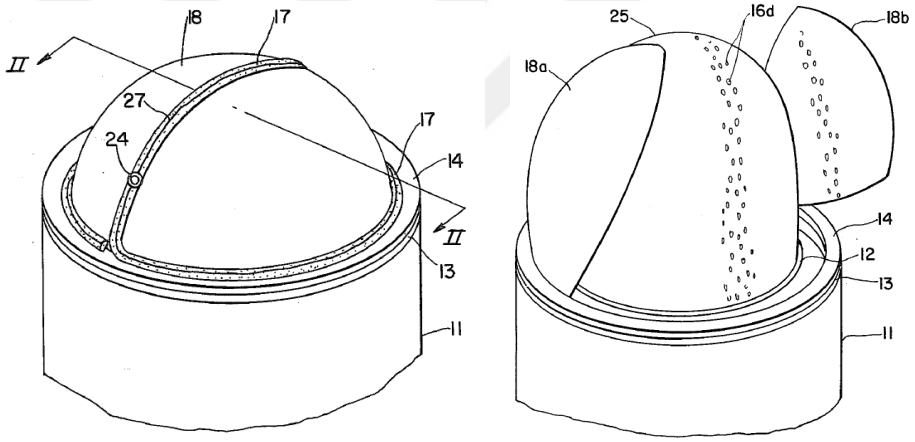

(a) (b)

Figure 15: Schematic View of Cover Before (Left) and After (Right) the Activation [28]

Pyrotechnic systems are chosen especially in submerged launch systems. Because they require large diameter and high strength covers that shall resist the pressure of the seawater. Frangible hard covers, foam type covers and other diaphragm type covers cannot provide this requirement.

Explosive charges can also be used to open the cover in a different way. In a launch system application, explosives are placed into the launch tube. In that system, the explosive is fired in the appropriate sequence before the rocket launch. When the diaphragm of the explosive charge is ruptured with the explosion, a shock wave is generated. Then, the shockwave inside the chamber of the launch tube removes the end caps as seen in Figure 16 [29].

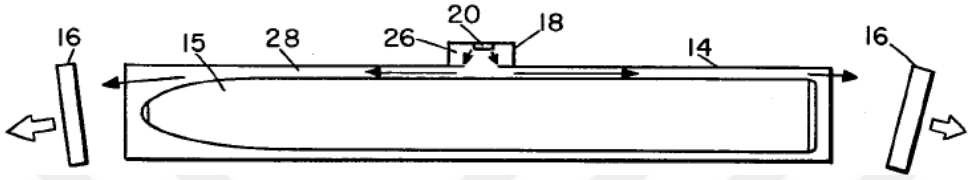

Figure 16: Schematic View of a Pyrotechnic Which is Used to Generate Pressure [29]

2.1.6 Other Type Covers

In this part, cover designs that cannot be categorized in previous sections are explained. One of the examples is a combination of two sub-component of the launch system in one structure. In that design which is seen in Figure 17.a, the cover works as a launch seal and a sabot. Typically, the sabot is an apparatus that holds the munition in the launch tube. The combination of sabot and launch seal is especially used in submerged launch systems. It reduces preparation time between two launches and increases the structural integrity of the sabot, cover assembly. Moreover, its manufacturing costs are lower than the other solutions. It is produced in a closed mold by using a flexible urethane based material [30].

Another example has also an innovative approach to the opening mechanism of the cover assembly. It has a hinged cover mechanism and between the hatch and opening of the cover, there is a membrane in order to fix the hatch and provide sealing. The membrane has an electrical heating wire on the periphery. Before the

firing, the wire is heated then the membrane ruptures and the hatch of the system is opened. The schematic of this cover is seen in Figure 17.b [31].

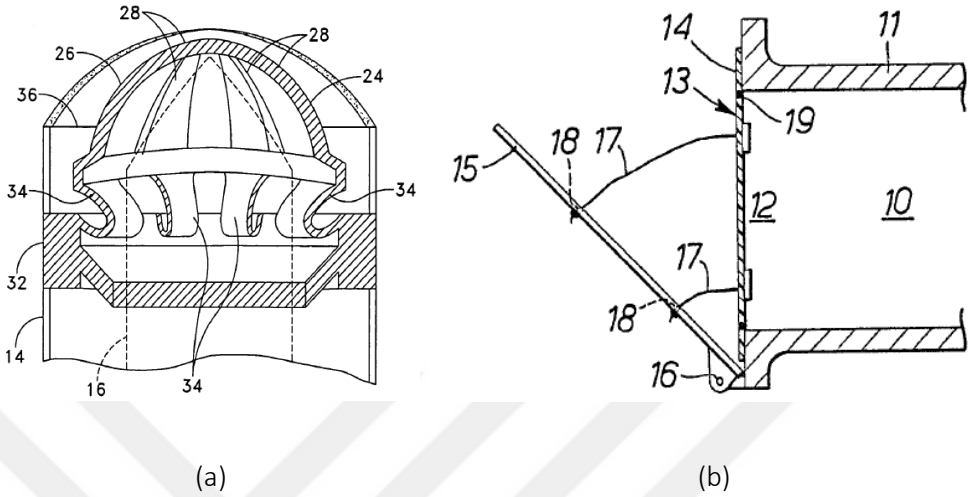

(a) (b)

Figure 17: Example Schematic Views of Other Type Covers [30, 31]

Topological interlocking is another way of obtaining a frangible launch tube cover. These covers possess similar features of other types but their main principal is interlocked subparts [32]. A typical schematic of this type of cover is seen in Figure 18.a. By using interlocking approach a structure with different inside and outside strength can be obtained. This design philosophy is analyzed and tested in the literature. Its geometry is optimized by using its boundary conditions [33]. In Figure 18.b free body diagram of typically interlocked dome-shaped geometry is seen. By using this approach, square-shaped geometries can also be produced as seen in Figure 18.c. In those systems, directional fracture is guaranteed as in the dome-shaped covers, but the different mechanical behavior between inside and outside face is not obtained. But it behaves in a different way when the same amount of point load or uniform load is applied [34].

Another example of the topologically interlocked cover mechanism is used in submerged launch systems. In this cover design, which is seen on Figure 18.d, interlocked subparts are covered and bonded with the thin outer layer. The outer

layer is rippable and it provides sealing to the system. It also applies a radial force to the interlocked subparts. By the help of this force, preload is obtained and subparts are held together [35].

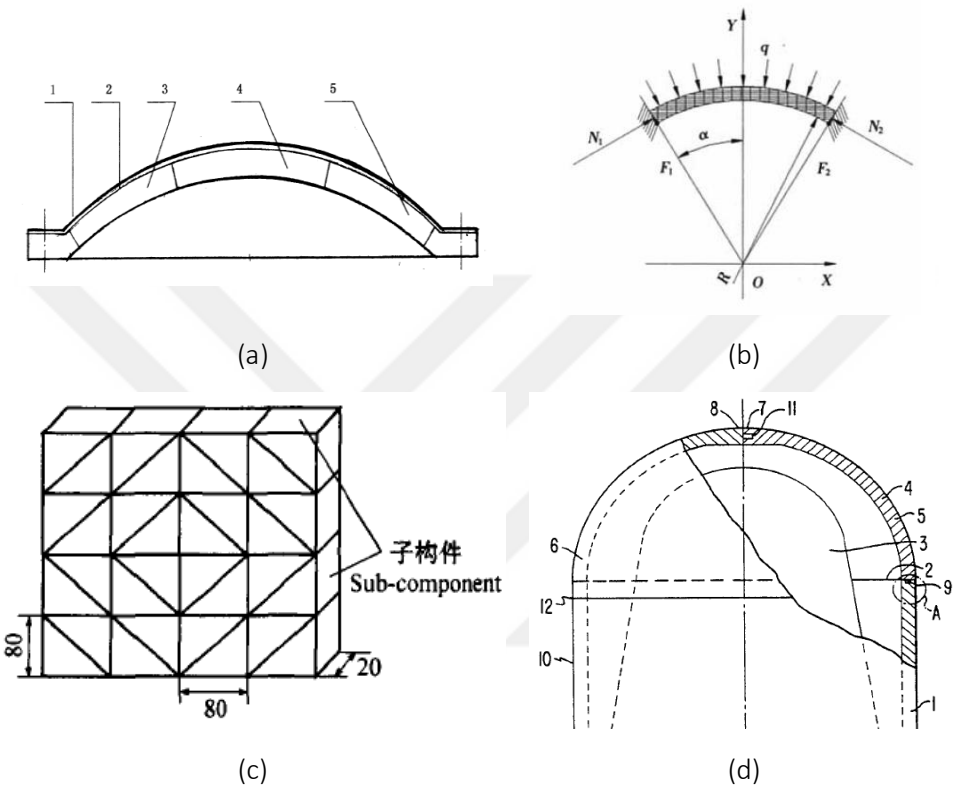

Figure 18: Schematic Views of Topologically Interlocked Cover Examples [32, 33, 34, 35]

2.2 Potential Use of Composite Material Technology

In this section, a brief description of the composite material and advantages of the composite materials will be presented. Moreover, composite material and manufacturing methods will be explained.

The very brief definition of composite materials is to use a combination of two or more dissimilar materials in order to combine their best properties. In practice, most composites consist of a bulk material (the "matrix"), and a reinforcement, added primarily to increase the strength and stiffness of the matrix. This reinforcement is usually in fiber form.

Today, the most common composites can be divided into three main groups, namely; Polymer Matrix Composites (PMC), Metal Matrix Composites (MMC) and Ceramic Matrix Composites (CMC). Polymer Matrix Composites are the most common type. They are also known as Fiber Reinforced Plastic (Polymer) and will be discussed in the following sections. Metal Matrix Composites are not widely used. In those composites, the matrix material is metal. Ceramic Matrix Composites are another type of composites. They are used in high-temperature application. Its matrix material is ceramic and it is generally reinforced with short fiber [36].

Using composites it is possible to build strong and lighter components. Increasing demand is originated from their apparent advantages. Aerospace, automotive, defense, renewable energy, oil, consumer products, pressure vessels, sporting goods are the examples of sectors that take advantage of composite material technologies.

Increasing demand for composite materials also increases the research activities. The research activities require different disciplines due to multidisciplinary nature of the composite material technologies. Research areas include material science, design, analyses, chemistry, manufacturing, automation, non-destructive inspection and destructive tests, raw materials, reliability, integration, mass production, recycling, robotics, textile and etc. Interdisciplinary structure of the composite material technologies makes the design process more challenging. Plurality of the options increases the difficulty of the selection. Therefore, it requires more knowledge when compared with metals. Thus, designers have to be

more qualified and they have to be aware of different disciplines in order to make a design that can use the advantages of the composite materials.

At a glance, it is difficult to find a relation between textile and aerospace industries. In aerospace structures, carbon materials are inevitable in most structures and they can be in fabric form. In order to produce the part, the fabric has to cover the surface without any wrinkles. But when the shape of the structure is complex, it is difficult to obtain a smooth overlap. This problem is solved with the weave type of the fabric. A fabric with a weave that has higher drapability is the solution as seen in Figure 19. This is the point that connects textile and aerospace industry. Moreover, due to the draping, the mechanical behavior differs and the designers have to consider these points in the design.

One of the subjects that are studied in the scope of the composites is Elastic Tailoring. From the nature of the composites, a composite lamina behaves anisotropic. Anisotropy means that the material's mechanical characteristic is different in different directions. This is one of the important features that composites possess. Besides, layered structure of a composite laminate makes possible to arrange orientation of each layer. When the layers are stacked up in necessary orientation angles and necessary positions the overall mechanical characteristic of the composite laminate can be obtained in a desired manner. This arrangement could make torsion/bending/axial load coupling and change the deformed shape under the applied load as seen in Figure 20. This approach is used in most of the advanced applications. For example, it is used to arrange the angle of attack of the helicopter blades [38].

At the previous paragraphs, the potential of the composites is briefly explained. In the scope of the thesis, composite material technologies will be implemented in a launch tube cover. In this respect, the objective of this work is to obtain an efficient design and proof of the concept of composite launch tube covers.

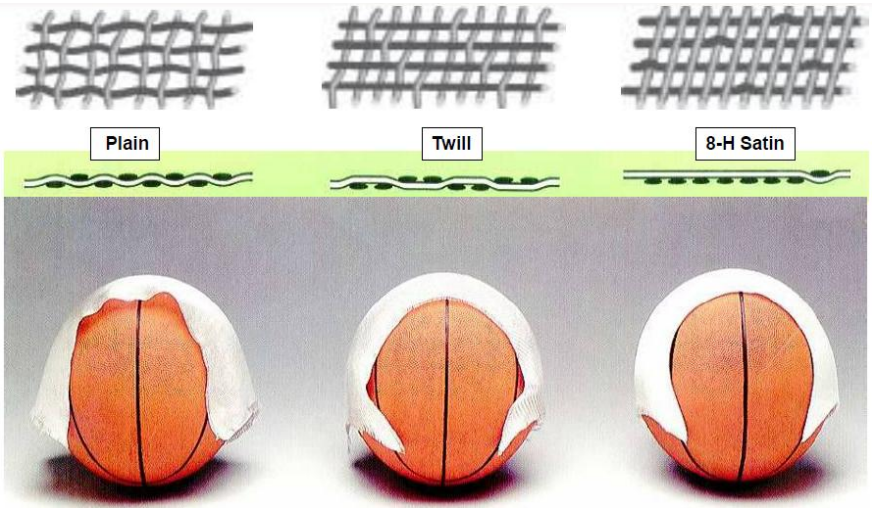

Figure 19: Effect of the Fabric Type on Drapability [37]

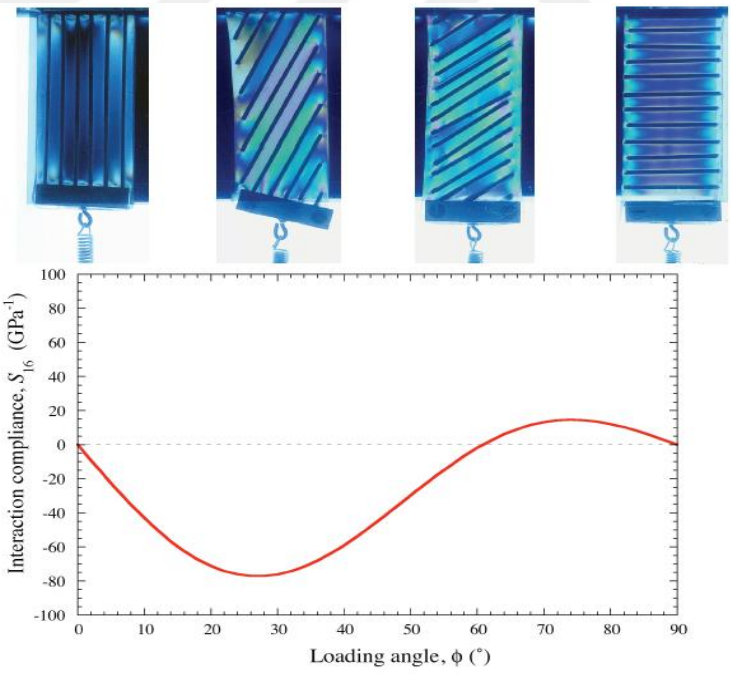

Figure 20: Variation of the Deformation for Different Lay-up Configuration under the Same Load [39]

2.2.1 Advantages of Composite Materials

As stated previously, it is clear that composites provide flexibility in design. They serve a wide range of materials, material forms, layup combinations. Also, complex shapes can be produced very efficiently. Composite materials can be shaped in a mold easily. It is easy to obtain a smooth surface, such as aerodynamic surfaces.

Flexibility in design also comes with flexibility in production. Composites can improve the productivity. An assembly that has different metal parts can be replaced with a single composite part. Thus, it can reduce the assembly cost and time, part count, production times of subcomponents. In Figure 21 a comparison of metal and composite productions of a floor pan assembly of an automobile is seen. Here the assembly of 28 metal parts is replaced with a single composite part that has 8 preforms and 5 cores. Since the whole assembly is produced in a single tool, better dimensional tolerances are obtained without any precise machining. Effort and waste in producing composite parts are generally lower than metals because in composites the part is shaped. On the other hand, in metals, the parts are machined and combined together. In these processes, energy consumption and material waste are relatively high.

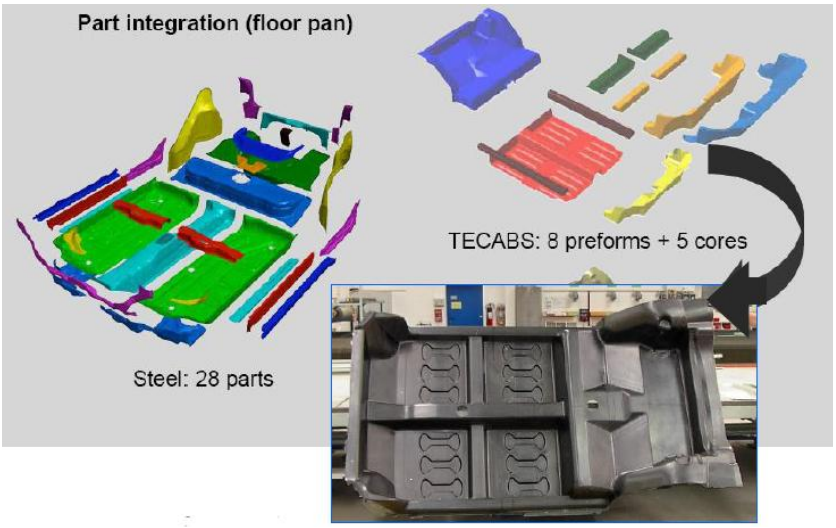

Figure 21: Composite vs Metal Floor Pan Production [37]

Besides, increasing efficiency in productivity and design, composites have other advantages. They are stronger than metals (for carbon, Aramid reinforcements). Strength and stiffness properties of composites and other materials are shown in Figure 22. Their specific strength is also usually higher than metals. This is the point that makes composites inevitable in weight critical structures. Significant weight savings are obtained. Moreover, their impact strength is also higher than metals. In ballistic armors and bulletproof vests, Aramid fibers are used due to their superior impact resistance.

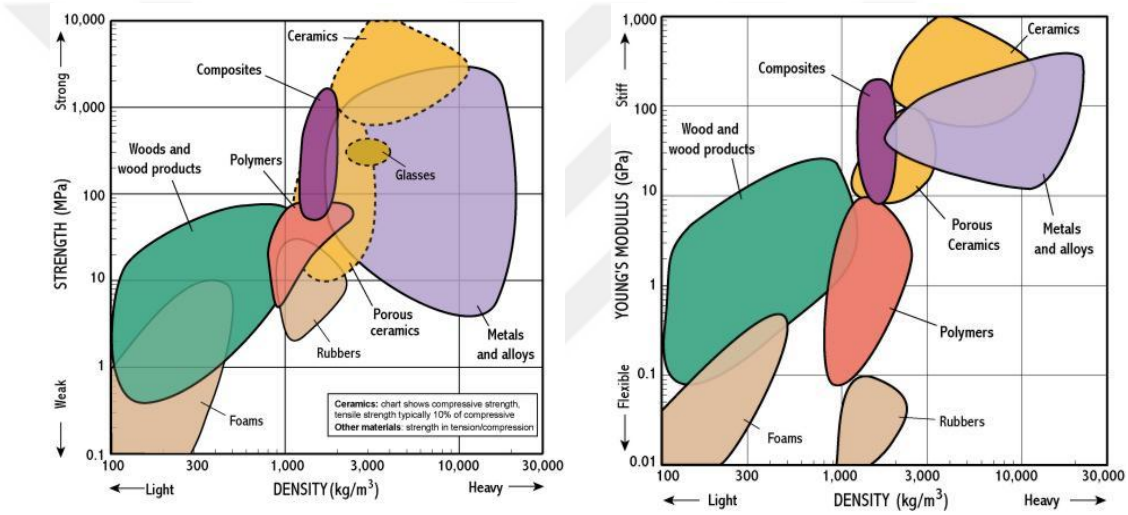

Figure 22: Strength (Left) and Stiffness (Right) per Density of General Materials [40]

Corrosion and chemical resistance of composites are also relatively high. They have a long service life and do not require maintenance as metal. Especially in marine applications, their usage is almost inevitable. They are dimensionally stable; they retain their shape in tough conditions.

Their coefficient of thermal expansion and thermal conductivity is relatively low. They can be used where thermal insulation is needed. Also, they can be tailored to obtain different thermal expansion characteristic. Therefore desired thermal behavior is achieved. For example, in some satellite antenna systems, thermally

stable structures (Figure 23) are needed, in order to prevent disturbance due to temperature changes. They have near-zero coefficient of thermal expansion carbon fiber reinforced truss structures [41]. Excellent heat sink properties can be achieved in carbon-carbon composites (both matrix and reinforcement are carbon) with lower mass. Those applications can be seen in aircraft brake systems.

From the nature of the polymer materials, nonconductive or nonmagnetic parts can be produced (Excluding carbon fiber which is electrically conductive to some extent). Composites are used very efficiently in the structures where electrical insulation is needed.

Also, they are used in magnetic resonance imaging equipment due to their nonmagneticity. This nonmagneticity makes composite material transparent to the radar signals. Therefore they are ideal for use in radar equipment or structures invisible to radar. Being invisible to radar is an important feature for tactical purposes in the defense industry. X-47B stealth drone is one of the example aircraft which is invisible to the radar [42].

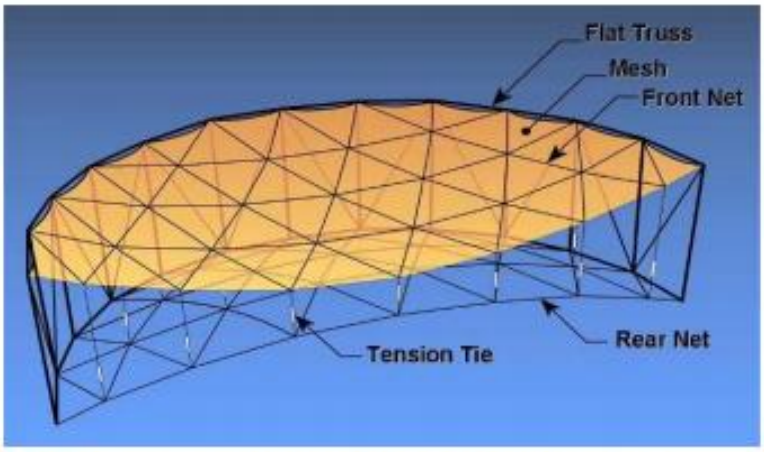

Figure 23: Schematic of Zero Coefficient of Thermal Expansion (CTE) Truss Structure [41]

Advantages of the composites and examples of their usage can be extended further. Main advantages of the composites are listed below:

- High strength and stiffness
- High specific strength and specific stiffness
- High impact resistance
- High fatigue resistance
- A wide range of coefficient of thermal expansion
- Tailoring capability to obtain the optimum structure
- Easy to produce
- Low cycle time to produce
- Low-cost manufacturing and raw materials
- Low investment cost required to produce
- High resistance to corrosion and chemicals
- Long service life
- Easy to obtain close tolerances
- Electrical, thermal insulation
- Transparent to magnetic signals
- Easy to obtain smooth surfaces
- Low part count assembly productions

Basic advantages of composites are presented in this section. In the scope of the thesis, the design of a composite launch tube cover will be conducted and those advantages will be considered in the scope of the thesis.

2.2.2 Alternative Materials

In this section alternatives to composite materials will be presented. When a general structure of a composite part is examined from micro level to macro level, it can be seen that it starts with at least two different material phases: matrix and reinforcement as seen in Figure 24. At the start, the matrix is in liquid form and

the reinforcement which is solid and generally in fiber form. Then, the fiber matrix impregnation is obtained and the mixture is consolidated by the help of heat (in some methods pressure is also applied in order to improve the consolidation).

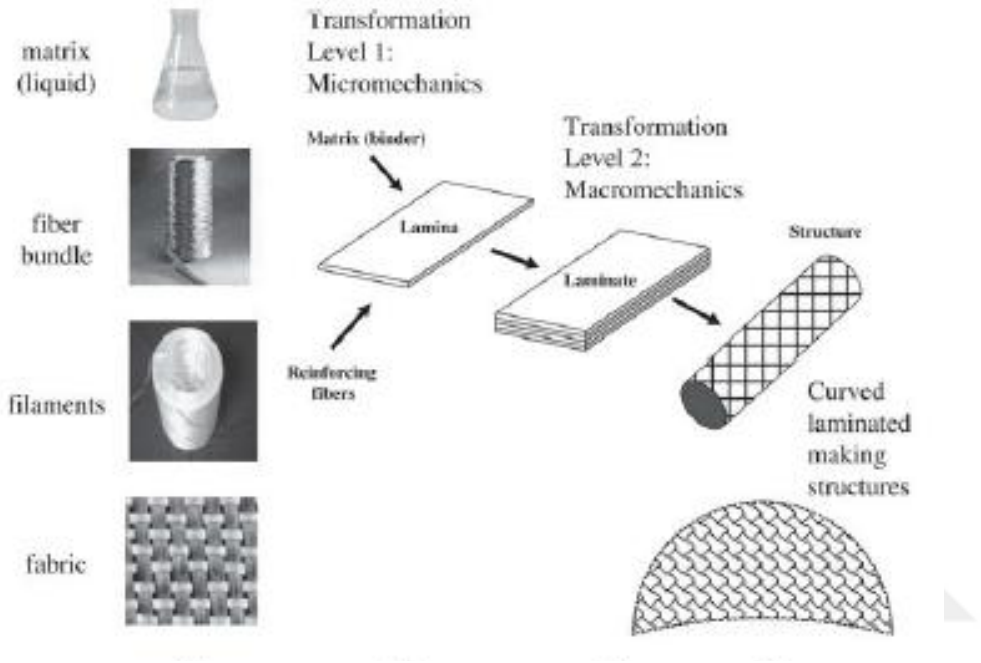

Figure 24: Stages of Constituents in the Manufacturing of Composites [43]

2.2.2.1 Matrix Materials

The matrix of a composite is mainly responsible for holding and supporting the reinforcement part. They provide dimensional stability to the composite and their strength is lower than reinforcement material. For a better understanding of matrix, their purposes will be discussed.

First of all, matrix aligns fibers to obtain the regular distribution of loads and displacements in the fibers. Another purpose of the matrix is to transfer the loads. Bonding between matrix and fibers must be good enough to transfer loads between fibers. Otherwise, the composite will fail. Moreover, matrix assists fiber

in compression. Due to the fibrous nature of the reinforcement, they cannot have good compressive properties. Matrix provides compression strength and stiffness. On the other hand, fibers usually have higher surface energy and they are prone to absorb moisture and other environmental effects. These effects not only damage fibers but also prevent the fiber matrix bonding [43]. In the scope of the thesis, only Polymer Matrix Composites (PMC) will be considered. It is possible to divide polymer matrices into two main groups; thermoset and thermoplastic. Thermoset resins perform nonreversible chemical reaction during curing. At this phase, cross-links are formed between long molecular chains (Figure 25) and they provide strength and stiffness to the matrix. When they are heated above the glass transition temperature, their strength and stiffness are decreased. On the other hand, in thermoplastic resins the process is reversible and when the material is heated up to a certain melting temperature it softens and it can be reshaped into a new geometry. This is the main difference between thermoset and thermoplastic resins, other main specifications are compared at Table 1.

In the scope of the thesis study, thermoset resins will be discussed. Since their dimensional stability, which is obtained by cross-links, is higher when compared with thermoplastic resins. Thermoplastic resins lose their shape when they are exposed to heat. Most common thermoset resins are epoxy, polyester, and vinylester.

Table 1: Comparison of Thermoset and Thermoplastic Resins [44]

Thermosets	**Thermoplastics**
Resin cost is low	Resin cost is slightly higher.
Thermosets exhibit moderate shrinkage	Shrinkage of thermoplastics is low
Interlaminar fracture toughness is low	Interlaminar fracture toughness is high
Thermosets exhibit good resistance to fluids and solvents.	Thermosets exhibit poor resistance to fluids and solvents
Mechanical properties are good	Mechanical properties are good
Dimensionally stable	Dimensionally unstable

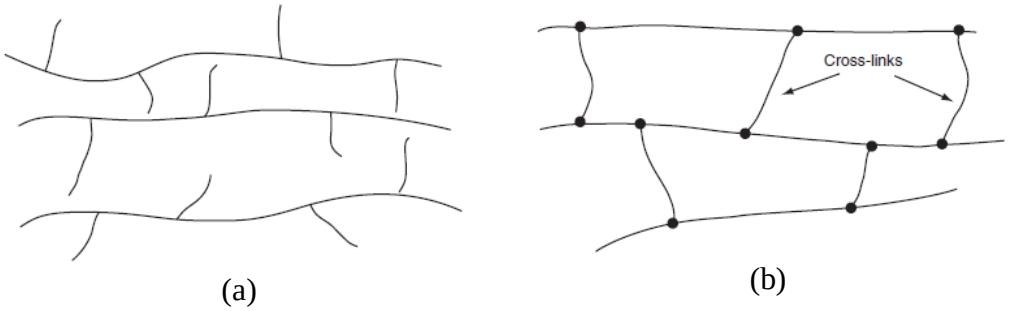

Figure 25: Schematic Representation Molecular Chain of (a) Thermoplastic Polymer and (b) Thermoset Polymer [45]

Polyester resins have been used for the longest period and their usage includes the widest range of structures. They are widely used due to their relatively low cost [46]. Polyester cures easily with the addition of a catalyst resulting in an exothermic reaction. This provides them ability to cure at room temperature. Therefore, they do not need curing oven or extra energy. Also, part size is not limited by oven [44].

Polyesters have relatively low mechanical performance, their tensile strength is between 34.5 - 103.5 MPa, tensile modulus of elasticity is between 2.1 - 3.45 GPa. Their heat deflection temperature ranges between 60 - 205ºC and they shrink 5-12% during curing [45]. Relatively high shrink rate and low mechanical performance make their usage inconvenient.

Epoxy Resins are the most widely used matrices for advanced composites. They are widely used in aerospace and defense industry applications. The main reason is their relatively high mechanical properties, as well as higher environmental resistance. They have advantages among other type matrices such as polyesters. They possess wide variety of properties due to their curing agent, modifier and starting material options. Main advantages of epoxies are [44, 45]:

- Absence of volatile and by-product forming during cure

- Low shrinkage during cure
- High resistance to chemicals and solvents
- High adhesion to a wide variety of fillers, fibers, and other substrates
- Good adhesion to reinforcement
- Good electrical properties
- Resistance to creep and fatigue
- Adjustable curing rate
- Wide range of curative options (high temperature or room temperature cure can be applied)

The principal disadvantages are its relatively high cost and long cure time. They have few inherent disadvantages. They are listed below [44, 45]:

- Physical properties and dimensions are changed by moisture absorption
- Heat deflection temperature limits the usage at temperatures up to 200°C
- Slow curing
- Resins and curatives are somewhat toxic before the curing operation
- Difficult to combine toughness and high temperature resistance due to the chemical structure of the resin
- Sensitive to ultraviolet light degradation

Tensile strength of epoxies ranges between 55 - 130 MPa, tensile modulus ranges between 2.75 - 4.10 GPa and they shrink 1-5% during cure [45].

Vinylesters are the most recent addition to the family of thermoset resins. They possess good characteristics of epoxy resins, such as superior chemical resistance and good mechanical performance, and of polyester resins, such as low viscosity and fast curing [44].

However, the volumetric shrinkage of vinylester resins is in the range of 5.4 - 10.3%, which is higher than that of the epoxy resin [45]. They also exhibit only moderate adhesive strengths compared with epoxy resins. It can be said that

vinylester ranges between polyesters and epoxies in terms of their cost and performance. The tensile strength of vinylester ranges between 73 - 81 MPa and tensile modulus ranges between 3 - 3.5 GPa. Heat deflection temperature ranges between 93-135℃.

Polyimides, **Cyanate ester**, **Phenolics** are the resins which are not as common as others. They are used in applications that have special requirements such as temperature resistance. Polyimides have extremely high working temperatures (up to 370 ℃). They have also high mechanical strength and fire resistance [44]. Cyanate ester is another resin that has high resistance to temperature. Its glass transition temperature ranges up to 265 ℃. Its moisture absorption is lower than epoxies and it has good chemical resistance dimensional stability [45]. Phenolics are other temperature resistant resins that have heat deflection temperature up to 260℃. They are cheaper than other high-temperature resistant resins and widely used in transportation industry [44].

2.2.2.2 Reinforcement Materials and Material Forms

In composites, different reinforcement types are used. They can be in the form of fiber, particle, whisker, flake or particulate, some of them are seen in Figure 26.

Fibers are essentially characterized that they are long in the longitudinal axis and they have circular or near-circular cross section [44]. Particles do not have any orientation in shape. Whiskers are shaped like small short fibers with the smaller cross-section. Different than other types, fiber form reinforcement could make composite part's mechanical behavior be tailorable by using the orientation of the reinforcement.

In the literature, this mechanical property is called as anisotropy and this property can be used as a tool to optimize the mechanical behavior of the composite part as desired.

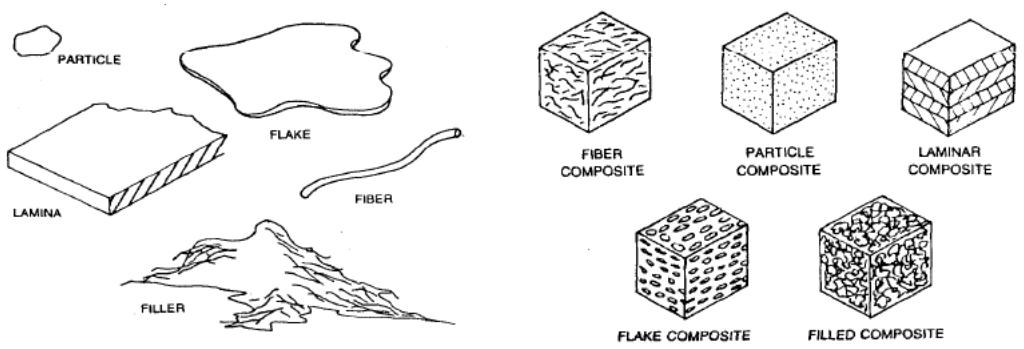

Figure 26: Different Reinforcement Forms [47]

In the scope of the thesis, fiber reinforced composites will be discussed. First of all, fiber material alternatives will be presented. Then, fiber forms and their architecture types will be mentioned.

The most commonly used fibers in composites industry are Glass Fiber, Aramid Fiber, and Carbon Fiber.

Glass Fibers are the most commonly used fibers in fiber reinforced composites due to their low cost, and relatively high strength and stiffness compared with the reinforced matrix material. In addition, they have high chemical resistance and excellent insulating properties.

Their disadvantages are high density and low tensile modulus among other fibers, low fatigue properties, high hardness, and abrasion sensitivity.

It has 3 types: E-Glass, S-Glass, C-Glass. E-Glass is the cheapest and the most widely used fiber type. S-Glass is developed to have higher mechanical properties. It has higher strength and stiffness among other glasses. It has a different chemical composition and higher manufacturing costs than the E-Glass. For this reason, it is relatively expensive. C-Glass is developed to be used in environments that require higher resistance to chemicals [45].

Aramid fibers have highly crystalline aromatic polyamide fibers that have long polymeric chains and aromatic rings. They are basically used in the applications that require high strength-to-weight ratio and high impact resistance. Their highly oriented molecular structure makes them impact resistant. In helmets and bullet-proof body armors, they are excessively used. They are very sensitive to moisture absorption, it is very important to protect them against the humidity. Moisture tends to crack the micro voids and produce splitting. Kevlar, Twaron, Technora are the commercial names used for Aramid [44, 45].

Carbon fibers are produced with different production techniques and basically, they have different graphitic carbon content ratio which differs mechanical properties. The tensile modulus of commercially available carbon fibers ranges between 207 GPa to 1035 GPa. They have an exceptionally high tensile modulus-to-weight ratio and tensile strength-to-weight ratio. They have intermediate modulus (IM), high modulus (HM) and ultra high modulus (UHM) types. Further, they have a very low coefficient of thermal expansion, high fatigue strength, and high thermal conductivity. Whereas, their impact resistance is relatively low. They are open to galvanic corrosion since they are electrically conductive. They are used in weight-critical applications due to their high specific strength value as seen in Figure 27. Those features increase demand for carbon fiber, furthermore their cost is relatively high [45].

Most widely used fibers are briefly explained in the previous paragraphs. Other than those, there are other fibers that are not as common.

One example is Boron Fiber. It has a relatively high tensile modulus which is ranging between 379-414 GPa. Its fiber diameter is relatively high that results with good buckling resistance. This property contributes their compressive strength. It used only in some aerospace applications due to its relatively high cost. Another one is silica fiber. It is purer glass fiber that has higher silica content. This difference increases its heat resistance up to 1600 ℃ [45].

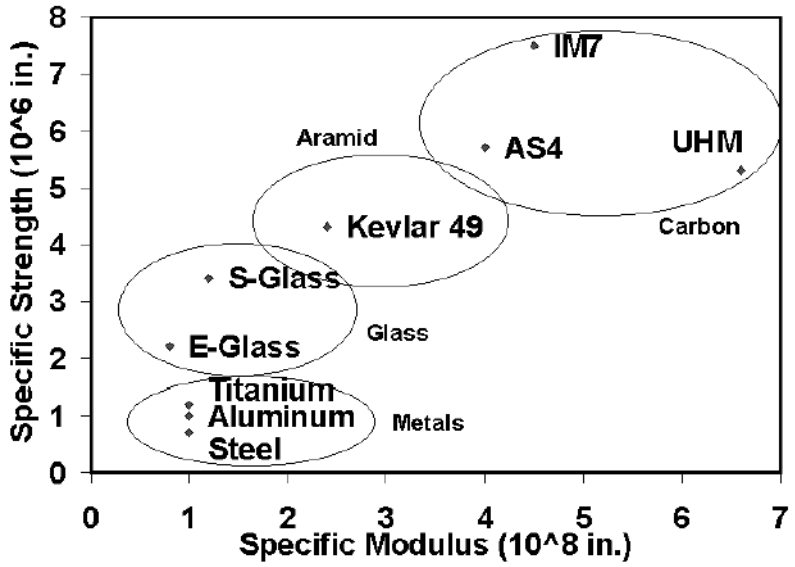

Figure 27: Specific Strength vs Specific Modulus Graph of Various Fibers [48]

Fiber material types are briefly explained above. As well as material type, form of the reinforcement has significant effect. The fiber can be in the form of tow, woven fabric, mat, stitched fabric, or braid. The form of reinforcement directly affects the fiber architecture which influences the mechanical and processing characteristics of the composite part. The difference in the fiber architecture includes continuity, orientation, crimping and interlocking of the fiber. Furthermore, it directly affects the resin flow during processing which influences other characteristics that determine performance of the composite part, such as void content, fiber wetting, fiber distribution, dry area and etc. Typical relation between fiber form and strength of composite part is explained in Figure 28 [45].

The simplest fiber form is tow. Definition of tow is an untwisted bundle of continuous filaments, generally with a specific count. It can be used directly in filament winding and pultrusion method or it can be used in chopped form in spray-up production method [43].

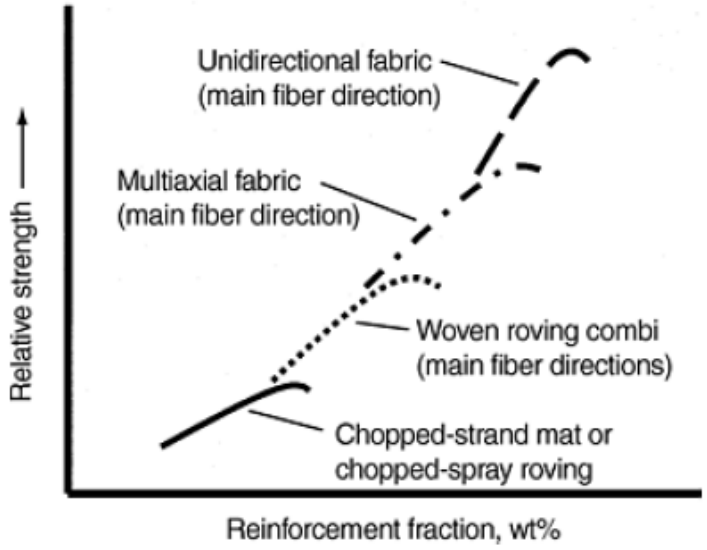

Figure 28: Influence of Reinforcement Type and Fraction on Mechanical Properties [49]

Another form is woven fabric. It is a planar material which is produced by interlacing yarns or roving in a specific pattern. Most common wave patterns can be seen in Figure 29. They are plain, twill, satin and basket waves. Plain is the simplest wave which is symmetrical and has good stability. However, it is difficult to drape the weaves in complex shapes. Different than plain wave there is an alternating pattern in twill weaves. It has higher wetting capability and its crimpling is reduced. Satin wave has higher wet out and a high degree of drapability. Low crimp increases its mechanical performance; however, its stability and asymmetry have to be considered during processing. The basket is an alternative wave to plain that has less crimp, higher performance but less stable. As well as 2D waves, 3D waves that have fiber reinforcement in through-thickness direction also exist. They require special production machines and they are used in some special applications in which interlaminar bonding strength is needed. [36, 43]

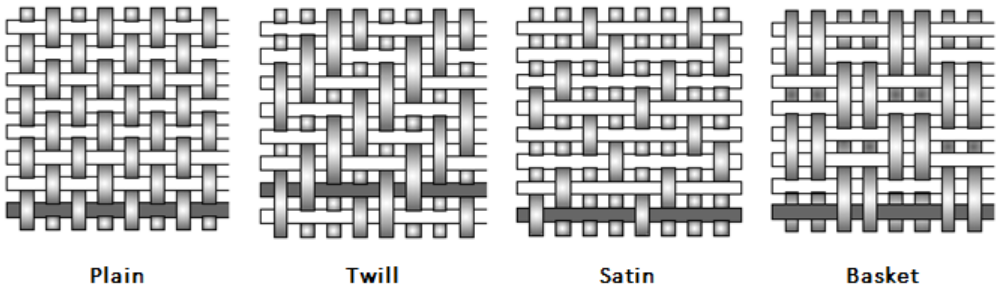

Figure 29: Illustration of Wave Types [36]

Mat is another type of reinforcement. It is a planar material form like fabric, but it does not have a specific wave pattern. In mat form, swirled continuous fibers or randomly oriented chopped fibers are bonded together. Due to its random fiber distribution, it shows isotropic behavior and its strength is lower than fabric forms.

The stitched fabric is a different form of fabric that can have uni-directional, bi-directional, or multi-directional fiber patterns that are hold together by means of stitches. In this type, different material combinations like carbon-glass, or material types like unidirectional fabric-chopped strand mat combinations can be obtained. Their draping capability is higher than woven fabrics and fiber density is higher so that they have higher mechanical performance. Properties of different reinforcements are given in Table 2.

Table 2: Properties of Different Reinforcements [49]

Reinforcement Type	Drapability	Shape Stability	Compaction	Permeability
Continuous Strand Mat	Poor - Good	Medium	Poor	High
Combination Fabric	Very good	Very good	Poor	Very High
Woven Roving (Plain weave)	Poor	Medium	Good	Medium
Woven Roving (Satin weave)	Good	Medium	Very Good	Low

Braids are produced by interlacing tows in the form of a tubular fabric. It is a special type of fabric that has a tubular shape. Also, it can be formed over a mandrel and from the nature of the braiding process; the whole surface of the mandrel can be covered, as seen in Figure 30.

They have high damage tolerance capability, torsional stability. They are used in high-performance applications, such as aircraft engine casings, missile bodies, or coupling shafts.

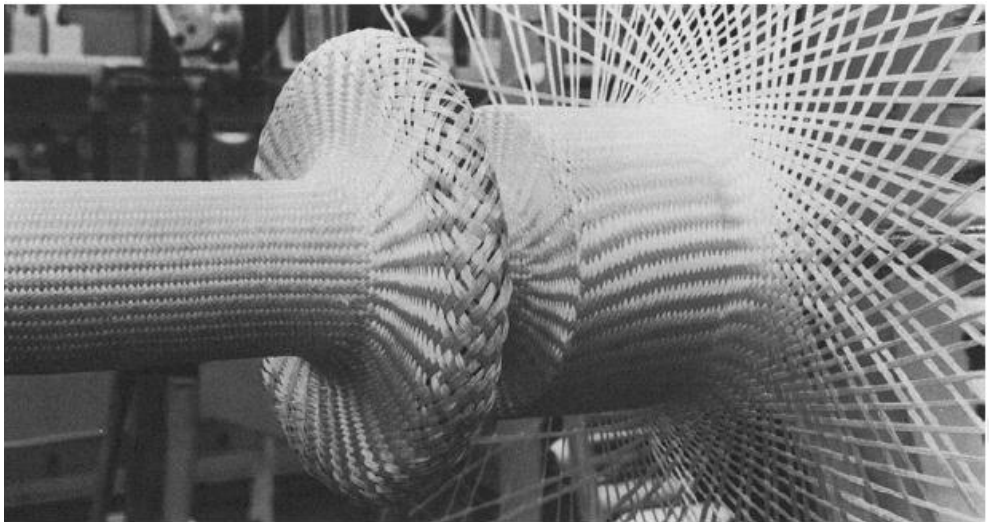

Figure 30: Formation of a Braided Coupling Shaft Preform [49]

2.2.3 Alternative Manufacturing Methods

When the composite manufacturing methods are considered, they are different in nature when compared with traditional production techniques. Other than traditional "material removal" approach applied on metals, composite manufacturing depends on "additive" production. For this reason, each method requires mold or mandrel in order to provide the shape of the product. In each manufacturing method, the reinforcement material is somehow impregnated with the matrix material, then consolidation is obtained with the curing process (Figure 31).

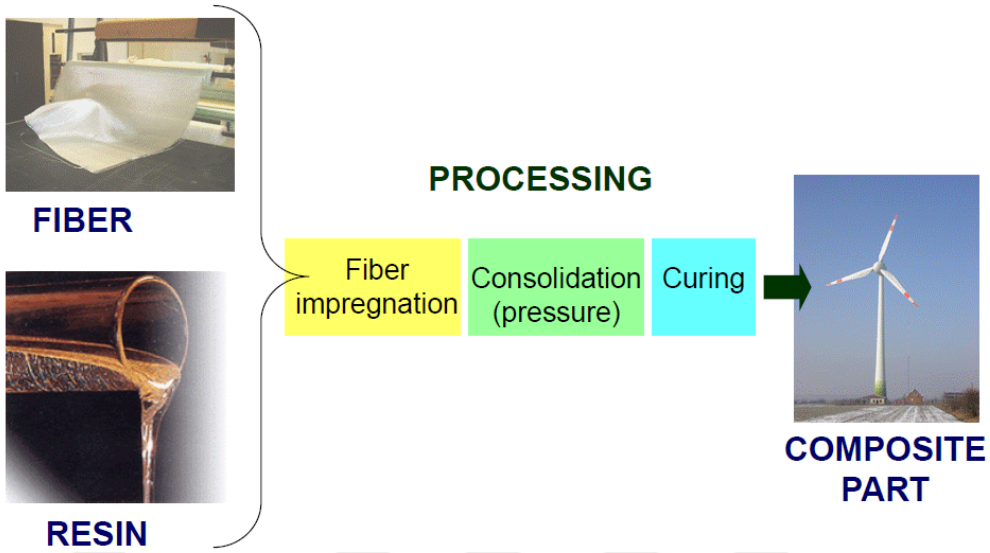

Figure 31: Processing of a Composite Part [37]

Basically, the curing type, supplementary consolidation, material impregnation method and mold shape specify the manufacturing method. Curing types are namely, oven curing, autoclave curing, room temperature curing and heated mold curing. Supplementary consolidation method can be vacuum pressure assisted, positive pressure assisted, and mechanical compression. Open mold, closed mold, constant cross-section pultrusion molds can be the mold alternatives.

The alternative manufacturing methods are various. In the following section, five alternative methods which are applicable to manufacture pod cover are briefly explained.

2.2.3.1 Wet Lay Up

This method is also known as hand lay-up or wet lamination. In this method, impregnation of resin into the reinforcement is obtained by hand (Figure 32). The wetting is generally obtained by spray, brush or roller. As a result, this is a very primitive process, but it is widely used. The reinforcement can be in fabric or mat form. Layers are added up to desired laminate thickness. Almost any type of

resins can be used, but generally, polyester is chosen. Since, the process is not suitable to produce high-performance parts, using a high-performance resin, such as epoxy, is pointless. It is suitable to build boats, chemical tanks, housings, city furniture etc.

Main advantages:

- Low investment costs
- Low mold and tooling costs
- Large parts can be produced
- A wide range of materials exists

Main disadvantages:

- Long cycle times
- Dependent on the operator skill
- Evaporation, exposure, and emission of volatile organic compounds (VOCs)
- Very low repeatability

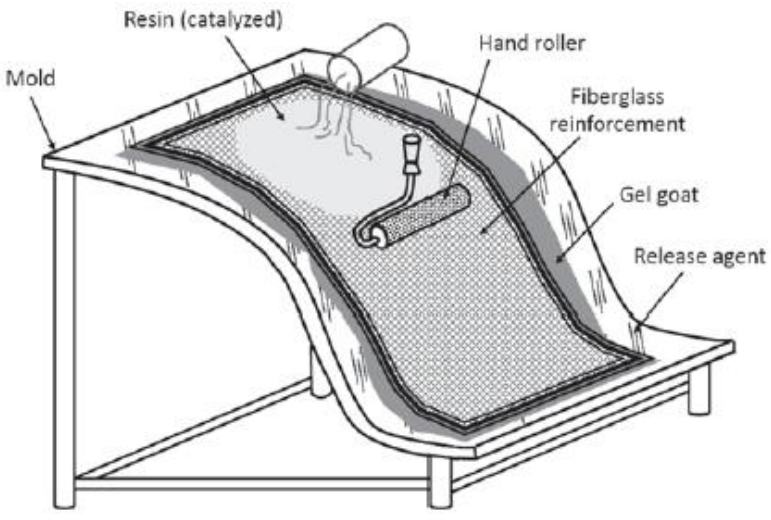

Figure 32: Schematic of Hand Laminating Process [43]

2.2.3.2 Sheet Molding Compound

Sheet molding compound (SMC) refers to both a material and a process for producing glass fiber reinforced polyester resin items. The material is typically composed of a filled, thermosetting resin and a chopped or continuous strand reinforcement of glass fiber. The additives allow the compound to be stored for months before processing. An SMC processing machine produces molding compound in sheet form (Figure 33, left). The glass fiber is added to a resin mixture that is carried onto a plastic carrier film. After partial cure, the carrier films are removed. The sheet molding material is cut into lengths and placed onto matched metal dies under heat and pressure (Figure 33, right) [44].

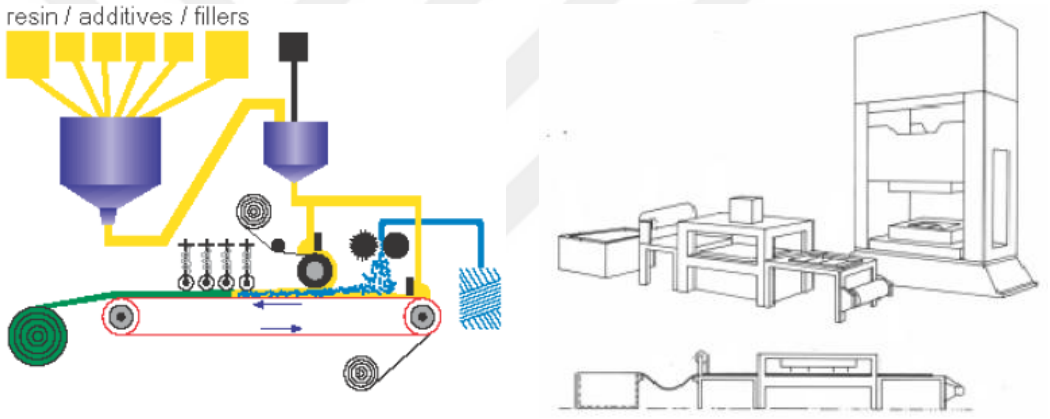

Figure 33: Sheet Molding Compound Precursor Production (Left) and Hot Pressing of the Sheet Molding Compound (Right) [37]

Since the cycle time is relatively low the process suitable for producing automobile parts such as tailgate or bumper.

Main advantages:

- Low cycle time
- Superior surface finish in all surfaces
- Automatic process
- Repeatability is relatively high

Main disadvantages:

- Necessity of special facility
- High cost tools
- Requires special precursor material

2.2.3.3 Resin Transfer Molding

In this method, dry reinforcement material is placed into the closed mold cavity and the liquid resin is injected to the mold by the help of the positive pressure (Figure 34). After the injection, heat is applied to the mold and curing is obtained. When the curing is finished, product is removed from the part. This method is applicable for production of the low/medium production rate, dimensionally precise and high performance parts. In this method, all surfaces are smooth; all the dimensions are fixed and depend on the mold geometry. Rocket/missile parts, UAV parts, helicopter blades are some of the examples that use this method.

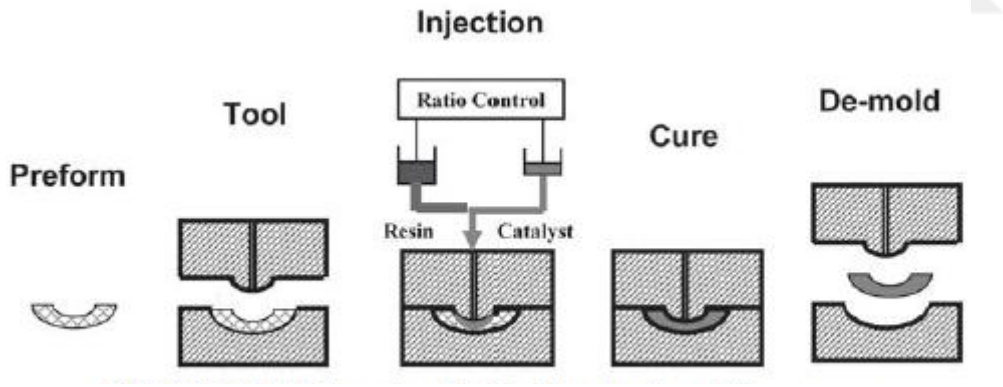

Figure 34: Schematic of the Resin Transfer Molding Process [36]

Main advantages:

- High fiber, low void content
- Dimensionally stable part
- Relatively low labor intensity

Main disadvantages:

- High mold cost
- Difficult to optimize process parameters
- Requires special equipment

2.2.3.4 Vacuum Infusion

Vacuum Infusion is another method that depends on resin transfer approach from outside of the system. Different than Resin Transfer molding, the mold is open and the reinforcement material is bagged on top of the mold surface (Figure 35). Resin impregnation is obtained with vacuum and atmospheric pressure applied on the bag. Due to the absence of the positive pressure, consolidation is not as good as RTM. Because of the one-sided mold, one side of the part has a smooth surface. Moreover, one-sided mold is relatively low cost when compared with RTM or other closed mold production techniques. Control of the process is easier than RTM due to the transparency of the vacuum bag. Flow of the resin can be observed during wetting and required action can be taken when necessary. Vacuum bag and other supplementary consumption materials are necessary for each process. This aspect adds recurring cost to the process.

Vacuum Infusion method is used to produce boat structures, wind turbine blades, ballistic panels very frequently. Generally, this method is efficiently used for large/medium parts with low production rate when medium or high performance is required. It is developed to replace with hand lay-up technique for the low volume higher performance part production.

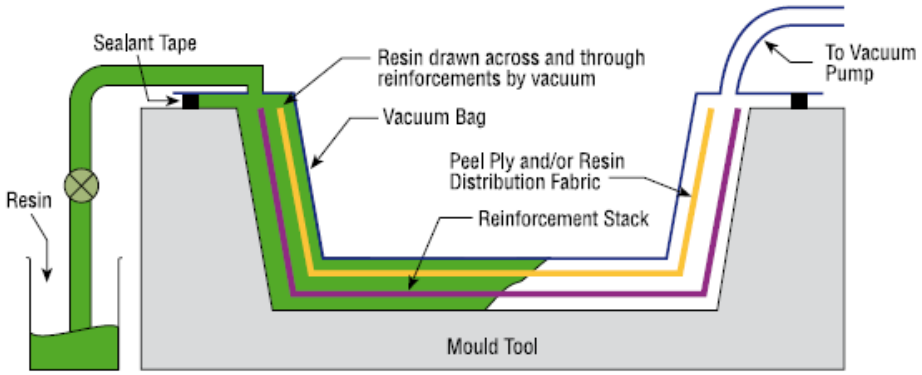

Figure 35: Schematic View of the Vacuum Infusion Process [36]

Main Advantages: [49]

- Low tooling cost
- Low investment cost
- Relatively low labor intensity
- Only method for very large parts
- Relatively high performance

Main Disadvantages:

- Only the tool surface is smooth and precise
- Waste of consumables for each production
- Higher void content than RTM

2.2.3.5 Autoclave

In the autoclave production technique, different than other methods, pre-impregnated reinforcement is used. This material is called prepreg and its basically preimpregnated resin and fabric material. In this material, resin is not fully cured and it allows the material to be used in the process under the required conditions. In this method, prepregs are laid up to the mold surface, similarly to the Vacuum Infusion process. Differently, the mold is placed into the autoclave

that applies pressure and heat simultaneously (Figure 36). Matrix and reinforcement consolidation is obtained with the pressure inside the autoclave chamber. Typically 5-6 atm pressure is used and 120-180 °C temperature is applied. It is used to produce high performance, small/medium parts. Helicopter/plane structural parts are typical examples using this method.

Advantages:

- High control of the resin/fiber ratio and repeatability
- High strength part
- Low void content
- The clean process due to the absence of liquid resin

Disadvantages:

- Investment cost is high
- Material cost is high
- Requires high skilled operator
- Cycle time is relatively high

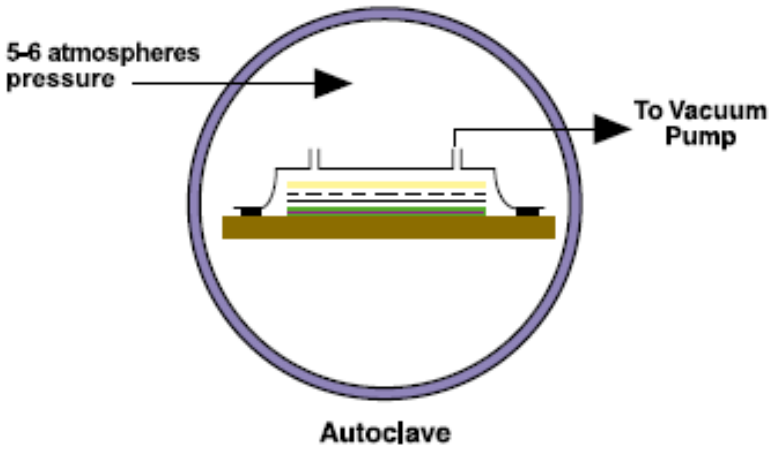

Figure 36: Schematic View of Autoclave [43]

2.3 Loads on the Cover

There are two load cases that must be considered for the cover design (Figure 37):

1. Inner Load:

The reflected pressure wave from the aft cover before the rupture and pressure induced due to backflow of the rocket nozzle inside the launch tube.

2. Outer Load:

The pressure effect of the rocket exhaust when the missile is fired from the adjacent launch tube.

Studies exist in the literature about the inner pressure effect on the fracture of the cover due to the rocket exhaust gases just after the ignition. According to Lee a pressure wave is reflected from the aft cover and propagates through the launch tube to the front cover. Change of the pressure profile with time for a typical missile is given in Figure 38. The reflected pressure wave coming from the aft side can be seen in this graph too [50].

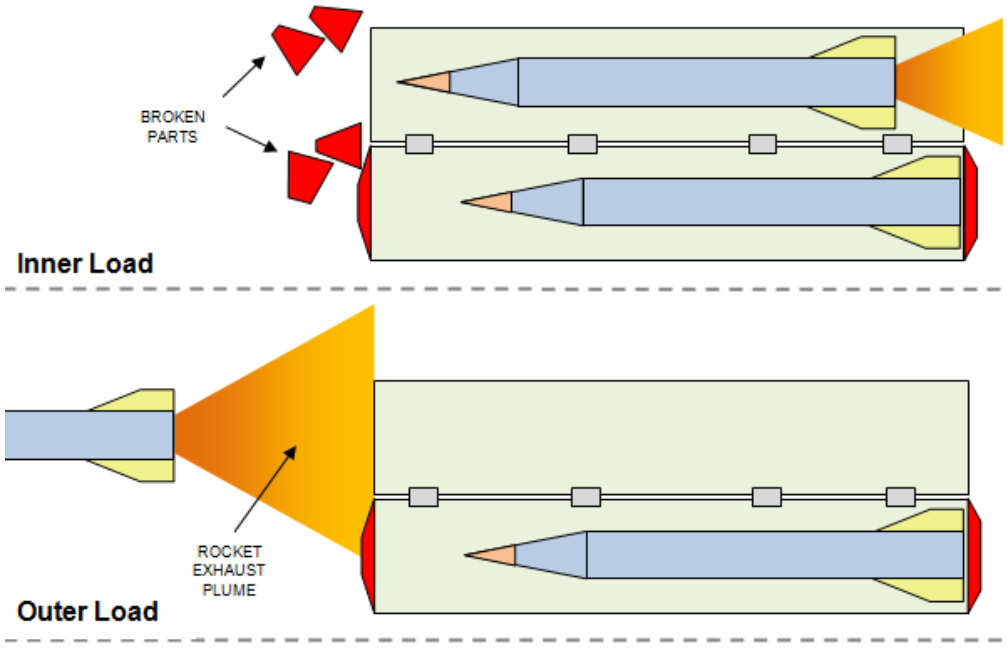

Figure 37: Schematic View of Loading Cases

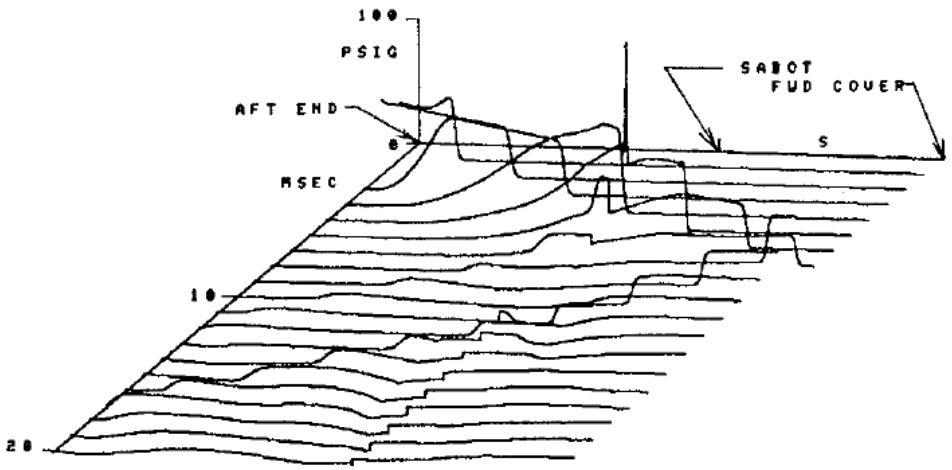

Figure 38: Pressure Profile vs Time Graph Inside the Launch Tube [50]

In the study of Fu and Jiang, it is stated that front cover of a launch tube can be broken by means of pressure waves inside the launch tube. This suggestion is corrected with simulations and tests [51].

In another source, it is stated that the pressure applied to the inner surface of the front cover is related with the backflow from the rocket nozzle and reflected shockwave from the aft cover. In Gas Dynamics modeling of the moving shockwave and its pressure effect is studied in detail [52].

Navy Vertical Launch System (VLS) consists of launch tubes which are integrated to the hull of the ship. In a study, pressure wave reflections inside the launch tube have been investigated. In that system, the pressure measurements are recorded and the below graph (Figure 39) is obtained. Reflection of the pressure wave can be observed as seen in the previous example. In that system, the front cover is not broken with the pressure, thus pressure wave reflects from the front cover [53].

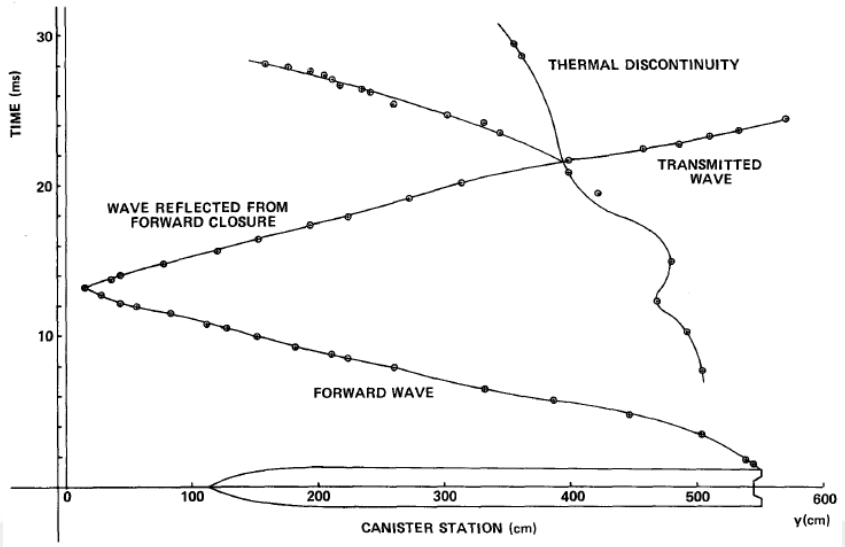

Figure 39: Wave Diagram for Pressure Transients in VLS Launch Tube [53]

M.J. Marongiu has been conducted simulation and test studies in order to model the plume-wall interaction in 1985. This study also gives information about the moving shock phenomena. In that study, strong non-steady pressure waves are generated inside the launch tube and recorded under the controlled laboratory conditions [54].

The outer load is different than inner load in some aspects. Pressure distribution at the outer side of the cover is non-uniform, and its magnitude changes with time and position of the nozzle. Additionally, the exhaust gas is at high temperature and contains alumina particles. Some researches are carried out for the investigation of outer loading. Generally, most of them are concerning about the effect of the missile exhaust plume on the launching equipment. These works basically are about CFD simulations and tests.

In the study of Ma, Jiang, and Yan the pressure and temperature distribution on the launching equipment are studied by using finite volume method. In order to simulate the phases of launching process, the missile is modeled at different distances from the launching equipment (Figure 40). This gives the variation of pressure distribution on the cover with time. [55]

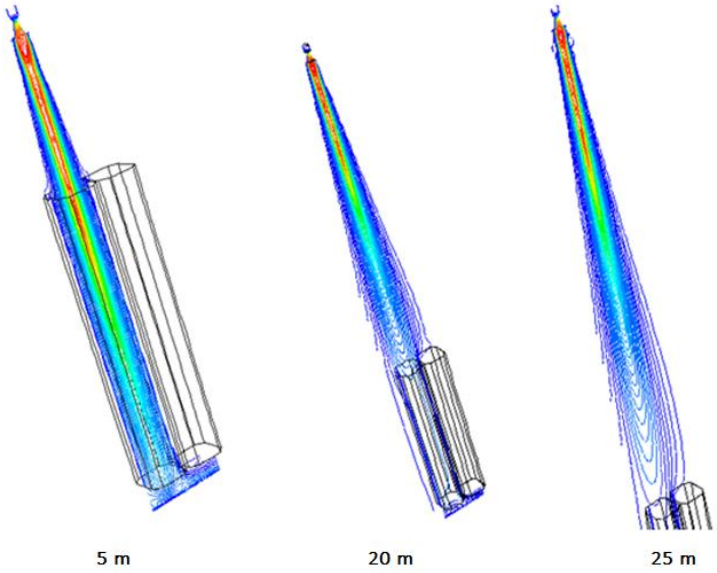

Figure 40: CFD Simulation for Different Instances Launching of a Missile [55]

In this work, simulation for the exhaust plume is carried out to find the pressure distribution on the cover. In these studies, the effect of the cover shape is also considered.

2.4 Scope of the Thesis

In the scope of the thesis, a hard cover will be designed by using composite material technologies. Basic properties of the composite production methods are summarized in Table 3.

RTM is chosen for manufacturing of the cover due to the reasons below:

- All surfaces are smooth and dimensions are controlled by the closed mold
- Labor intensity is lower than wet lay-up and vacuum infusion
- Reproducibility is relatively high
- Cycle time is lower than other methods except for SMC

Table 3: Comparison of Composite Production Methods

Property	Wet Lay Up	SMC	RTM	Vacuum Infusion	Autoclave
Labor Intensity	High	Moderate	Moderate	High	Moderate
Tooling Cost	Low	High	High	Low	High
Geometry	Simple	Simple	Complex	Simple	Complex
Surface Quality	Moderate	High	High	Moderate	Moderate
Number of smooth surfaces	One	All	All	One	One
Reproducibility	Low	Moderate	Moderate - High	Low	High
Mechanical Properties	Low	Low	Moderate - High	Low - Moderate	High
Cycle Time	High	Low	Moderate	High	High

For the resin material epoxy is chosen due to its better mechanical properties, higher reproducibility, and better aging properties. Also, epoxy has the lowest shrinkage during curing. For this reason, dimensional stability is higher and residual stress level is lower in epoxy matrices.

Glass fiber, carbon fiber, and aramid fiber are the example reinforcement materials that can be applicable to RTM and can be bonded to epoxy resin. Carbon is used for the applications where the weight and strength are critical. Aramid has superior resistance to impact loadings. Both aramid and carbon are expensive when compared with glass fiber. Since impact resistance and weight is not critical for launch tube cover, E-Type glass fiber is chosen. It has moderate properties with low cost and it is easy to supply without any restriction.

In the scope of this study, loads on the pod cover will be investigated. Load investigation consists of both inner and outer loads acting on the cover. In order to determine load levels, measurement and simulation approaches are used. Effect of cover geometry is also considered in the simulations. In order to measure the outer

load, a custom adapter is designed and used in the firing tests. The results of simulation and measurement are compared.

In the design phase, first of all, the problem definition is obtained and corresponding design requirements are derived. Technical solutions are developed for each requirement. The concept is developed step by step starting with the simplest solution of a plate cover ending with preliminary dome-shaped designs leading to a general form of the cover design.

After obtaining the general form of the design, sizing is conducted by using parameters which are defined in the design phase. In this study Abaqus FEA software is used. FEA results for each parameter is investigated and compared with each other. In order to obtain material properties, literature information and results of coupon tests are used. At the end of this study, all the dimensions of the cover are determined.

In order to manufacture the cover, an RTM mold is designed and manufactured with respect to the final dimensions of the cover model. Cover prototypes are produced by using this mold.

In order to test and obtain burst pressures, burst test set-up is designed and manufactured. By using the set-up inner and outer burst pressures are obtained for the first batch of the cover prototypes. Test results are compared with the results obtained in analyses. After all these tests, the cover is used in firing test for the proof of the design

Due to confidentiality some of the numerical values (i.e. force, pressure, dimension) are replaced with parametrical variables.

CHAPTER 3

DETERMINATION OF LOADS ON POD COVER

3.1 Applied Method for Load Measurement

In order to measure the inner load, pressure transducer is used. During a test fire, the pressure is measured by using a transducer mounted to the inner surface of the front cover (test configuration).

For the outer load prediction; CFD analysis has been conducted. Pressure and load measurements are also applied.

3.1.1 Method for Measuring Inner Load

For the inner load measurement, piezoelectric pressure transducer is used. The transducer is integrated into the test cover as shown in Figure 41. The sensing element of the transducer is directed to the inner side of the cover.

Figure 41: Pressure Transducer Integrated Cover

Position and orientation of the pressure transducers are given in Figure 42. During the experiment since only the upper missile is fired, pressure transducers in the upper pod cover are oriented to measure the inner pressure. On the other hand, transducers at the lower tube are located such that the outer pressure (i.e. the pressure created by the exhaust of fired upper missile) can be measured.

During the measurement sampling rate of the data logger is set to 102 kHz. This sampling rate provides accurate measurement of pressure oscillations which are expected within175-200 Hz range [54].

The transducer records pressure from the missile launch until it is damaged by the exhaust of the rocket engine. It is expected that a pressure wave shall reach to cover before the missile's nose cone.

Properties of the transducer and its schematic view are given in Table 4 and Figure 43, respectively.

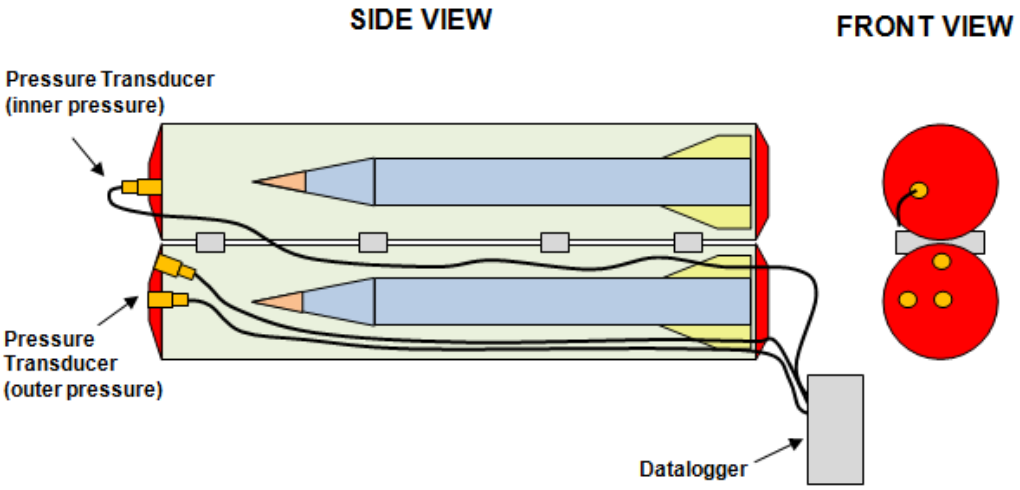

Figure 42: Pressure Transducer Integrated Covers

Table 4: Properties of the Pressure Transducer [56]

Producer Name	PCB Piezotronics
Model Number	CA102BXX
Measurement Range	0-3450 P
Resolution	0.014 P
Sensing Element	Quartz
Resonant Frequency	>500 kHz

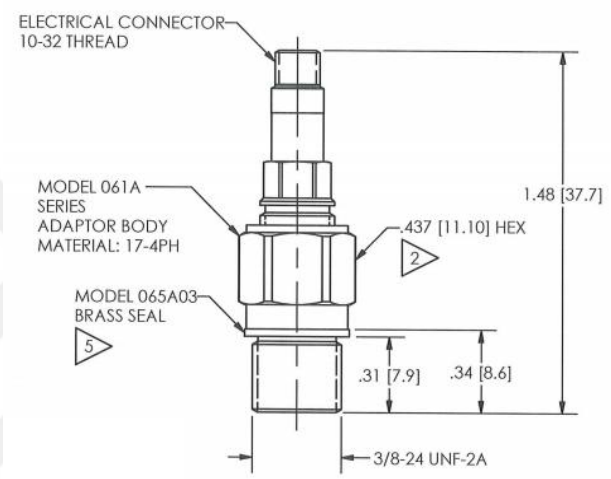

Figure 43: Schematic View of the Pressure Transducer [56]

3.1.2 Method for Measuring Outer Load

For outer load measurement, pressure transducers and load cells are used.

Different than inner pressure measurement, outer pressure measurement is more challenging due to high temperature and alumina particles of the exhaust plume. Two different types of transducers are used. One of them is the same transducer which is used at the inner pressure measurement. The orientation of the pressure transducers is given in Figure 42.

In order to protect the pressure transducers from the high-temperature exhaust plume, thermal grease was applied to the sensing element of the pressure transducer. However, meaningful data recording could not be obtained and it was sacrificed.

When the transducer has failed, another transducer which was suitable for high-temperature applications was used. Such a transducer can be used to measure the plume pressure and vibration response. In this measurement, only one transducer was used at the nearest point of the adjacent tube [57]. Properties of the transducer are given in Table 5 and technical drawing is given in Appendix A.

However, this measurement was also failed and the transducer was sacrificed. The main cause of failure is the flow direction which is directed almost perpendicular to the sensing element. In the literature, it is used parallel to the flow direction as seen in Figure 44.

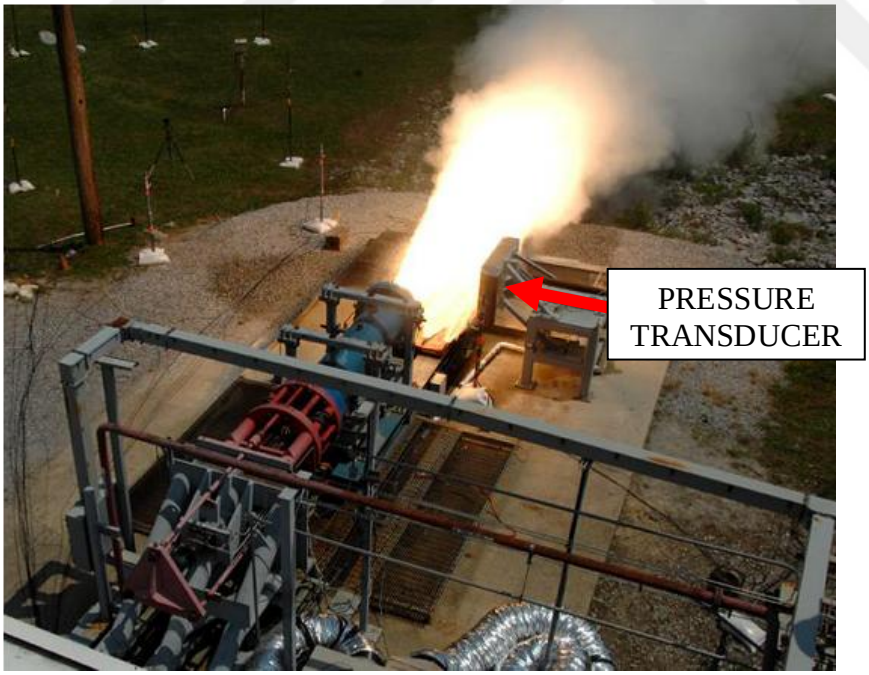

Figure 44: Example of the Pressure Level Measurement by Using Second Type of Pressure Transducer [57]

Table 5: Properties of the Pressure Transducer [58]

Producer Name	Kulite Semiconductor Products, Inc
Model Number	XTEH-10L-190 (M)
Measurement Range	0-70 P
Resolution	Infinitesimal
Pressure Sensing Principle	Fully Active Four Arm Wheatstone Bridge Dielectrically Isolated Silicon
Resonant Frequency	500 kHz
Operating Temperature Range	-55°C to 538°C

The third option for the load measurement is to use load cells. Due to the failure possibility as of the pressure transducers, load cells are placed under the test cover. By using load cells the resultant force applied to the cover is measured instead of the pressure. Load measurements are taken with 3 load cells simultaneously. By using three load cells, total force (axial) and application point of the force are obtained.

In order to integrate the load cells, an adapter is designed between the cover and the launch tube. The adaptor can be seen in Figure 45.

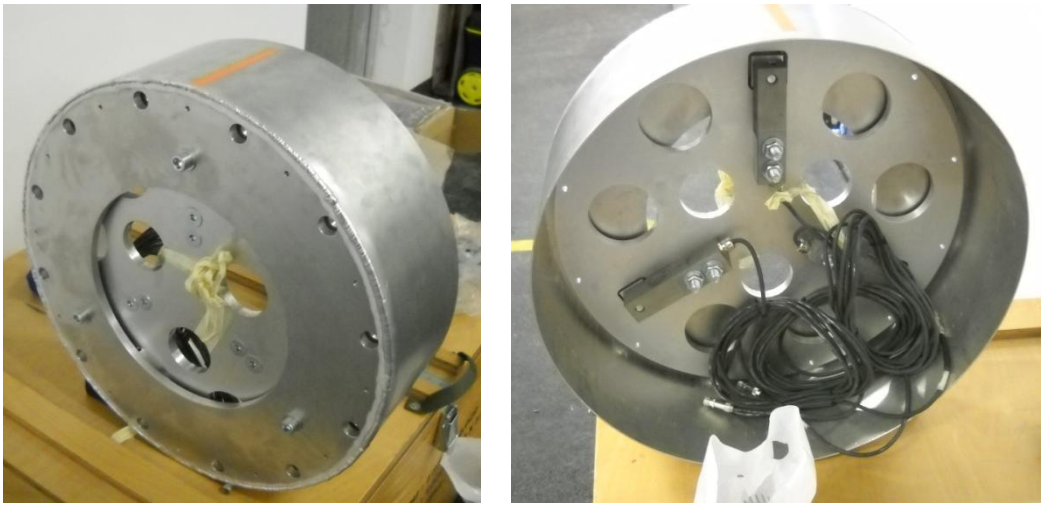

Figure 45: Photographs of Load Cell Adapter

The alignment of the load cells is given in Figure 46. Properties of the load cell given in Table 6 and technical drawing is given in Figure 47.

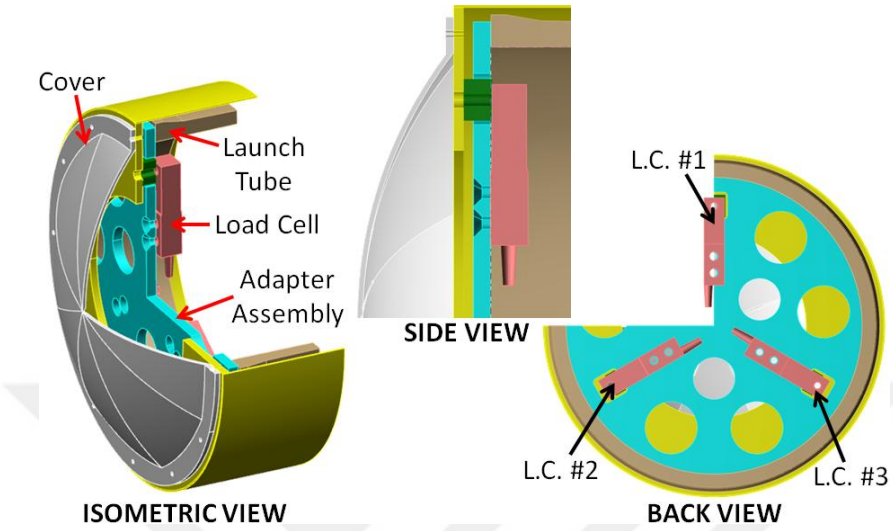

Figure 46: Schematic Explanation of Load Cell Adapter Assembly

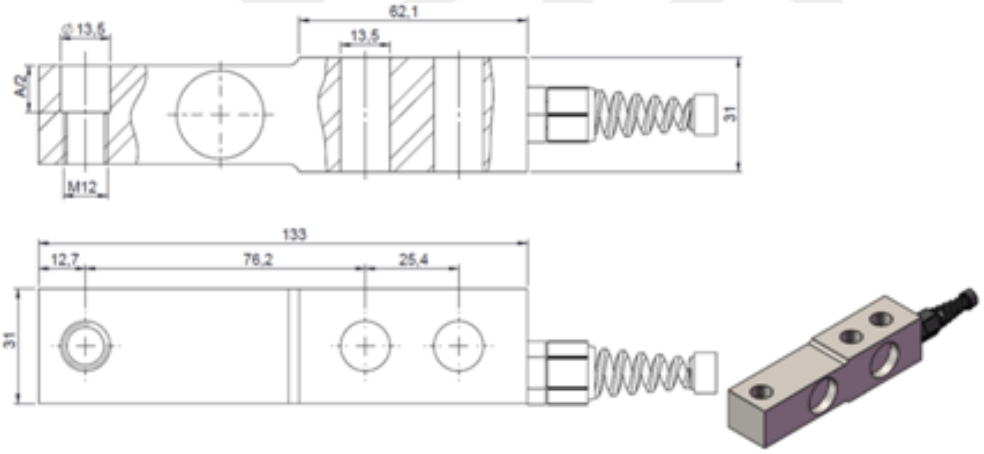

Figure 47: Technical Drawing of Load Cell (Dimensions are in mm)

Table 6: Properties of Load Cell

Producer Name	ESİT Electronics Co
Model Number	BS X
Type of Load Cell	Shear Beam
Capacity	40 F
Minimum verification interval	0.004 F
Material	Stainless Steel

3.2 Load Measurement Results

3.2.1 Inner Load Measurement

Inner pressure measurement can be seen in Figure 48. In the figure, “t0” stands for the firing instant. A sudden pressure increase exists as expected. This peak is observed at 8 t after firing. After sudden pressure increase, which can be interpreted as a shock, the gradual pressure increase is observed.

In the literature and section 2.3, it is stated that a shockwave moves with the speed of sound. It is assumed that when the rocket engine is fired a pressure wave is generated and it is reached to the front cover after reflecting from the aft cover.

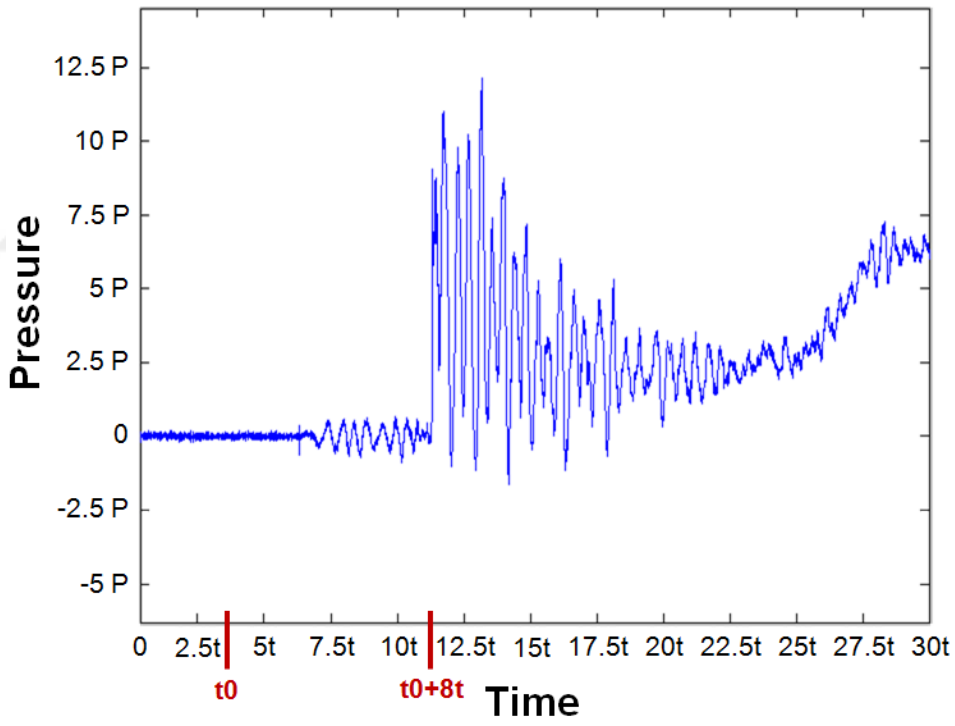

Figure 48: Inner Pressure Recording of Cover Surface During Launch

The time between the fire and the instant of the pressure wave reached to the front cover is used to calculate the speed of the wave. The distance from the aft cover to the front cover is 21.9 L and the time between firing and the pressure observation at the front cover is 8 t. By using this distance and elapsed time, speed of the wave is calculated as 342.5 m/s and it is approximately equal to the local speed of sound which is 340 m/s.

3.2.2 Outer Load Measurement

Since the pressure transducers are failed, the only data available is load cell records for the effect of the exhaust gas pressure at the outside of the cover. The load cell measurements are given in Figure 49 and Figure 50.

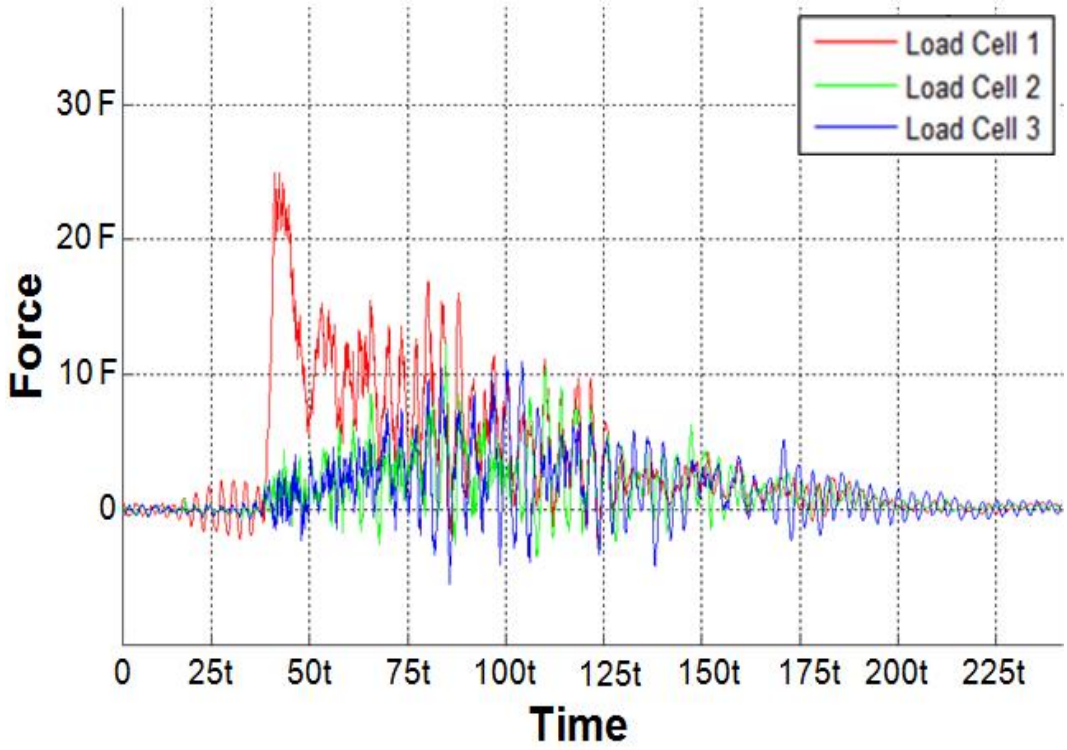

Figure 49: Load Cell Recordings During Launch of the Adjacent Missile

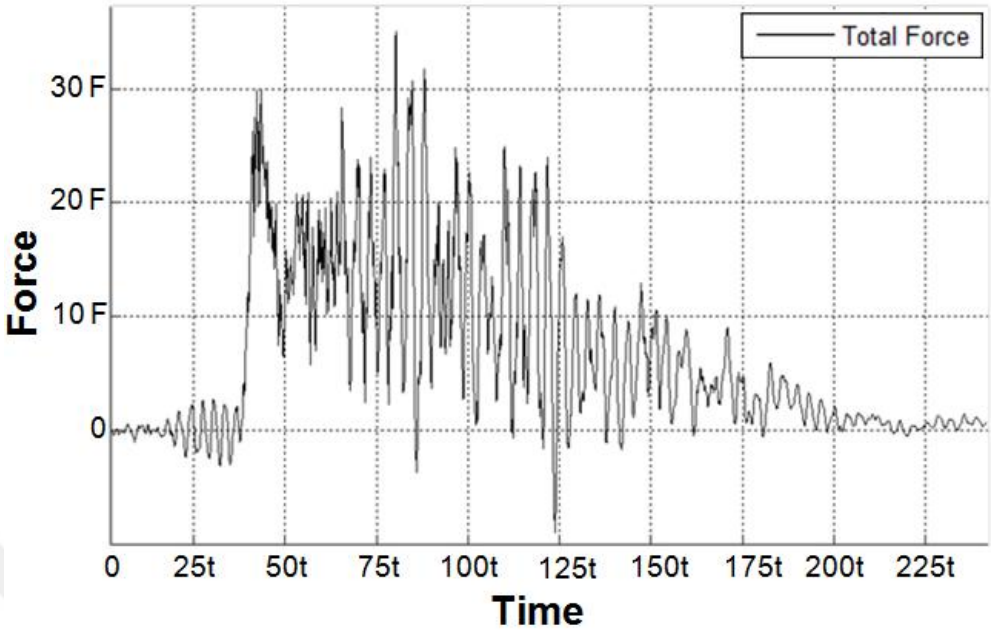

Figure 50: Load Cell Recordings Measurement (Total Load) During Launch of the Adjacent Missile

The upper load cell (load cell 1) shows higher load since the exhaust plume is closer at the upper side of the cover. While the missile is moving away from the cover the pressure cone of the exhaust plume gets bigger and the magnitude of the resultant force increases simultaneously. After a certain point, resultant force reaches a maximum value starts to decrease afterward.

The load cell record data is not synchronized with the instant of firing. Therefore it is difficult to detect the position of the missile and corresponding force. But it is possible to detect approximate position of the missile when the force is maximum. When Figure 49 is examined, it can be seen that upper load cell (load cell 1) peaks suddenly. It is assumed that the load is started to increase just after leaving the missile's nozzle from the launch tube. After this instant, approximately 37 t passes until the peak of the force. In other words, the missile flies 37 t after leaving the tube until the force peak occurs. It is possible to investigate the position of the missile by using high-speed camera recordings. Therefore, the distance between the missile and launch tube can be found approximately 24 L as seen in Figure 51.

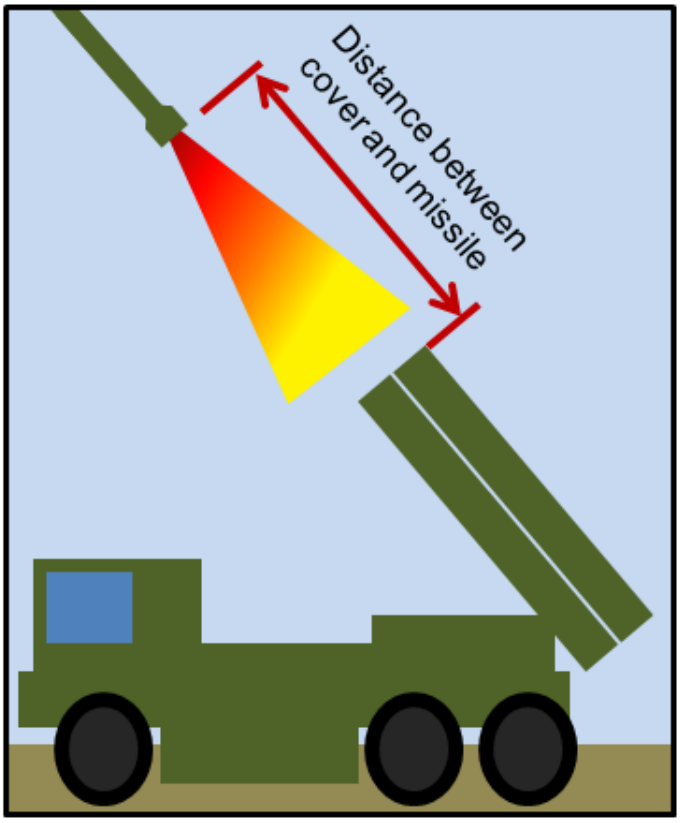

Figure 51: Schematic Explanation of Measurement of Position of Missile from High-Speed Camera Image

3.3 Interaction Analysis by Using CFD

3.3.1 Analysis Method

In the previous sections, literature information about the load on the cover is explained. Moreover, experimental approach is also discussed and pressure and load cell measurements are given. In this section, computational approach is considered in order to obtain the load on the cover.

Design of the cover is basically a solid mechanics problem. On the other hand, the outer surface of the cover has an interaction with the outflow of the rocket exhaust

plume. Therefore, fluid dynamics is another element that is used to find out the loading on the cover.

For computational fluid dynamics analysis, FloEFD (V15) software is used. Since the scope of the thesis is not fluid dynamics, this section is not given in detail. FloEFD is unique software and does not require expert level computational fluid dynamics knowledge. For this reason, it is reasonable to use in designing of the cover.

FloEFD software has an algorithm to obtain solution by using adaptive meshing. By the help of this feature, the software automatically refines the mesh in required zone and it updates the mesh when necessary during solution. For example, when the high gradient flow is obtained in the solution, then the resolution in the mesh is updated in that zone during the analysis run. Therefore, the accuracy of the result is increased with optimized mesh that has minimum number of elements. FloEFD also has the ability to detect the fluid domain automatically. Analysis definition is obtained step-by-step by selection of the scenarios. Therefore, by using this software fluid flow analysis can be carried out without deep knowledge in CFD.

In the CFD analyses, the effect of the adjacent rocket on the cover is investigated. As stated before, the most critical loading condition is the outer plume force. In order to investigate the effect of the adjacent rocket, different instants and different positions of the rocket are modeled. The perpendicular distance between the nozzle (Figure 52) and the boundary conditions are parameters used as variables for each instant. The rocket is assumed to be stable. This assumption is applicable since the speed of the fluid flow through the nozzle is relatively too high when compared with the speed of the rocket [54].

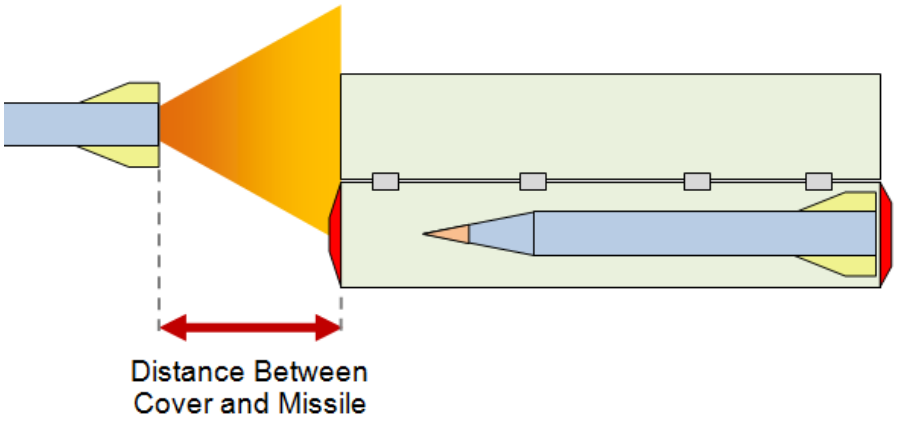

Figure 52: Schematic View of the Distance between Cover and Missile

The instants and the corresponding positions are given in Table 7. The time and corresponding distance are obtained by using high-speed camera images of firing.

Table 7: Distance of the Adjacent Rocket at the Corresponding Instants

Elapsed Time After Ignition	Perpendicular Distance Between Nozzle and Cover	Elapsed Time After Ignition	Perpendicular Distance Between Nozzle and Cover
90.5 t	0.25 L	111.5 t	14 L
92 t	2 L	114 t	16 L
94 t	3 L	117 t	18 L
95.5 t	4 L	120 t	20 L
97.5 t	5 L	122.5 t	22 L
99 t	6 L	125 t	24 L
102 t	8 L	130 t	28 L
105.5 t	10 L	135 t	32 L
108.5 t	12 L		

As seen in the upper table, instants are not evenly distributed. The change in outside pressure is more sensitive when the distance between the nozzle and the cover is smaller. Therefore sampling is increased at 0-6 L distance. By using the elapsed time after ignition, exit pressure, density, and velocity of the outflow at the nozzle is obtained. Additionally, molecular weight of the fluid material is

obtained from the characterization of the exhaust products of engine fuel. Moreover, after defining the material as gas, the flow of gas at each instant can be modeled. FloEFD model for the instant when the distance is 6 L is seen in Figure 53. Missile engine is modeled as cylinder. The cover is assumed as a dome-shaped geometry. Asymmetry or other design features are neglected. Half of the whole model is used during computations since the model is symmetric to the plane that cut along the longitudinal axis.

As stated previously, FloEFD software has an algorithm to obtain optimum mesh structure automatically and it refines it where and when necessary.

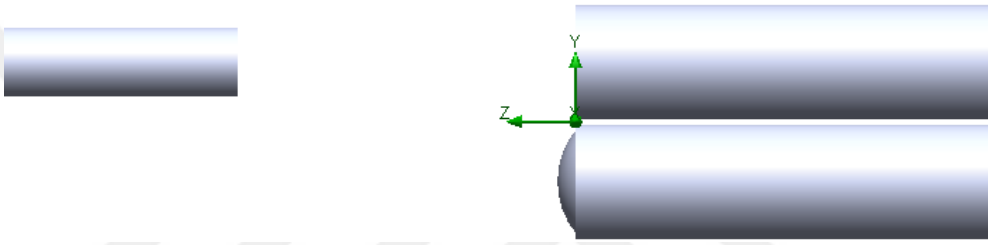

Figure 53: Solid Model Used in FloEFD Software

3.3.2 Analysis Result

Force on the cover and pressure distribution on the cover are obtained as output of the analyses. The results are given in Table 8. Variation of the force in the axial direction with distance is given in Figure 54. Moreover, the maximum outer pressure versus distance graph (Figure 55) is also obtained. The maximum pressure is observed at the flange of the cover and it is near to the vicinity of the adjacent tube. The highest value of the maximum pressures is observed at the instant when the distance is 5L, afterwards it sharply decreases and it is almost constant after 8L distance.

Force (axial) peak is obtained when the nozzle is 5 L away from the cover. Secondly, the force drops but later increases gradually up to the instant when the distance is 18 L. The force value of the second peak is close to the first value, but

the pressure distributions are different. Pressure distributions at different instants are given in Figure 57.

Table 8: CFD Analysis Results

Distance	Time	Force (Axial)	Max. Pressure
1 L	90.5 t	7.8 F	8.0 P
2 L	92 t	11.6 F	34.9 P
3 L	94 t	19.8 F	70.1 P
4 L	95.5 t	22.8 F	51.3 P
5 L	97.5 t	31.4 F	99.7 P
6 L	99 t	22.7 F	28.7 P
8 L	102 t	21.5 F	15.3 P
10 L	105.5 t	26.4 F	16.5 P
12 L	108.5 t	26.9 F	17.9 P
14 L	111.5 t	28.9 F	14.5 P
16 L	114 t	27.7 F	14.8 P
18 L	117 t	30.1 F	13.0 P
20 L	120 t	28.9 F	14.2 P
22 L	122.5 t	27.5 F	12.3 P
24 L	125 t	29.1 F	11.4 P
28 L	130 t	23.1 F	9.5 P
32 L	135 t	11.6 F	9.1 P

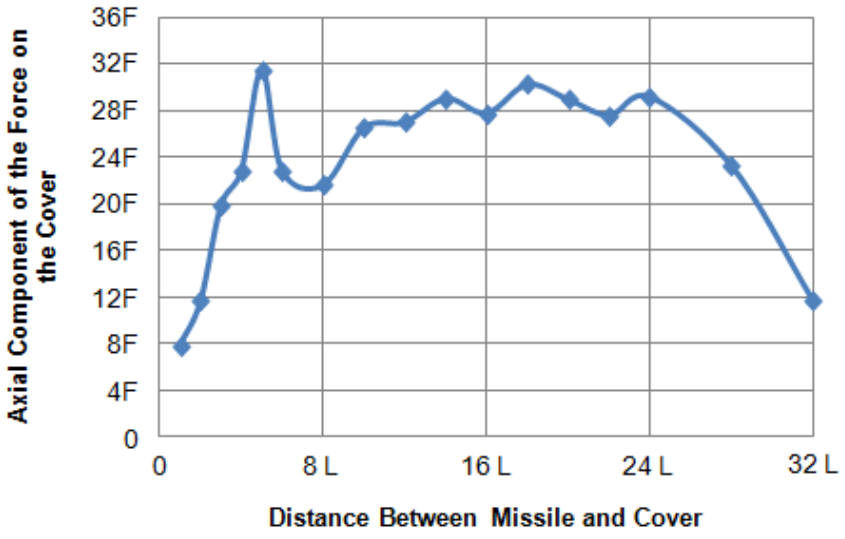

Figure 54: Graph of Axial Component of the Force on the Cover Surface vs Distance (for 200d dome height)

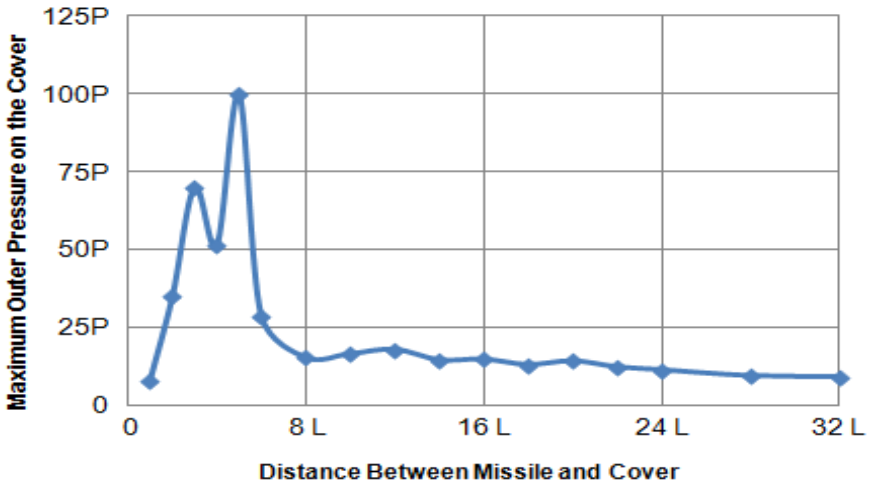

Figure 55 : Graph of Maximum Outer Pressure vs Distance Between Missile and Cover

Axial load which is obtained from FloEFD software is plotted with respect to time and compared with load cell measurements (Figure 56). In load cell recordings, instant of missile launch (t0) is not known. However, the instant when the axial load starts to increase sharply is assumed as the instant of missile's exit. The portion of the theoretical graph between 0-25t (Figure 56.a) and portion of the experimental measurement between 0-25t (Figure 56.b) are very similar in shape and numerical values.

After that duration of time, oscillation in the recordings starts to increase and even negative values are observed. For this reason, oscillation peaks are neglected in that area. It is considered that, these oscillations are originated from the vibration of the whole launch system (pod, cradle, launch vehicle). Oscillation exists at the beginning and increases when missile's exhaust plume starts to affect the launch system. When the results are compared, it can be concluded that, load levels are compatible with each other and results are slightly higher at FloEFD. Therefore, one can conclude that numerical force values are reliable and therefore corresponding pressure values are used for the calculation of stress in the cover due to the outer exhaust pressure of the missile.

Flow trajectories and Mach numbers of the flow for 4, 8, 16 and 24 L distances are given in Figure 58.

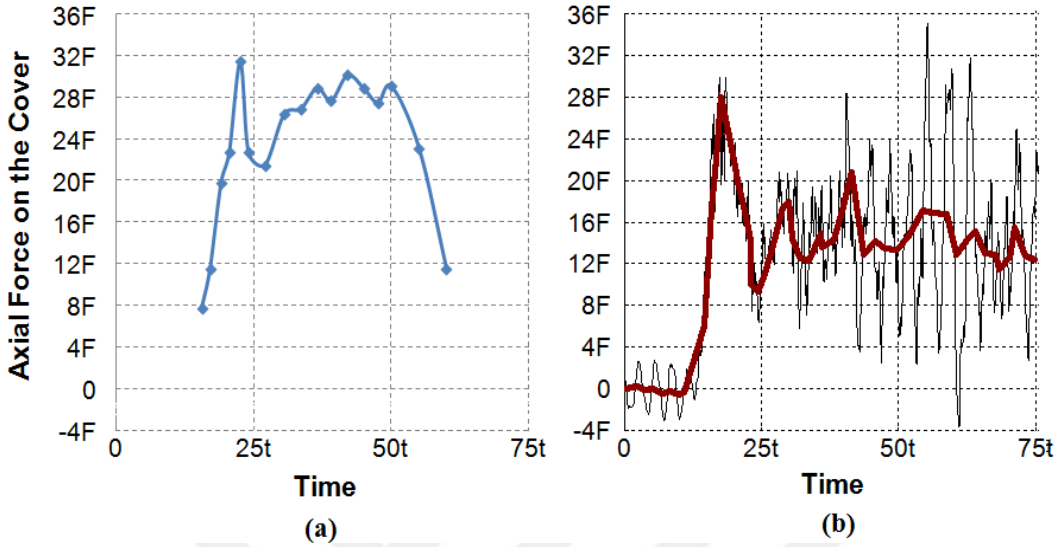

Figure 56: Theoretical (a) and Experimental (b) Results for Axial Load

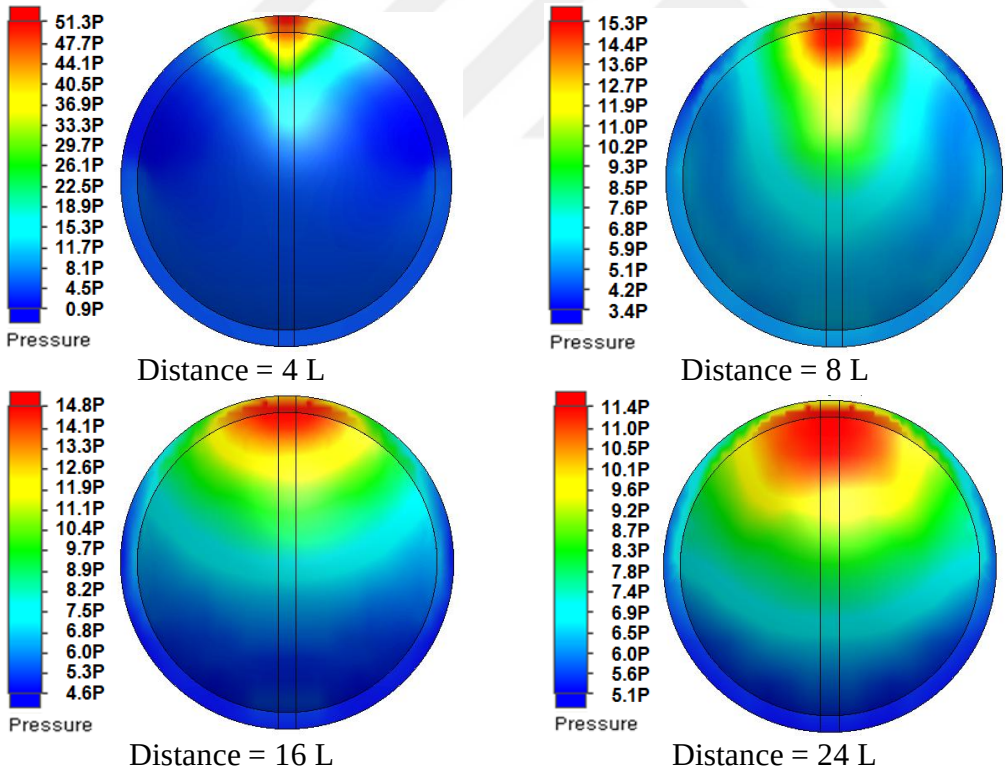

Figure 57: Pressure Distribution on the Cover Surface at Different Instants

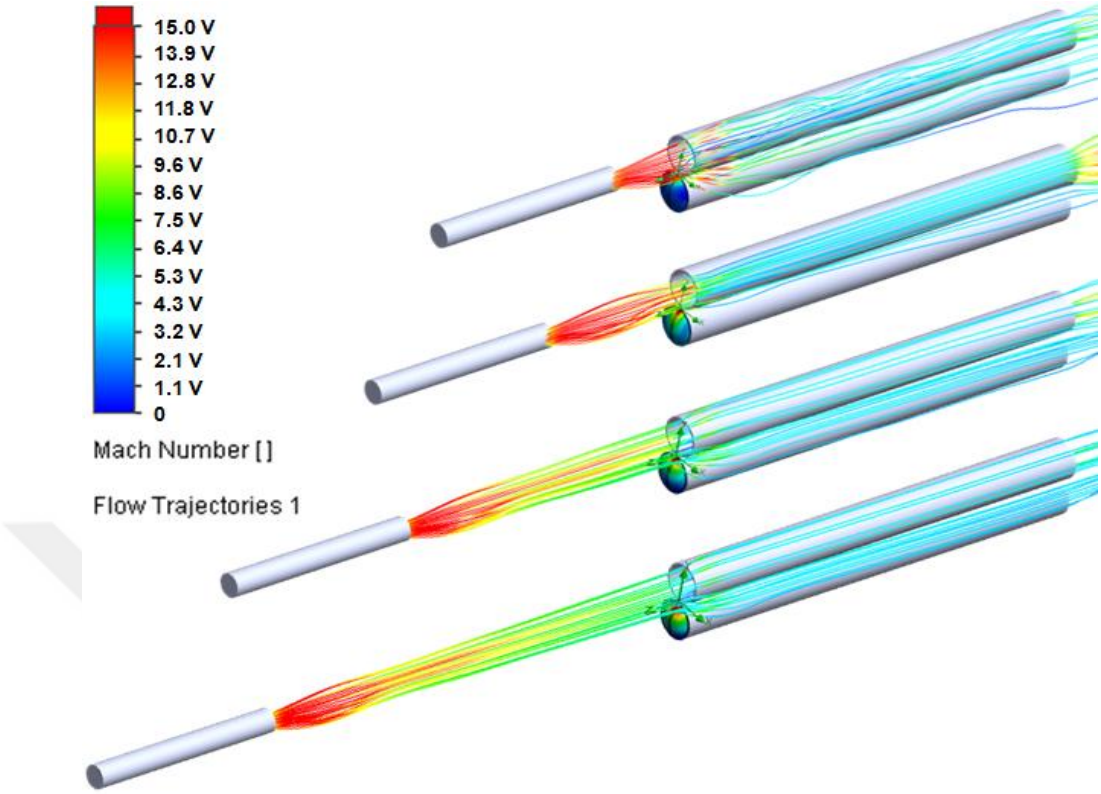

Figure 58: Flow Trajectories

3.3.3 Effect of External Geometry of Cover

Effect of the cover shape is also investigated by using FloEFD software. The analyses are repeated for different dome heights at 5 L and 18 L distances from the nozzle. The dome height of the cover is changed between 0-350 d with 25 d steps. Side views of different dome heights with 50 d increments are given in Figure 59.

Axial force resultants with respect to different dome heights are given in Figure 60 and Figure 61. As seen in the figures, axial force tends to decrease slightly with increasing dome height. Moreover, decreasing trend is smoother for 18 L distance case.

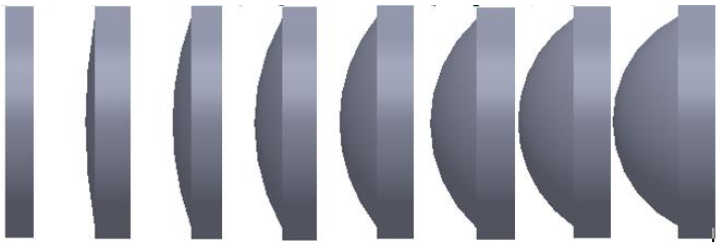

Figure 59: Side View of Covers that Have Different Dome Heights

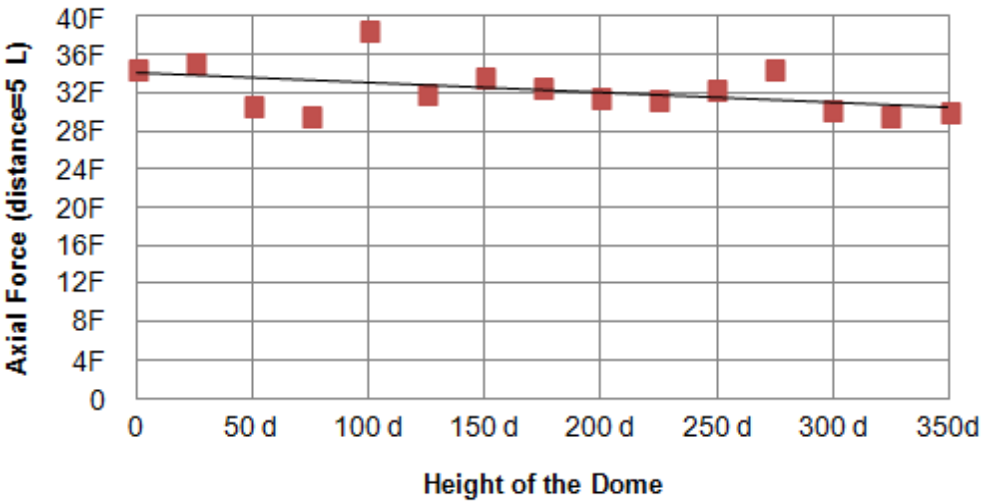

Figure 60: Graph of Axial Force vs Height of Dome When Distance is 5 L

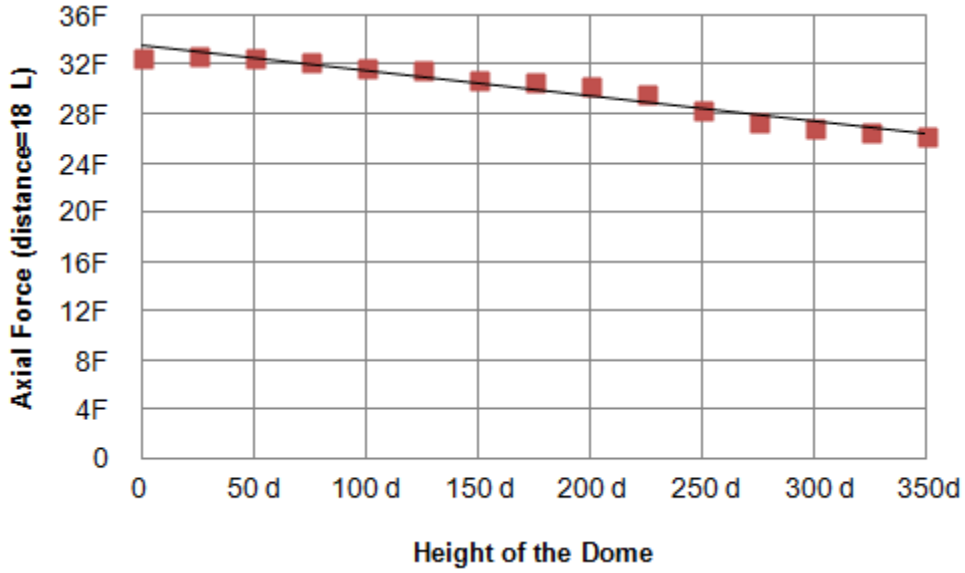

Figure 61: Graph of Axial Force vs Height of Dome When Distance is 18 L

CHAPTER 4

DESIGN OF COVER

4.1 Problem Definition and Design Requirements

Launch tube covers are one of the major subsystems of a launch system. They take role in every step of the lifecycle of the system. Therefore, they must satisfy all requirements of the phases of the lifecycle.

Three main phases exist in the life cycle of the launch tube:

1. Storage
2. Transportation
3. Operation

For storage and transportation phases, the purpose of the launch tube cover is to isolate the inner volume of the launch tube from the environment. By this means, necessary storage conditions can be provided for the missile and its subsystems.

For the operation phase, in addition to the environmental protection, it must resist the exhaust plume of the adjacent launch tube. Moreover, it must provide ejection of the missile without any interaction.

Therefore, the aim of the launch tube cover is to protect the missile until the launch and to provide ejection of the missile without any interaction with the missile during the launch.

As mentioned in Chapter-2, the cover is produced from composite materials by using Resin Transfer Molding (RTM) process. Its materials are chosen to be fiberglass and epoxy resin.

Other main constraints are briefly summarized below:

1-The cover shall not interact with the missile during launch.
2-The cover shall isolate the internal volume of the launch tube from the environment.
3-The cover shall resist the exhaust plume of the adjacent missile.
4-The cover shall be compatible with the interface of the front opening of the launch tube.
5-The cover shall not contain mechanism or actuator.
6-The cover shall not increase the length of the launch tube more than 200 d.

4.2 Requirement Analysis

Requirements are analyzed and sub-requirements are derived. Each requirement shall be satisfied and a technological solution will be proposed by using this sequence.

In the requirement analysis, three major design considerations are derived.

1- The cover shall be gas tight. Therefore, necessary sealing must be provided at the interface and the cover itself.
2- The cover shall resist the force applied by the plume of the adjacent missile. Therefore, it must be strong enough for the plume force at the outside.
3- The cover shall be frangible. It must be weak enough to be broken with the effect of the inside pressure of the launch tube during firing.

These design considerations are derived as seen in Figure 62. 1st main requirement which is tightness can be solved by using common solutions. 2nd and 3rd

requirements contradict each other. Therefore, this contradiction and its solution become the basis of the solution. Design considerations are handled according to this aspect on a large scale. Solution of this contradiction requires creative solutions and these solutions are derived in the preliminary design phase.

Another important issue that must be considered during the requirement analysis is the evolution of the product. When patents and similar systems are investigated in chronological order, the evolution of the pod covers can be observed. The information of product evolution guides the design and reveals some of the properties that a pod cover should possess. When the literature is investigated evolution of pod covers have the following steps.

1. Necessity and idea of the pod cover
2. Invent the first pod cover
3. Make the pod cover working better
4. Make the pod cover safer and more reliable
5. Make the pod cover more practical
6. Make the pod cover autonomously working
7. Reduce the cost
8. Standardize the pod cover

Properties of the pod cover matured from basic through the advanced. Therefore, the pod cover design already possesses basic properties. Moreover, it must have advanced or new aspects, in order to create better pod cover. Thus, stages of the design aspects are taken into consideration in addition to the requirements.

Being frangible is the major aspect of the cover design. By the help of this property, the cover can be opened by the effect of the inner pressure. Since the inner pressure increased just after the firing but before the missile launch, it can be used to break and open the cover. Therefore, the cover can be opened autonomously and this autonomy is gained only by making the cover frangible.

This is an example of efficient use of the sources. Instead of using complex actuator mechanisms, the pressure of the engine is used.

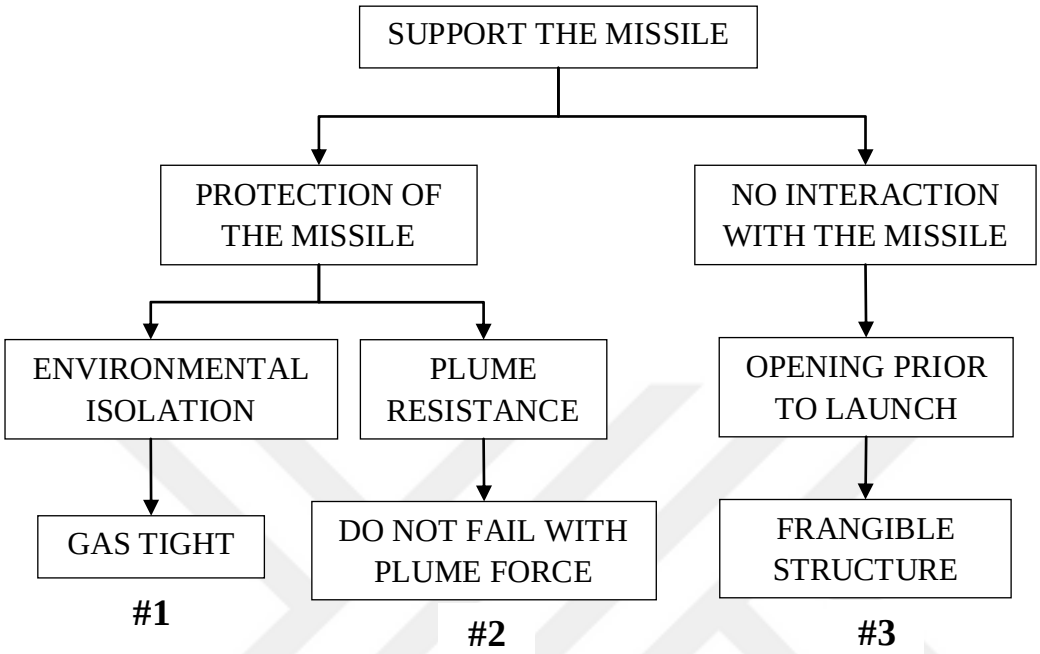

Figure 62: Derivation of Sub-requirements

4.3 Preliminary Design

Creative solution (Figure 63) is the most important output of preliminary design phase. It is the main element that creates diversity and awareness. Also, it determines the quality of the design. Therefore, this is one of the most important steps that shapes the design.

In the continuity of this section, the design process is explained step by step. The design starts with the simplest condition and it is evolved through a more complex phase.

1- The simplest geometry that the cover should possess is a simple plate. Therefore, the design starts with the simple plate as seen in Figure 64. In this phase, the cover has two parameters. They are the outer diameter and thickness of

the plate. The outer diameter is fixed due to the known launch tube diameter but the thickness is to be determined.

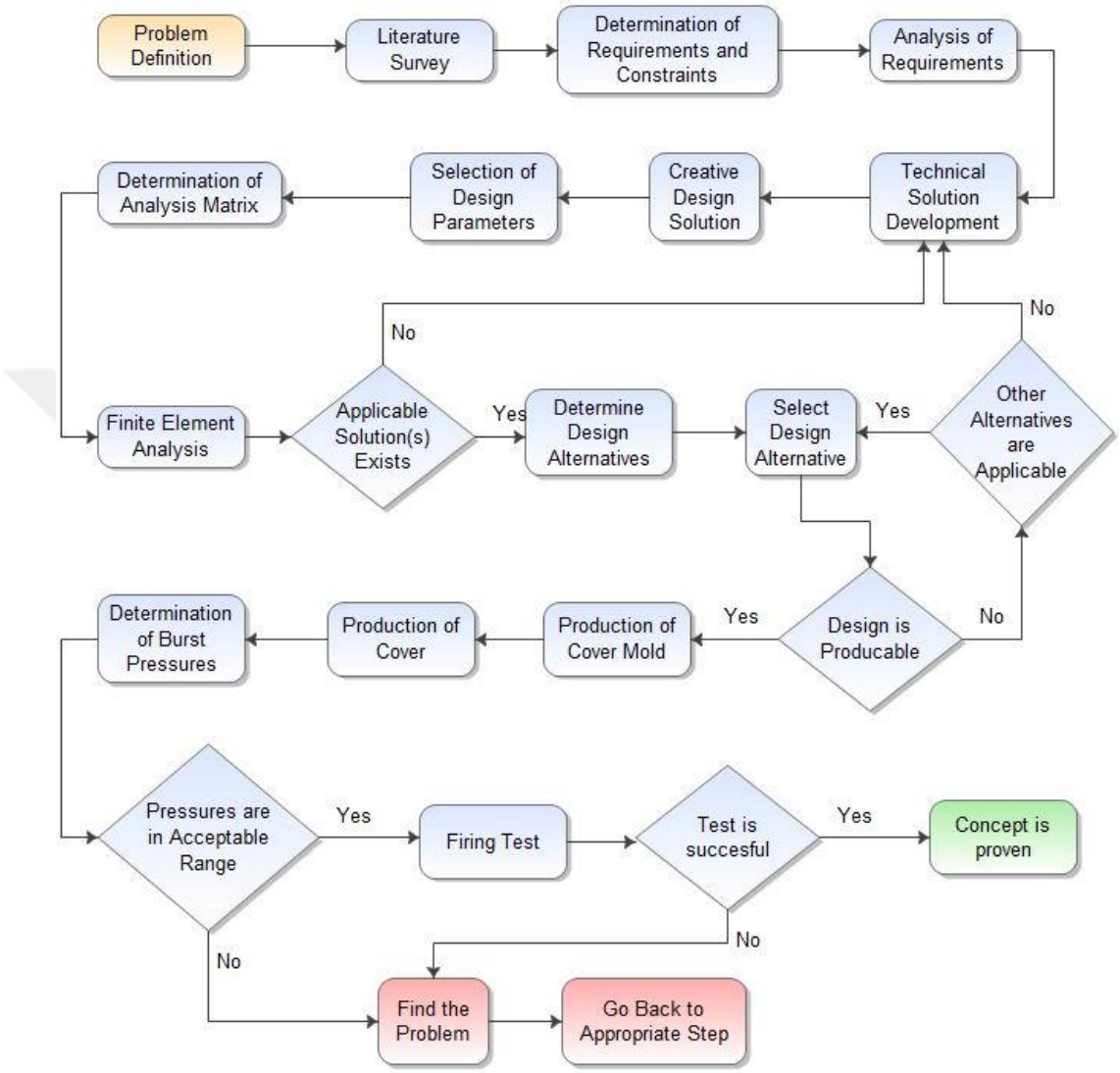

Figure 63: Flowchart of the Design Process

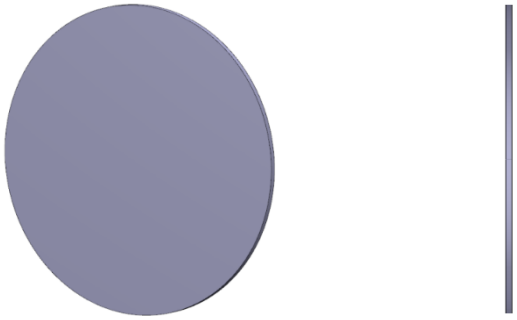

Figure 64: Illustration of the Design (Step-1)

2- In order to provide a certain pattern for controlled fracturing (Figure 65) the plate should have weak lines (or curves) having comparatively low strength. These weak lines should possess different material or different thickness. Therefore, dimensions of these weak lines are new parameters.

3- The cover should have dome-shaped protrusion geometry in order to be more resistant against pressure acting from outside due to the plume of the adjacent missile (Figure 66). The dome height becomes another parameter which is constrained by the length requirement of the launch tube.

4- Pyramid like segmented geometry helps fragmentation due to the discontinuity of the surface (Figure 67). The number of surfaces becomes a new parameter.

5- Increasing the number of surfaces (Figure 68) increases the number of parts which are fragmented after the fracture (burst). In addition, it decreases the size of the flange area (Figure 69). Flange area is important due to the limitation of the launch tube opening. The launch tube opening should be large enough for missile ejection. The number of surfaces is another parameter.

6- Spheroidiality distributes the load and increases the strength of the part (Figure 70). Therefore level of spheroidiality is one of the parameters.

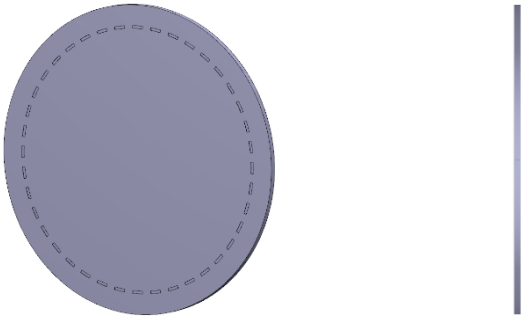

Figure 65: Illustration of the Design (Step-2)

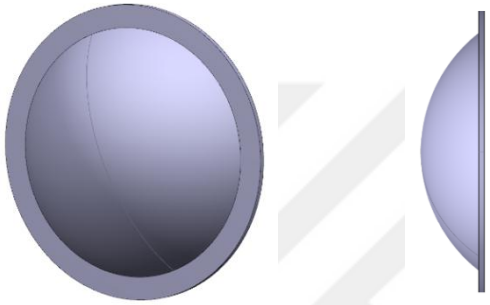

Figure 66: Illustration of the Design (Step-3)

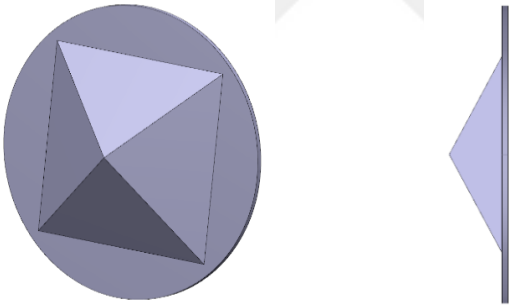

Figure 67: Illustration of the Design (Step-4)

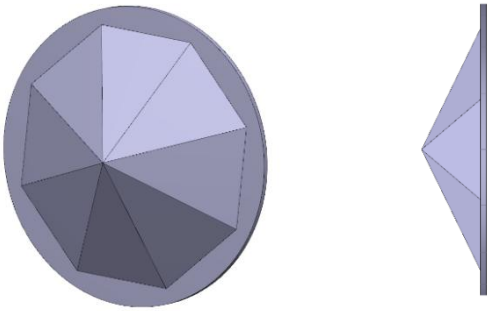

Figure 68: Illustration of the Design (Step-5)

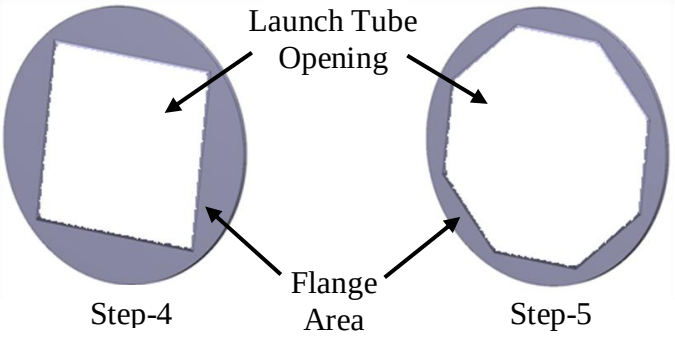

Figure 69: Explanation of Flange Area and Launch Tube Opening

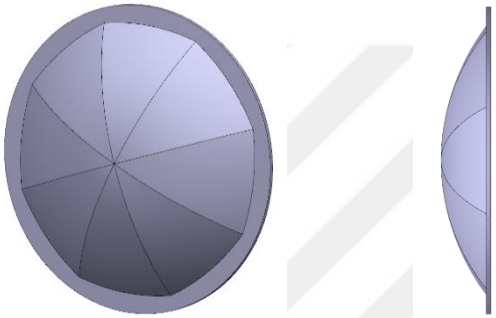

Figure 70: Illustration of the Design (Step-6)

7- A notch at the center creates stress intensity (Figure 71). It initiates the fracture at the center of the cover. Therefore, fragmentation and separation may occur due to high pressure created during firing. The suitable shape and size of the notch are determined by the depth and length of the notch.

8- In composite materials at least two different materials are used. Therefore, by arranging the material configuration it is possible to obtain zones with different mechanical behaviors. A typical stress-strain behavior of composite materials is seen on the left of Figure 72. As addressed here, the resin is the weaker element in terms of strength and if the stress exceeds a certain value it fails. When the resin and composite phase of the material is manufactured in separated sections, it can be said that the section made of only resin is the weakest one. When the force is applied, the coupon which is seen on the right side of Figure 72, fails at the resin section.

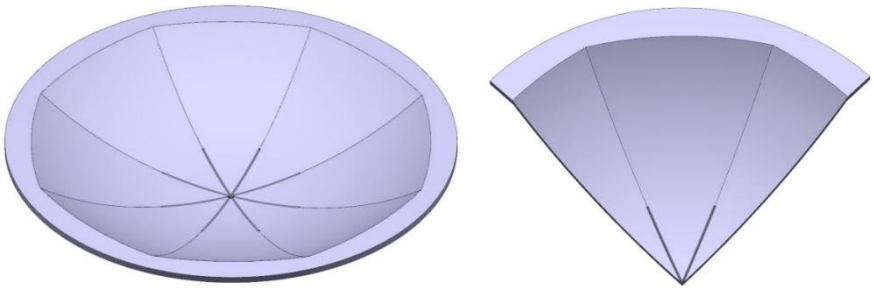

Figure 71: Illustration of Notch at the Center (Step-7)

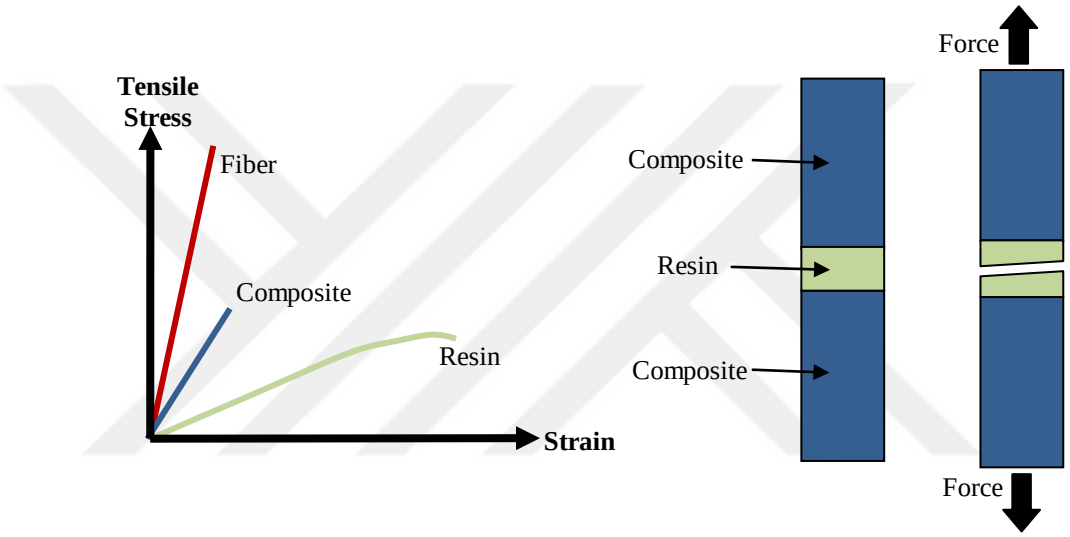

Figure 72: Mechanical Behavior of the Resin Section

When independent surfaces of the cover are manufactured by separated reinforcement fabric slices it is possible to create resin areas between fabrics. Therefore, resin areas coincide with the edge of the surfaces where stress is already concentrated due to the geometrical discontinuity. These resin corners and the notch at the center helps the cover to fragment when inner pressure applied. The line of resin areas is given on (Figure 73).

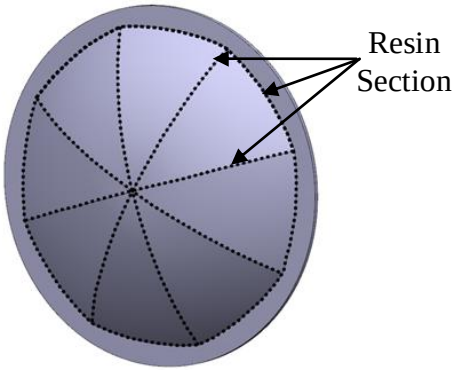

Figure 73: Illustration of the Resin Section (Step-8)

4.4 Detailed Design

In general, Detailed Design includes a series of decision-making process that uses related disciplines where necessary.

In Preliminary Design process a frangible cover design is explained with technological solution suggestions. Further, sizing of the design parameters will be conducted. Major parameters to be determined are:

- The height of the dome shape
- The thickness of the cover
- The depth and length of the notch
- Asymmetry of the cover

Investigation of these parameters and the sizing of the cover are explained in Chapter 5.

In Preliminary Design phase, a weak section is proposed by using resin area. In this way, frangible structure will be obtained. Proof of this concept is investigated with coupon level tensile tests. Photographs of test coupons are given in Figure 74.

Three different types of coupons are produced:

1. Fabrics are completely separated and the cavities between the fabrics are filled with only resin. (Figure 75)
2. Fabrics are separated but they have butt contact, and the thickness of the resin section is negligibly small. (Figure 75)
3. Fabrics are overlapped with each other and there is no resin section. (Figure 75)

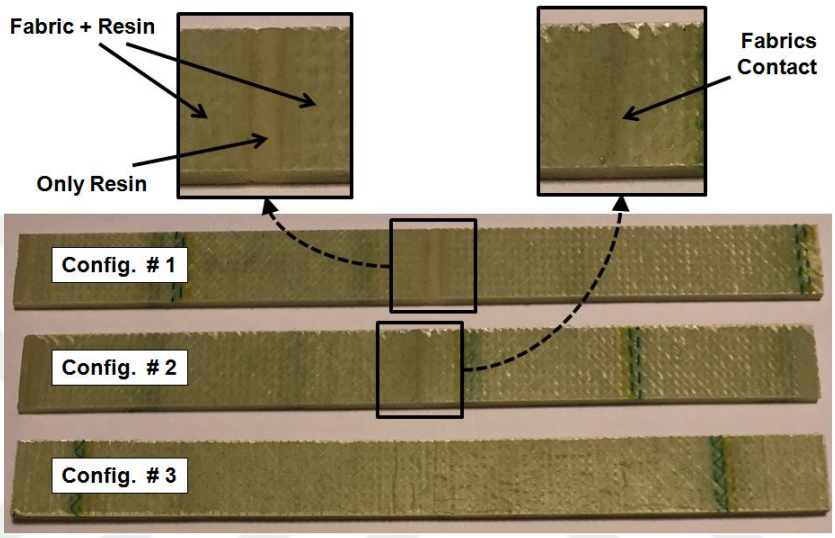

Figure 74: Photograph of Test Coupons

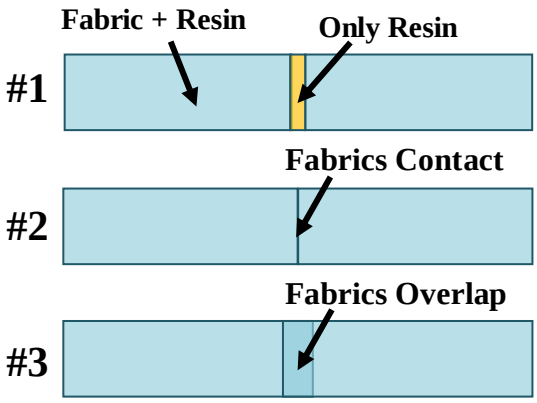

Figure 75: Test Coupon Configurations

Dimensions of test coupons are given in Figure 76. Failure modes differ in these coupons with the weak section. In the first one, in which fabrics are completely separated, the failure mode is the resin cracking. The one whose fabrics have butt

contact has a resin cracking and fiber pull-out type failure mode. In these specimens, tensile strength increases about 15%. The third one, which has overlapped fabrics, is approximately 3.5 times stronger than the first one. The failure mode is in the form of delamination and the failure is determined by interlaminar shear failure. Tensile test results are given in Table 9.

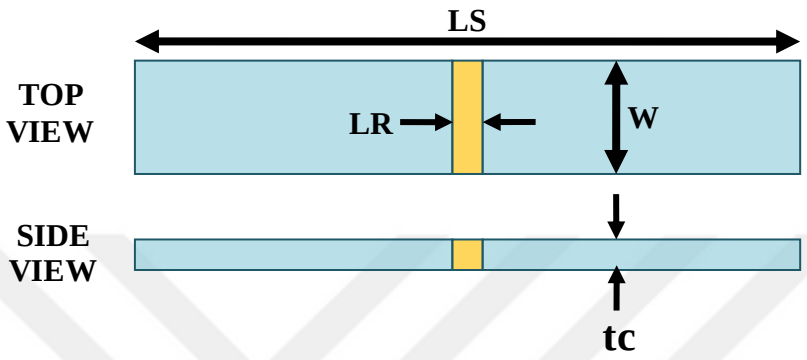

Figure 76: Test Coupon Dimensions

Table 9: Test Coupon Results ("-" Indicates Overlap)

	COUPON PARAMETERS					RESULTS		
Config.	Test No	LS (mm)	W (mm)	tc (mm)	LR (mm)	Load (kN)	Stress (MPa)	Mean Stress (MPa)
# 1 (Figure 75)	1.1	261	24.90	4.05	6.05	4.11	40.76	37.11
	1.2	254	25.10	3.90	3.90	3.55	36.27	
	1.3	257	25.20	4.05	3.50	3.59	35.18	
	1.4	262	25.12	3.95	5.05	3.14	31.65	
	1.5	255	25.15	4.05	3.50	4.20	41.23	
	1.6	260	24.90	4.05	5.50	3.84	38.08	
	1.7	256	25.10	4.05	3.70	3.72	36.59	
# 2 (Figure 75)	2.1	248	25.00	4.20	2.00	4.79	45.62	43.72
	2.2	250	24.95	4.20	2.00	5.11	48.76	
	2.3	249	24.50	4.25	2.00	4.51	43.31	
	2.4	247	25.00	4.20	2.00	4.31	41.05	
	2.5	252	25.10	4.15	2.00	5.00	48.00	
	2.6	251	25.10	4.20	2.00	4.60	43.63	
	2.7	247	25.10	4.00	2.00	3.58	35.66	
# 3 (Figure 75)	3.1	249	24.80	3.95	-	14.15	144.45	137.07
	3.2	249	24.70	4.10	-	14.35	141.70	
	3.3	249	24.70	4.00	-	13.50	136.64	
	3.4	249	24.70	3.95	-	11.10	113.77	
	3.5	249	24.40	4.00	-	14.36	147.13	
	3.6	25	24.40	4.00	-	13.54	138.73	

When the tensile test results given in Table 9 are investigated, they show that predetermined weak lines can be created by resin sections. However, the width of the resin section must be kept controlled.

Another requirement is the sealing of the launch tube. In order to satisfy this requirement, the cover should be gas-tight and a gasket should be used on the mounting interface.

In order to assemble the cover to the launch tube interface, bolts will be used on the mounting surface. Therefore, bolt holes should exist at the flange surface. Another issue that must be considered is the production of the cover. The geometry of the cover does not have any detail that prevents production.

This design approach is considered as an invention and utility model certificate is obtained. [59]

CHAPTER 5

NUMERICAL SIMULATION OF COVER

5.1 Description of the FEA Model

In this section details of the finite element analysis are given. Sizing of detailed design is conducted. Thus detailed design is finalized in this section. In the sizing process, configurations are compared and the configuration that ensures the requirements is selected. Therefore, the effect of the geometrical parameters is also referred in this section.

In order to conduct analysis, Abaqus 6.12-3 software is used. For small finite element model, a computer that has 2.27 GHz dual-core processor and 4 GB ram and another computer that has quad-core 3.60 GHz processor and 16 GB ram are used as workstation for models having larger numbers of elements.

A parametrical solid model is prepared in accordance with the detailed design described in Chapter-4. 1/2 and 1/16 of the solid model are used in analyses. When the pressure loads are assumed to be uniform, 1/16 model is used, since the model and the load condition is symmetrical and the smallest segment that carries all the details of the whole model. Similarly 1/2 model is also used when the pressure distribution is not uniform but symmetrical to the plane that divides the model in to two halves. This simplification is applied in order to reduce the processing cost of analyses. Views of the full model, ½ and 1/16 models are given in the Figure 77.

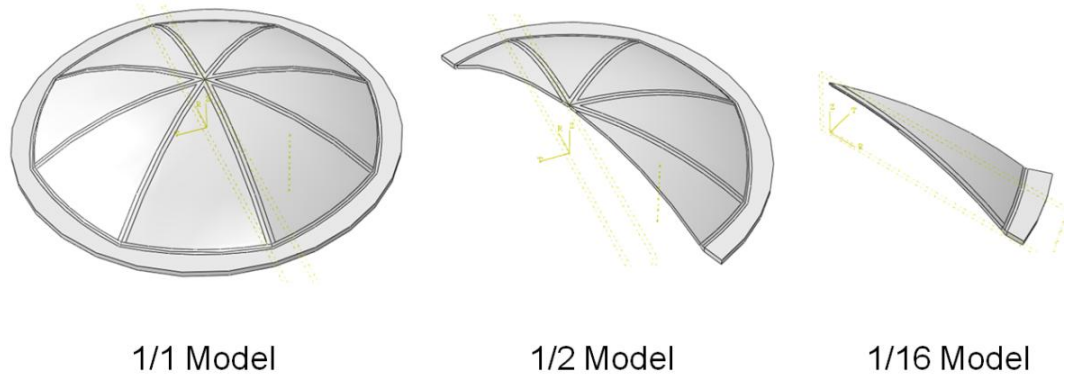

Figure 77: Views of 1/1, 1/2 and 1/16 Solid Models

Parameters that are examined in this section are: The height of the dome (DH), the thickness of the dome (DT), the height of the notch (NH), length of the notch (NL) and asymmetry of the cover (ASY). Asymmetry is defined as the distance between the center of the cover and center of the dome slices. Visual explanations of parameters are given in Figure 78. Values of the parameters that are used in the analysis matrix are given in Table 10.

The thickness of the flange section is arranged such that its thickness is higher than the thickness in the section of the dome. This difference is created in order to make the flange section of the cover stronger. Since the cover is fastened to the launch tube by bolts to provide airtight connection.

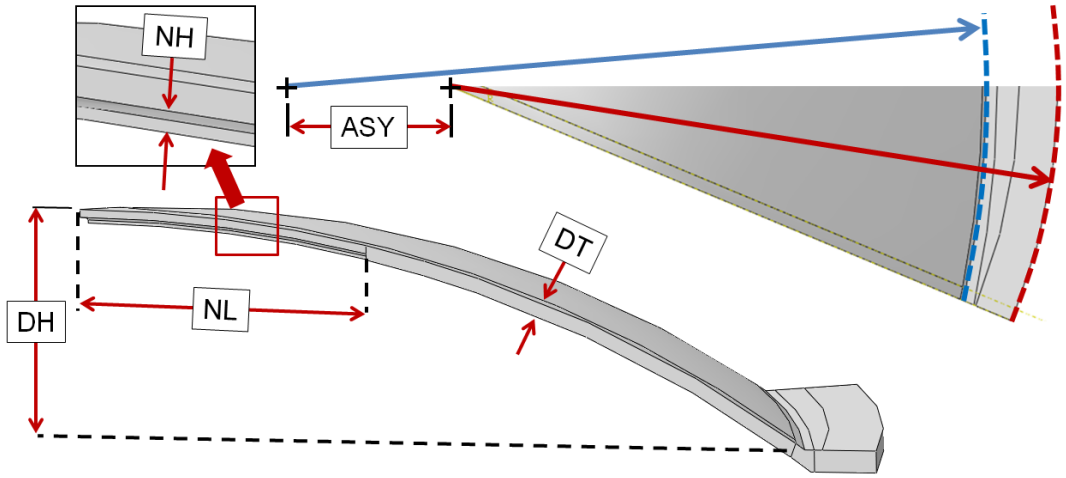

Figure 78: Explanation of Dimensional Parameters

Table 10: Parameters Used in the Model (DH: Dome Height, DT: Dome Thickness, FT: Flange Thickness, NH: Notch Height, NL: Notch Length, ASY: Asymmetry)

Model Number	DH	DT	FT	NH	NL	ASY	Control Parameter
1	50 d	11.25 d	12.5 d	5 d	225 d	375 d	DH
2	100 d	11.25 d	15 d	5 d	225 d	375 d	
3	150 d	11.25 d	17.5 d	5 d	225 d	375 d	
4	200 d	11.25 d	17.5 d	5 d	225 d	375 d	
5	250 d	11.25 d	17.5 d	5 d	225 d	375 d	
6	200 d	11.25 d	17.5 d	0	225 d	375 d	NH
7	200 d	11.25 d	17.5 d	2.5 d	225 d	375 d	
4	200 d	11.25 d	17.5 d	5 d	225 d	375 d	
8	200 d	11.25 d	17.5 d	7.5 d	225 d	375 d	
9	200 d	7.5 d	15 d	3.75 d	225 d	375 d	DT (DT/NH is constant)
10	200 d	10 d	17.5 d	5 d	225 d	375 d	
11	200 d	11.25 d	17.5 d	2.25 d	225 d	375 d	
12	200 d	12.5 d	18.75 d	5.625 d	225 d	375 d	
13	200 d	15 d	20 d	7.5 d	225 d	375 d	
14	200 d	11.25 d	17.5 d	5 d	0	375 d	NL
15	200 d	11.25 d	17.5 d	5 d	75 d	375 d	
16	200 d	11.25 d	17.5 d	5 d	150 d	375 d	
4	200 d	11.25 d	17.5 d	5 d	225 d	375 d	
17	200 d	11.25 d	17.5 d	5 d	300 d	375 d	
18	200 d	11.25 d	17.5 d	5 d	225 d	0	ASY
19	200 d	11.25 d	17.5 d	5 d	225 d	125 d	
20	200 d	11.25 d	17.5 d	5 d	225 d	250 d	
4	200 d	11.25 d	17.5 d	5 d	225 d	375 d	
21	200 d	11.25 d	17.5 d	5 d	225 d	500 d	

In order to obtain the mesh structure C3D8R (8-node brick element) and C3D10 (10-node tetrahedral element) type elements are used. Sizes of the elements are obtained after conducting the mesh sensitivity study. Effect of the element size to the maximum principal stress is given in the following graph (Figure 79). According to those results, 1 mm element size is enough for convergence of the analysis. 0.5 mm element size is selected at the zones where the stress level and

stress gradient is relatively high. The same mesh structure and element size is used in both 1/2 and 1/16 models of the cover

The intensity of the mesh structure is seen in Figure 80. Mesh intensity is higher at the section of the notch area and the edge of the dome section within resin section. 391184 Elements are used for 1/2 model (Figure 81) and about 95000 elements are used for 1/16 models.

In the Abaqus software quasi-static stress analysis is conducted. It is one of the simple analysis procedures that are used to examine the level of the load that causes failure or the zone where the failure occurs.

It is assumed that there is no inertial effect. Otherwise, static analysis cannot be conducted. Moreover, the material model is linear and does not have time-dependent material properties. It is also assumed that strains are small enough to neglect the nonlinear geometrical effects. Therefore, the large-displacement formulation is not used in analyses. By the help of this assumption, the analysis has a linear response. This makes the process to find the burst pressure easier. There is no contact in the model that causes non-linear boundary condition.

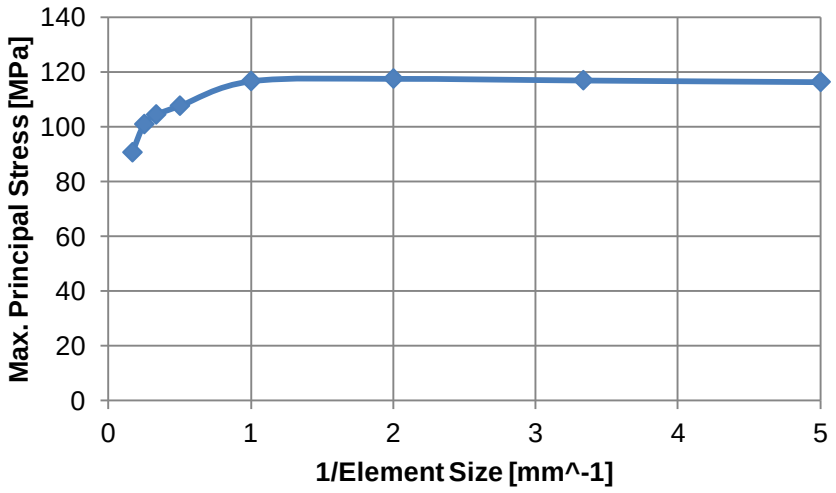

Figure 79: Mesh Sensitivity Study

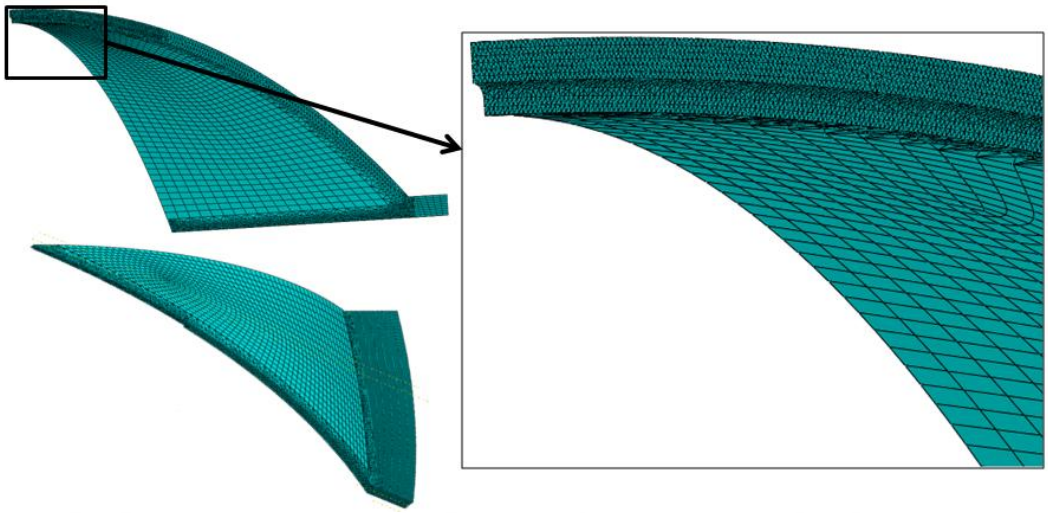

Figure 80: View of Mesh Structure on 1/16 Model

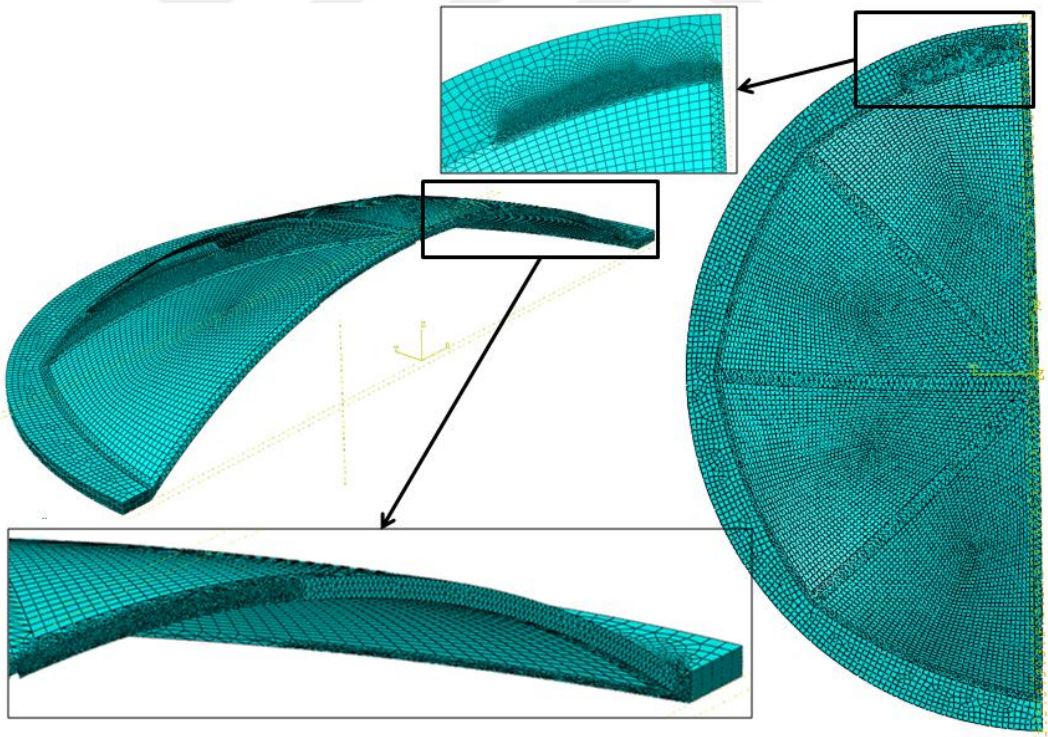

Figure 81: View of Mesh Structure on 1/2 Model

5.2 Material Properties

The cover contains two material phases:

1. Resin Section: Contains only epoxy resin

2. Fiber Reinforced Section: Contains epoxy resin and fiber reinforcement

These two sections have different mechanical (elastic modulus, Poisson's ratio and strength) properties. In order to determine the mechanical properties; material data sheets, literature information and coupon level tests are used. In order to obtain the properties of the resin section, a test is conducted in accordance with ASTM D 683. On the other hand, the properties of the reinforced section are obtained by conducting a test in accordance with ASTM D 3039.

Test coupons are produced for each test (Figure 82). In the tensile tests, Instron 5500 R tensile test machine is used. The strain is measured by 2663-821 Advanced Video Extensometer (Figure 83).

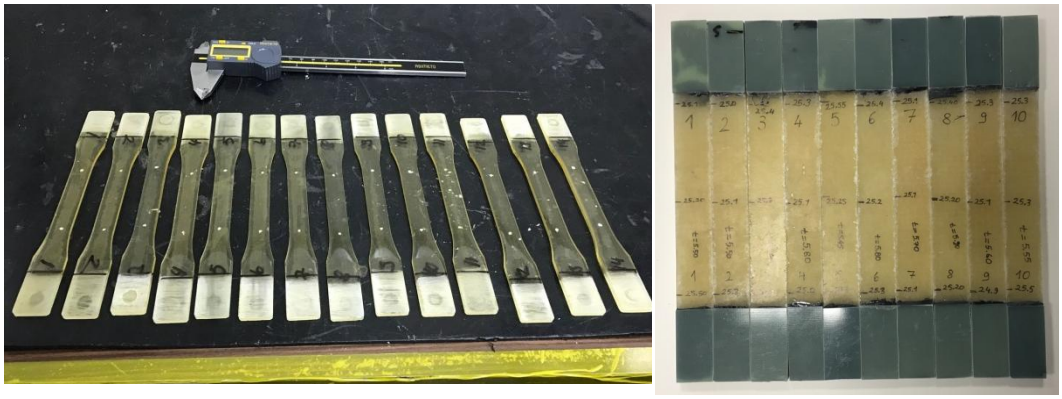

Figure 82: Photographs of Test Coupons

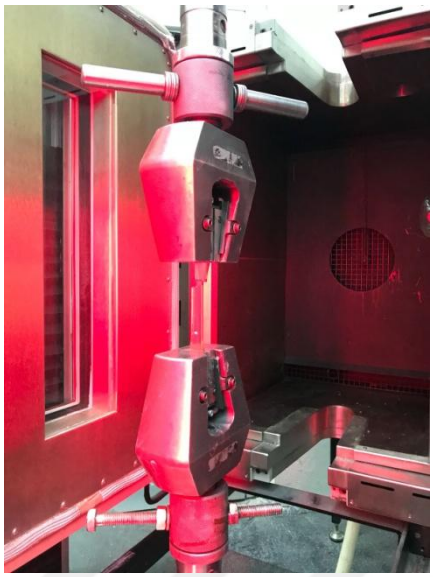

Figure 83: Photograph of Tensile Testing

The force at the jaw of the test machine and strain at the marking of the gauge section is recorded simultaneously until the failure of the specimen. This data and dimensions of the specimen are used to obtain the stress/strain graph. Then, modulus of elasticity and tensile strength of different materials are obtained.

The collected data cannot be interpreted to determine transverse strain. Therefore, Poisson's ratios cannot be obtained experimentally. For this reason, literature information is used for Poisson's ratio.

Results of the experiments are given in Tables 11 and 13. In Table 11 modulus of elasticity and tensile strength of resin section for each coupon is given. Moreover, comments about failure are stated. Similarly, Table 12 is prepared for reinforced section. Tensile strength is not used in this table since material failure will not be investigated in reinforced sections. Some of the specimens are failed at the outside of the gauge length. They are considered as premature failure and not taken into consideration. Stress concentration at the jaw section could be the reason for such failures. Such unsuccessful tests are indicated in the last column. The mean value of the applicable results is calculated and given in the last row.

Table 11: Tensile Test Results for Epoxy

Coupon Number	Modulus [MPa]	Tensile Strength [MPa]	Failure Location	Applicability
1	3325.55	34.01	Inside the jaw area	Nonapplicable
2	1162.17	31.33	Inside the jaw area	Nonapplicable
3	3138.01	82.70	Multiple locations	Applicable
4	3067.86	57.37	Inside the gauge length	Applicable
5	3162.13	69.32	Near the jaw	Nonapplicable
6	1219.39	32.82	Inside the gauge length (Crack exists before test)	Nonapplicable
7	3013.09	78.90	Multiple locations	Applicable
8	3304.57	45.59	Inside the gauge length	Applicable
9	3238.82	43.57	Applicable	Applicable
10	3145.50	54.45	Inside the gauge length	Applicable
11	3430.01	57.15	Near the jaw	Nonapplicable
12	3035.50	72.83	Inside the gauge length	Applicable
13	3139.53	76.20	Multiple locations	Applicable
14	3045.11	81.13	Multiple locations	Applicable
Mean	3125.33	65.86	(Nonapplicable values are neglected)	

Table 12: Tensile Test Results for FRP (Fiber Reinforced Plastic) Material

Coupon	Modulus [MPa]	Failure Location	Applicability
1	6485	Inside the gauge length	Applicable
2	5794	Inside the gauge length	Applicable
3	7325	Inside the gauge length	Applicable
4	5741	Outside the gauge length	Nonapplicable
5	6873	Outside the gauge length	Nonapplicable
6	7034	Outside the gauge length	Nonapplicable
7	5918	Outside the gauge length	Nonapplicable
8	5819	Inside the gauge length	Applicable
9	5561	Inside the gauge length	Applicable
10	6636	Inside the gauge length	Applicable
Mean	6270	(Nonapplicable values are neglected)	

Example of the premature failure is seen in Figure 84. Another observation that causes premature failure, in addition to the concentrated stress at the jaws, is micro bubble formation in the resin. In the production of the cover, precautions

will be taken in order to minimize the bubble formation. Degassing will be taken into account in order to eliminate bubbles during resin injection. In literature tensile strength of this epoxy resin is given as 75-85 MPa [60] Mean value of applicable test results is 66 MPa, which is relatively consistent when compared with literature data.

In the assessment of the finite element analysis, the compressive strength of the resin is also needed in order to determine the load that causes failure. In the literature, it is stated that the ratio of compressive strength to tensile strength of epoxies is approximately 2.2 when the average values are considered [61, 62]. Therefore, compressive strength is assumed to be 2.2 times the tensile strength. Similarly, Poisson's ratio is assumed as 0.375 for epoxy resin and 0.26 for the reinforced section by using the literature information [63, 64, 65, 66]. Material parameters obtained from coupon tests and literature are summarized in Tables 13 and 14. Approximately 10% difference exists between literature and experimental values. Experimental results will be used in analyses.

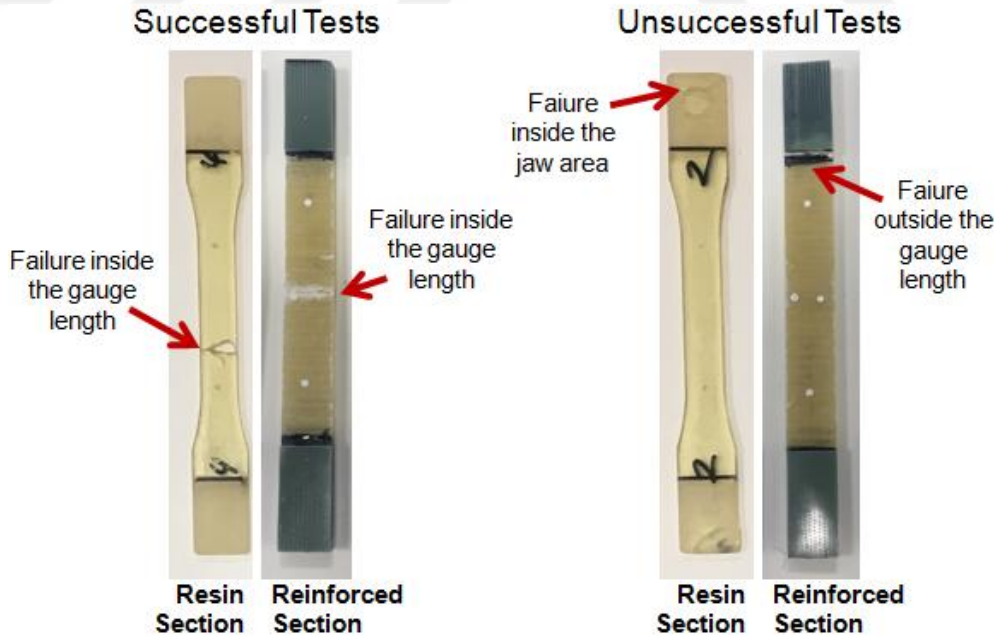

Figure 84: Photograph of Test Coupons After Testing (Left: Successful Tests, Right: Unsuccessful Tests)

Table 13: Mechanical Properties of Epoxy

	Experimental	Literature	
	Value	Value	Source
Elastic Modulus, E [MPa]	3125	3200-3800	[60]
Poisson's Ratio, υ	-	0.375	[63, 64, 65]
Tensile Strength, S_{UT} [MPa]	66	75 - 85	[60]
Compressive Strength, S_{UC} [MPa]	-	145 (S_{UT} * 2.2)	[61, 62]

Table 14: Mechanical Properties of FRP

	Experiment	Literature	
	Value	Value	Source
Elastic Modulus, E [MPa]	6270	-	-
Poisson's Ratio, υ	-	0.26	[66]

5.3 Boundary Conditions and Loads

In the previous sections, finite element model is described. In this section, the definition of loads and boundary conditions are explained.

Basically, there are two loading conditions which are going to be considered. They are inner and outer loading conditions. At the real working condition, the cover is exposed to inner loading which is due to uniform distribution of the inside pressure and a load due to non-uniform distribution of the pressure acting on the outer surface of the cover. In addition to pressure, the cover is also exposed to high-temperature effect of the exhaust products of the solid engine. There are aluminum particles in exhaust products which create abrasive effects.

In analyses, 3 loading conditions are taken into account. They are due to uniform inner pressure, non-uniform outer pressure and uniform outer pressure as seen in Figure 85.

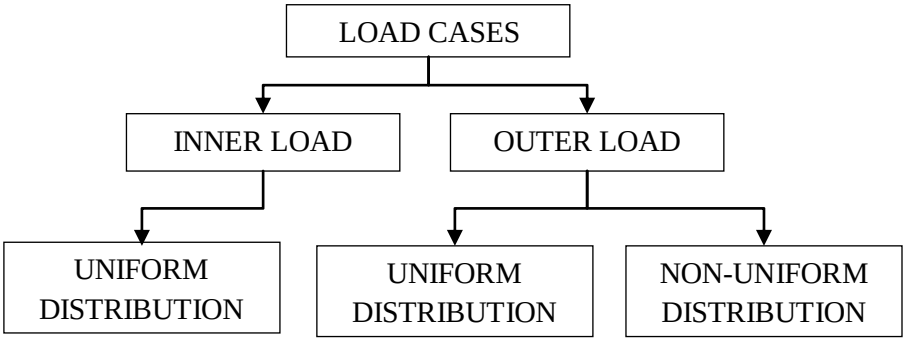

Figure 85: Diagram of Load Cases

Although non-uniform pressure distribution is the only loading scenario for outer surface, the uniform outer pressure distribution is also examined. It is due to the fact that, non-uniform pressure distribution cannot be applied at the burst tests. In the burst tests, only uniform pressure distribution can be applied to inner and outer surfaces. Uniform pressure distribution is taken into consideration, in order to compare the test results with the analysis results.

Analyses are linearly modeled as explained previously. In this way, stress values corresponding to any load level can be found by using linear relations between load and stress. Moreover, burst pressures can be determined easily with this linear ratio. In order to obtain load-stress relation, 5 P pressure is applied and corresponding stress values are investigated. Comparison of inner and outer burst pressures becomes possible by using this approach. Inner and outer surfaces used to define pressure are given in Figure 86.

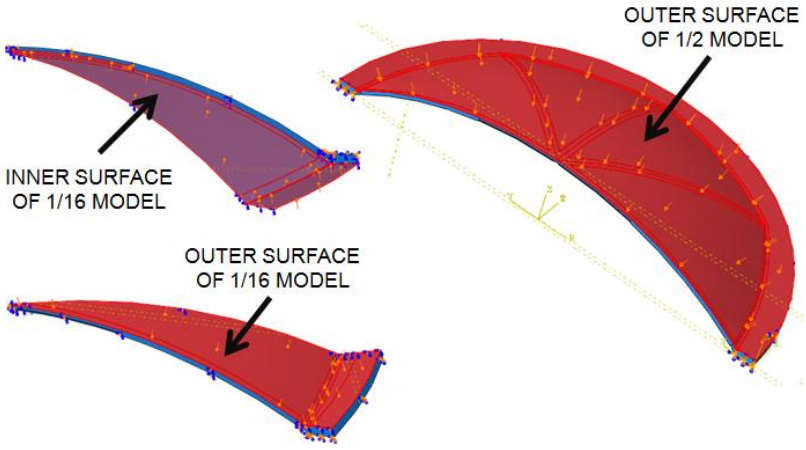

Figure 86: Views of Inner and Outer Surfaces of the Model

Application of non-uniform pressure is a different case. In this case, 1/2 model needed to be used instead of 1/16.

In CFD software pressure distribution is found for various instants. Instants which have higher pressures are previously determined. Instants when the distance between the cover and engine nozzle is 5 L and 18 L, are chosen to obtain pressure profile. Axial forces have maximum value at those instants (Figure 54). As seen in Figure 54, effective area due to the pressure expands with increasing distance between engine nozzle and the cover. Similarly, high-pressure zone is more localized for 5 L distance when compared with 18 L (Figure 87).

Asymmetry on the surface of the cover that creates umbrella like detailed cover geometry is neglected in CFD software. Instead, a simple dome shape is used in CFD analysis. Therefore, the solid model in CFD software is different than the model used in Abaqus software. For this reason, it is not possible to map the pressure profile onto the model used in Abaqus. Analytical approach is used to define the pressure profile corresponding to non-uniform pressure distribution. Continuous function of two variables (X and Y coordinates) is adapted to pressure profile which is obtained from FloEFD software.

Surface fitting is used in order to define the function of the pressure profile. First of all, pressure and coordinate information of the point cloud of the surface is exported from CFD software and 3-D scatter plot is obtained as seen in Figure 88. In this figure, Z-axis corresponds to pressure value; X and Y axes correspond to the X and Y coordinates as given in Figure 87 and Figure 91.

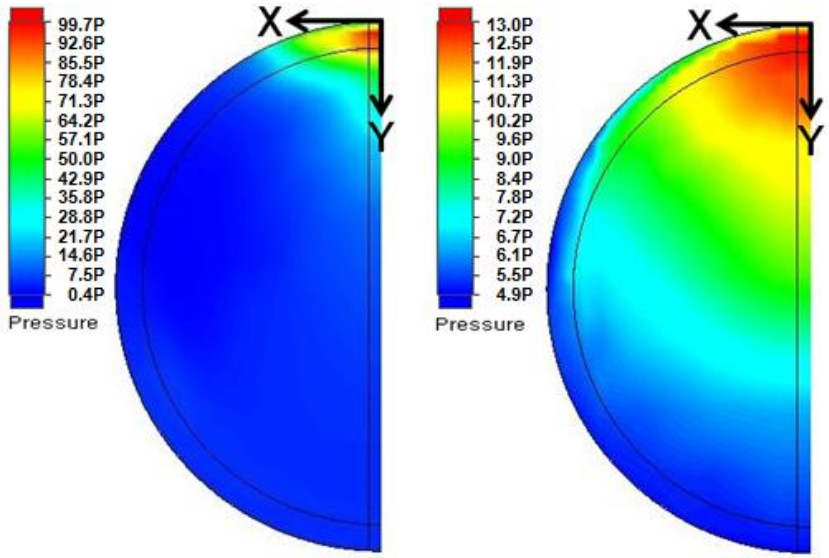

Figure 87: Pressure Distribution Obtained from FloEFD (Left: 5 L Instant, Right 18 L Instant)

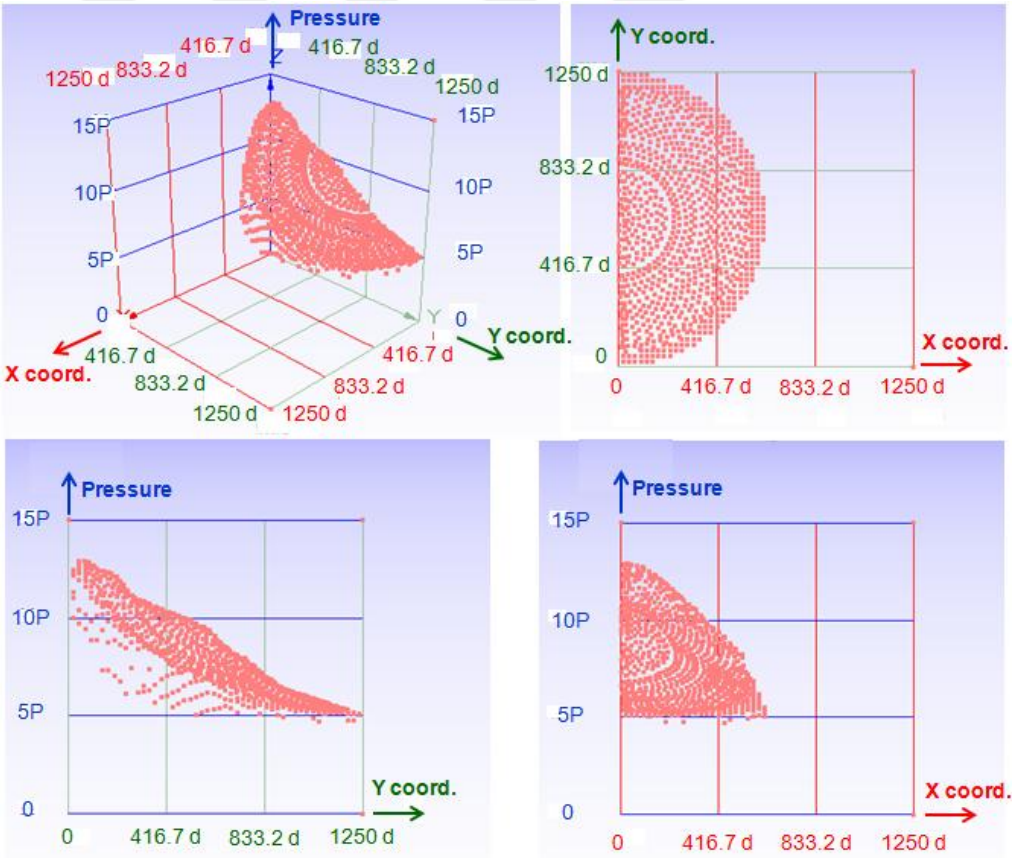

Figure 88: Isometric and Perpendicular Views of 3-D Scatter Plot of Pressure Distribution Obtained from FloEFD at 5 L Instant

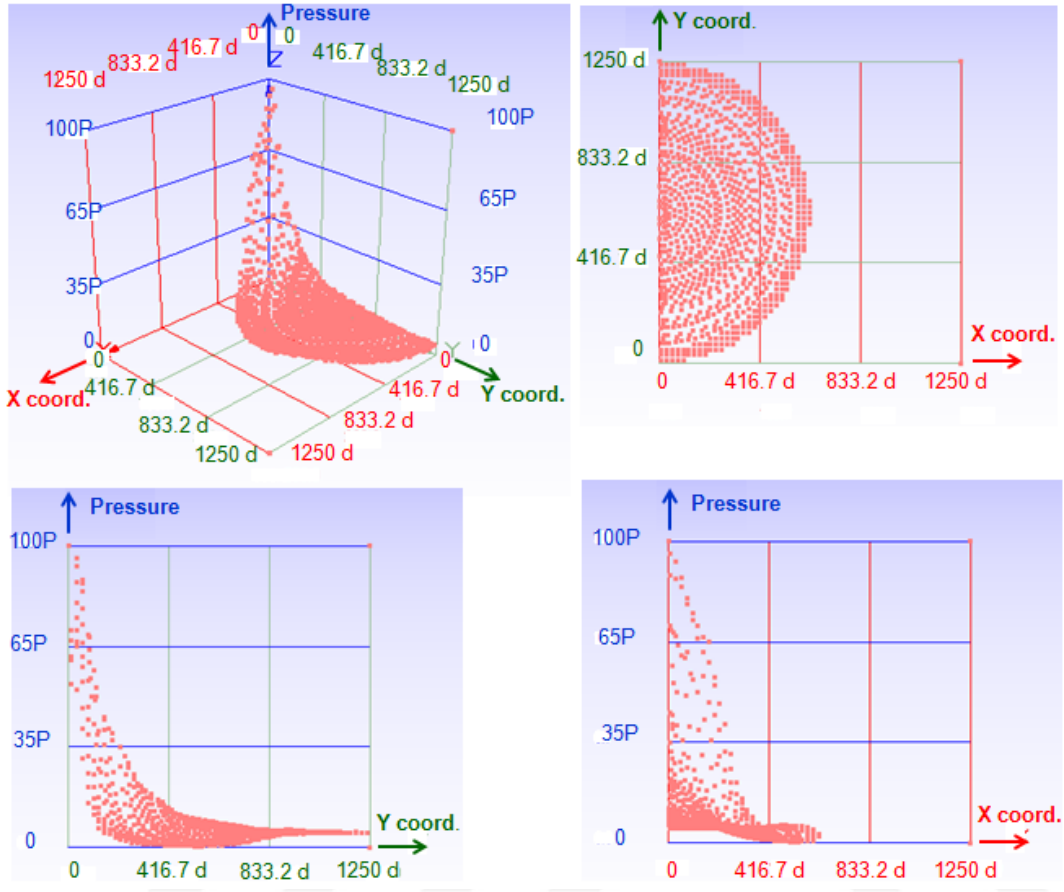

Figure 89: Isometric and Perpendicular Views of 3-D Scatter Plot of Pressure Distribution Obtained from FloEFD at 18 L Instant

Surface fitting functions are obtained by using ThreeDify XLGrapher (Excel Add-on) software. From its equation library; best possible equation family and its constants are chosen with the software by using the lowest sum of squared absolute error. Surface fitted points and the data points are compared at Figure 90.

Surface fit equations for pressure distributions at 5 L (P_1) and 18 L (P_2) distances are given in Equation 1 and 2. The output of these equations is absolute pressures [MPa] at corresponding coordinate.

$$P_1(X,Y) = \frac{4*a*b^2}{\left(1+4*b^2*(X^2+Y^2)\right)^2} + c \qquad (1)$$

where a, b, and c are numerical parameters and they are not given due to confidentiality.

$$P_2(X,Y) = e^{\frac{-a}{X+b}} * e^{-c*Y} \qquad (2)$$

where a, b, and c are numerical parameters and they are not given due to confidentiality.

Contour plot of these equations in Abaqus and axis definitions are given in Figure 91.

In addition to nonuniform outer pressure, uniform 0.101325 MPa inner pressure (atmosphere) is defined in the model.

Boundary conditions are also defined in software. The inner surface of the flange section is defined as encastre (Figure 92) for outer pressure loading condition. Similarly, the area corresponds to contact surface of the outer metal ring is defined as encastre for inner pressure loading condition.

In order to define the model as repeating element of the whole model, symmetry boundary condition is used. Symmetry surfaces are defined as seen in Figure 93.

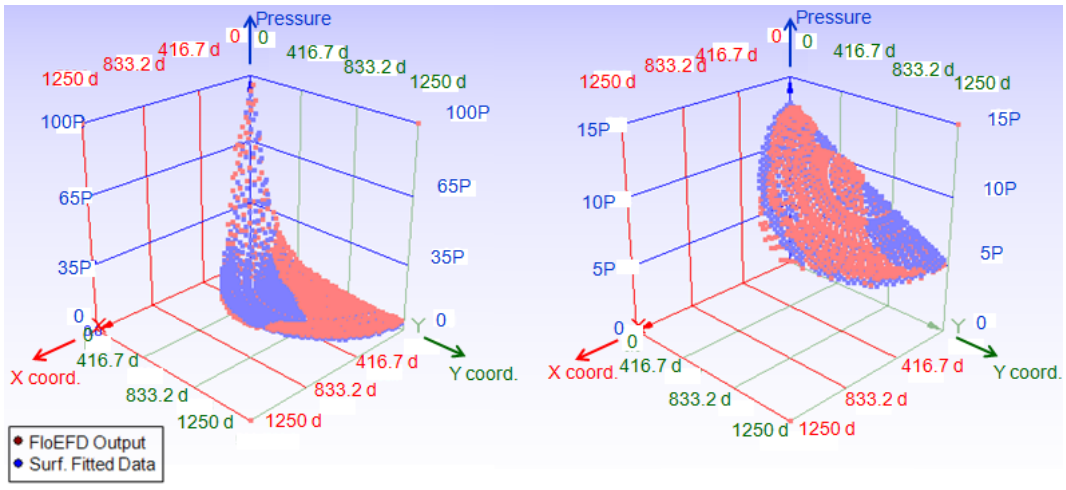

Figure 90: 3-D Scatter Plot of Pressure Distribution Obtained From FloEFD and Data Obtained with Surface Fitting (Left: 5 L Instant, Right 18 L Instant)

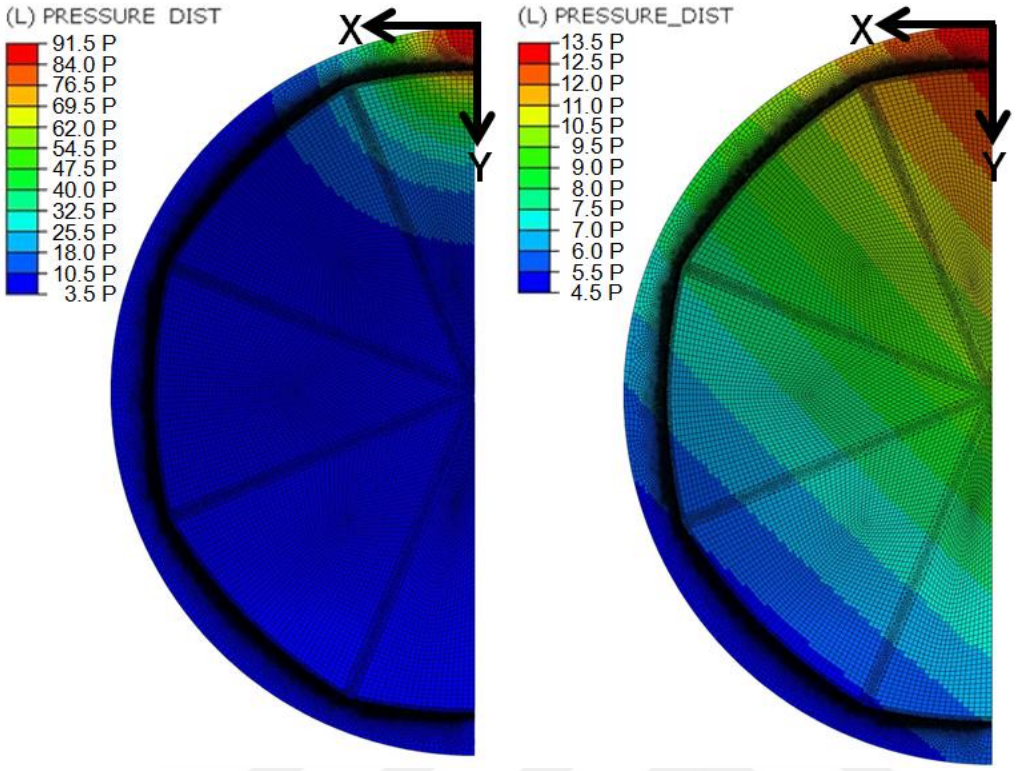

Figure 91: Contour Plot of Pressure Profiles Defined in Abaqus (Left: 5 L Instant, Right: 18 L Instant)

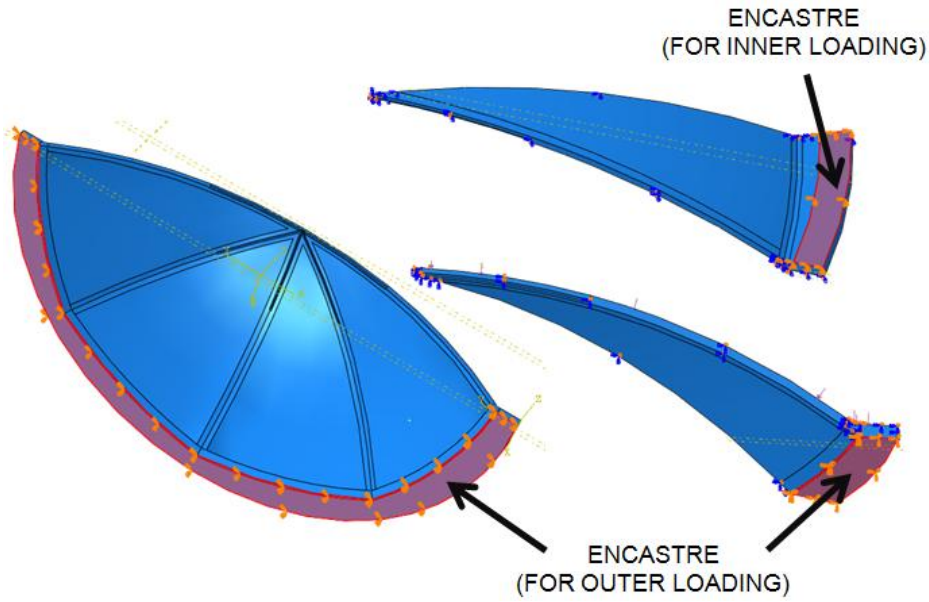

Figure 92: View of the Surfaces with Encastre Definition

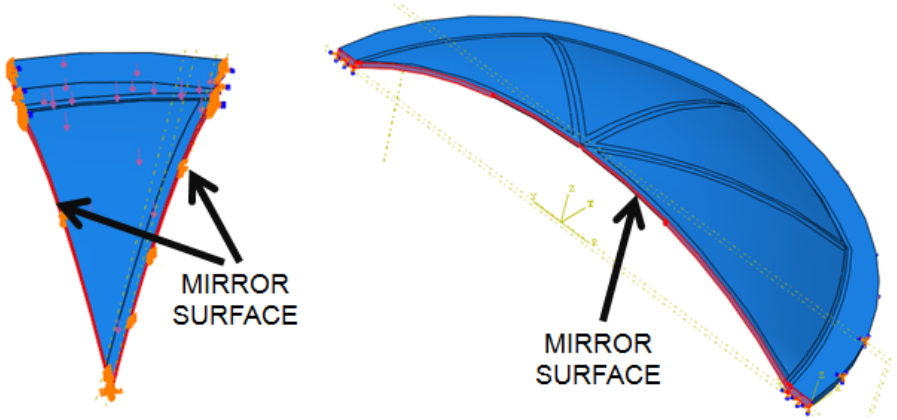

Figure 93: View of Surfaces with Mirror Boundary Condition Definition

In analyses, holes at the flange surface are not modeled. Effects of these holes are neglected. Pre-stress caused by tightening of the bolts is neglected. It is assumed that the surface of the cover is bonded without sliding. Similarly, the metal ring which is fixed at the outer surface of the flange is assumed to be rigid.

5.4 Results and Configuration Selection

Review and interpretation of analyses are referred in this section. Stress distributions and deflections are analyzed and corresponding burst pressures are examined. Moreover, effects of different parameters are investigated according to the analysis matrix. Results corresponding to all parameters are compared and applicable values are chosen for each parameter. Therefore, sizing of the cover is provided in this section.

5 P pressure is applied for each configuration and stress state is investigated. 5 P value is used only as a reference. Pressure value corresponding to critical stress level is calculated by the help of linear relationship between load and stress state. Therefore, burst pressure is able to be determined in this way. This procedure is applied to all models and burst pressures are obtained for each configuration.

Graph of maximum and minimum principal stresses of a typical analysis for one load condition is given in Figure 94. Linear load-stress relationship is also seen in the graph.

In addition to the stress state, a failure criterion is also needed to determine the burst pressure. When the stress state satisfies failure condition, corresponding pressure level is considered as burst pressure.

In this cover design, the weak sections are created by using weak material at predetermined lines. Failure occurs at these predetermined sections and the material in that section is epoxy.

When the cover bursts, fragments should separate away from flying path of the missile in order to prevent interaction. It is assumed that best possible separation is obtained when the fracture is started at the center of the cover. If the fracture is started at the corner section of the cover, fragments can stay in the flight path. For this reason, numerical simulations are used to determine not only failure load but also failure location. Dome and corner of the cover are shown in Figure 95.

Contour plots of maximum and minimum principal stresses when 5 P inner and outer pressure is applied are given in Figures 96 - 99 for model 4.

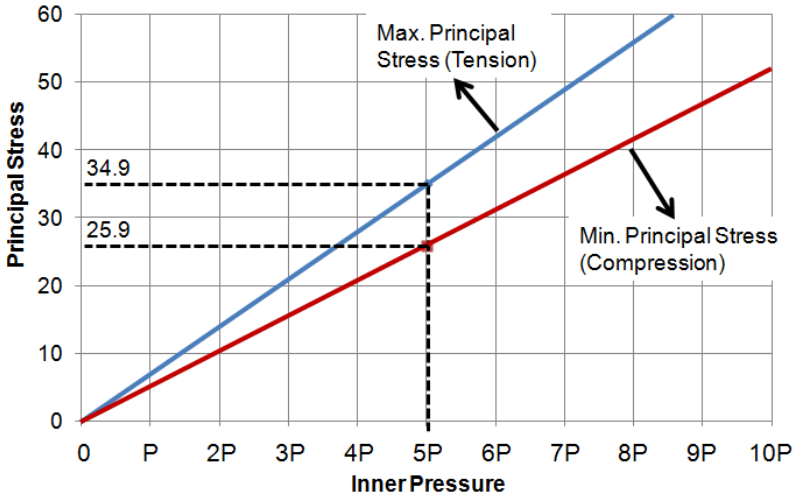

Figure 94: Graph of Inner Pressure vs Principal Stress for Model 4

When the inner pressure is applied tensile stress occurs at the inner section of the notch area (Resin at Dome). On the other hand, compressive stress is observed at the resin at corner. When the inner pressure is applied, the cover expands and the corresponding deformation induces compressive stress at the upper side of the resin at corner. Groove of each notch is merged together at the apex of the cover. The thickness of the cover in the apex zone is therefore constant. For that reason the stress concentration effect is not present in the apex zone. For this reason, the stress in the apex zone is not higher than the stresses in the notch section where the maximum stress occurs. As a result of this, the fracture starts at notch section and proceed towards the apex and flange side simultaneously causing fragmentation of the cover.

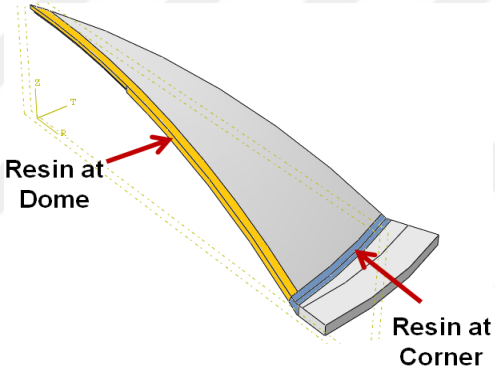

Figure 95: Schematic Explanation of Dome and Corner Locations

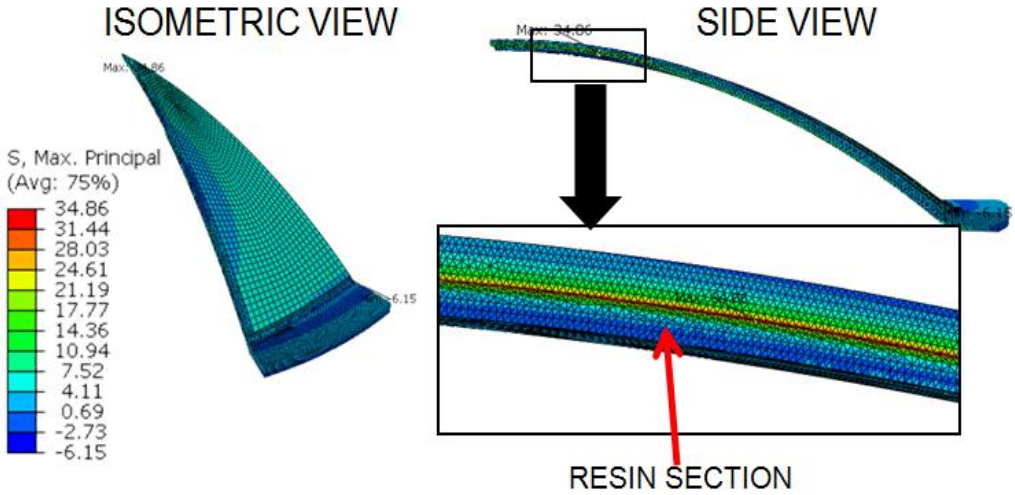

Figure 96: Contour Plot of Maximum Principal Stress When 5 P Inner Pressure is Applied to Model 4

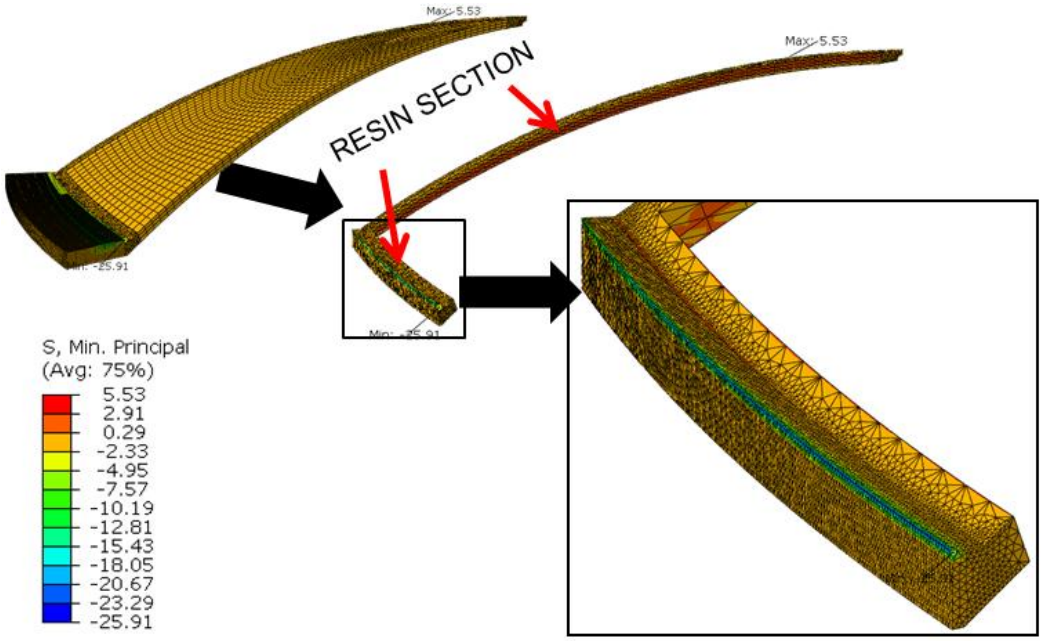

Figure 97: Contour Plot of Minimum Principal Stress When 5 P Inner Pressure is Applied to Model 4

When the outer pressure is applied, compressive stress is induced at the inner section of the notch. Moreover, tensile stress occurs at the interface between the outer surface of the cover and the flange part of the cover.

Displacements of the same configuration for 5 P inner and outer pressures are given in Figure 100.

Von-Mises which is the most widely used failure criteria is not applicable in this failure analysis since it is valid for ductile materials. On the other hand, epoxy resin is a kind of glassy material and its failure behavior is brittle. In the material tests its brittle failure is observed (Failure strain, $\varepsilon_f < 0.05$).

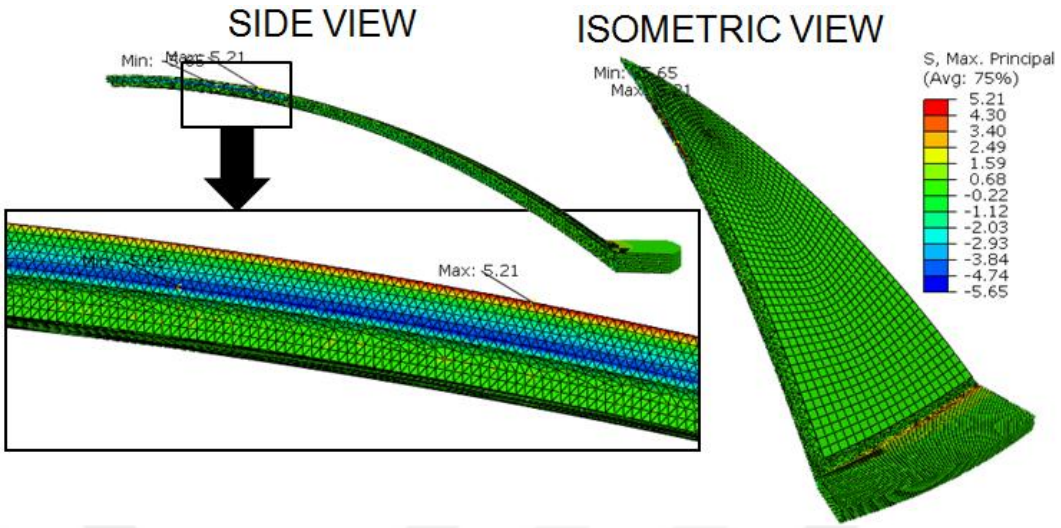

Figure 98: Contour Plot of Maximum Principal Stress When 5 P Outer Pressure is Applied to Model 4

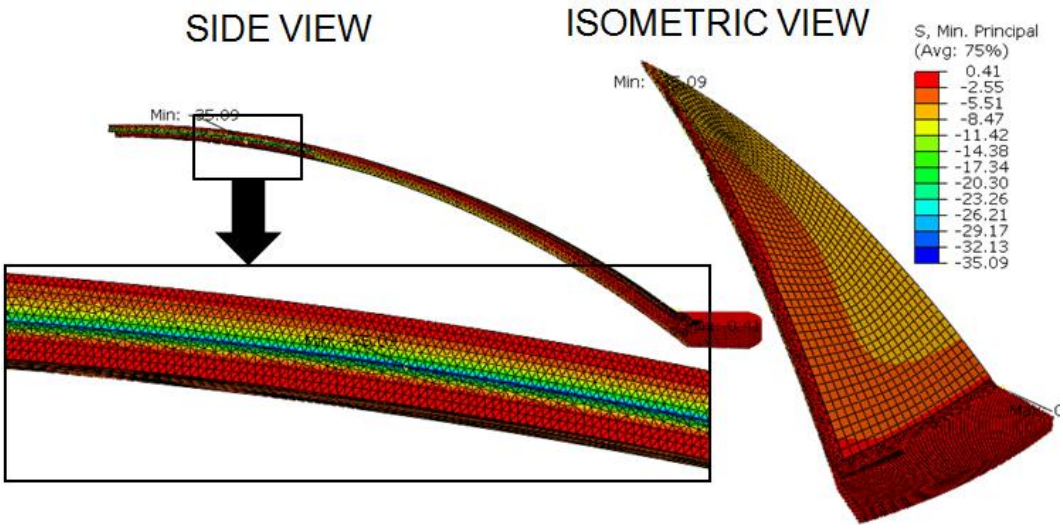

Figure 99: Contour Plot of Minimum Principal Stress When 5 P Outer Pressure is Applied to Model 4

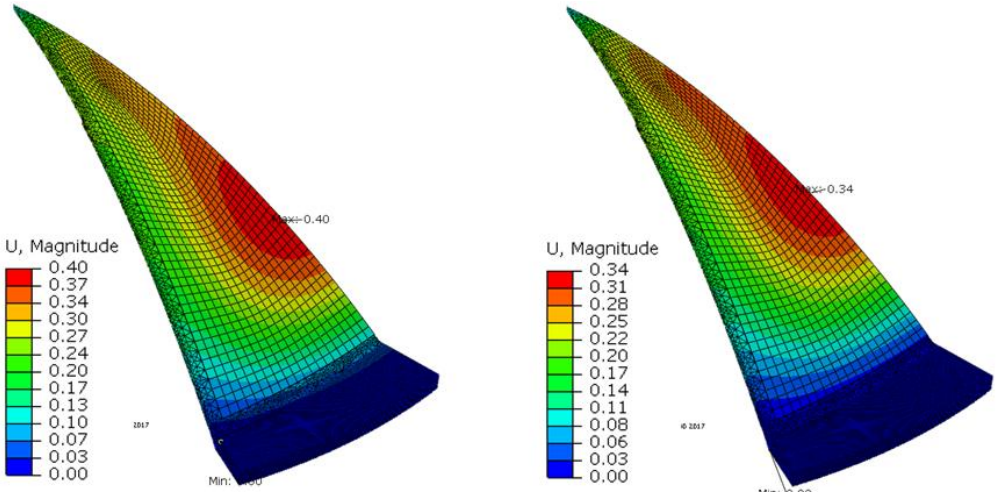

Figure 100: Contour Plot of Displacement for 5 P Inner (Left) and Outer (Right) Pressures (Values are in [mm] unit)

Modified Mohr Theory (MMT) is used as failure criteria for resin section. It is used for brittle materials and it has better agreement with experiments than Coulomb-Mohr Theory. Its graphical representation is given in Figure 101.

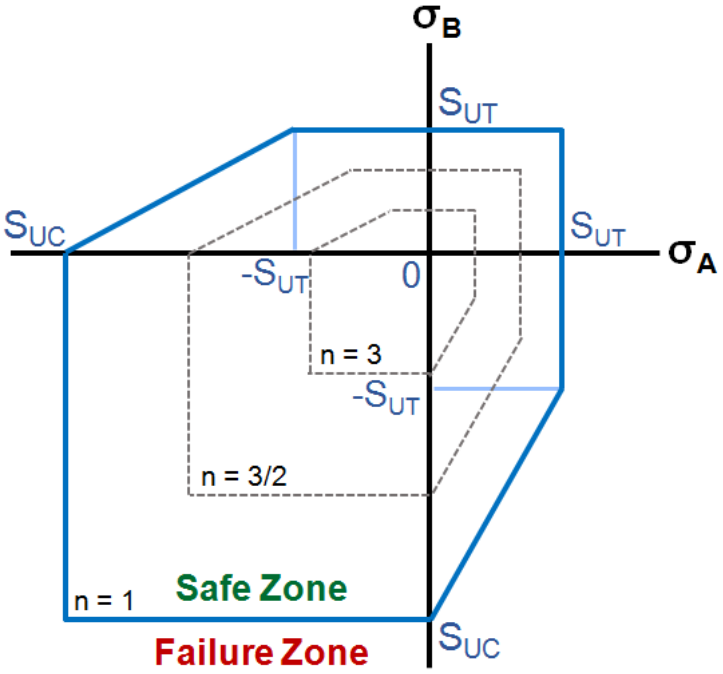

Figure 101: Graphical Representation of Modified Mohr Theory

Quadrant conditions and corresponding failure criterion are given in Equation 3.

Quadrant Condition:	Failure Criteria:	
$\sigma_A \geq \sigma_B \geq 0$	$\sigma_A = \frac{S_{UT}}{n}$	(3.a)
$\sigma_A \geq 0 \geq \sigma_B$ and $\lvert\frac{\sigma_B}{\sigma_A}\rvert \leq 1$	$\sigma_A = \frac{S_{UT}}{n}$	(3.b)
$\sigma_A \geq 0 \geq \sigma_B$ and $\lvert\frac{\sigma_B}{\sigma_A}\rvert > 1$	$\frac{(S_{UC} - S_{UT})\sigma_A}{S_{UC}S_{UT}} - \frac{\sigma_B}{S_{UC}} = \frac{1}{n}$	(3.c)
$0 \geq \sigma_A \geq \sigma_B$	$\sigma_B = -\frac{S_{UC}}{n}$	(3.d)

Stress condition which makes n equal to 1 is the failure condition and corresponding load (pressure) gives burst pressure. Linear relationship between load and stress is previously mentioned. Therefore the load which is equal to burst pressure can be easily calculated by the same way. First of all, quadrant condition is determined then the necessary equation is selected. In order to determine the quadrant conditions, maximum and minimum principal stresses (σ_A and σ_B) of each element are determined. By using scatter plot of σ_A and σ_B critical quadrant is graphically examined.

The plot of model 1 is given in Figure 102. In this figure principal stress state of each element is given according to loading condition (inner or outer) and location of the element (dome or corner). In addition, failure envelope of Modified Mohr Theory is also plotted. As seen from the figure; for 5 P inner pressure failure occurs at the dome and tensile failure is observed (bottom left corner of Figure 102). It can be concluded that failure stress (σ_A) for inner pressure can be calculated by using Eq. 3.a. Moreover, when the outer pressure is 5 P, the cover does not fail. If the pressure is increased up to failure, compressive failure will be observed (top right and bottom right corner of the figure). Thus, failure stress (σ_B) can be calculated by using Eq. 3.d.

Maximum principal stress (σ_A) in model 1 is 123.1 MPa for 5 P inner pressure. When σ_A and S_{UT} are substituted into Eq. 3.a, n is calculated.

$$\sigma_A = \frac{S_{UT}}{n} \rightarrow n = \frac{S_{UT}}{\sigma_A} = \frac{66\ MPa}{123.1\ MPa} = 0.536 \quad (4)$$

n is equal to the ratio of failure stress to the applied stress (5 P). Therefore, burst pressure (P_{Burst}) is calculated as given in Eq. 5.

$$n = \frac{P_{Burst}}{P_{Applied}} = \frac{P_{Burst}}{5\ P} \rightarrow P_{Burst} = n * (5\ P) \quad (5)$$

when n = 0.536 is substituted into Eq. 5; corresponding inner burst pressure is calculated as given in Eq. 6:

$$P_{Burst} = 0.536 * (5\ P) \cong 2.7\ P \quad (6)$$

Outer burst pressure can be calculated in the same way. Different than inner burst pressure calculation Eq. 3.d is used instead of Eq. 3.a. When σ_B (122.2 MPa) and S_{UC} (145 MPa) is substituted into equation 3.d, n is calculated. Since 122.2 MPa is compressive stress, it is substituted as negative.

$$\sigma_B = -\frac{S_{UC}}{n} \rightarrow n = -\frac{S_{UC}}{\sigma_B} = -\frac{145\ MPa}{-122.2\ MPa} = 1.187 \quad (7)$$

P_{Burst} is calculated similarly by substituting n into Eq. 5.

$$P_{Burst} = n * (5\ P) = 1.187 * (5\ P) \cong 5.95\ P \quad (8)$$

The similar approach is applied for inner and outer loading conditions for all configurations. Results are compared in order to gather information about the effects of the parameters. Change of inner and outer burst pressures with respect to dome height (DH), dome thickness (DT), notch height (NH), notch length(NL) and asymmetry (ASY) are given in the Figures 103-107. After investigating the effects of these parameters, a selection of an appropriate configuration is conducted.

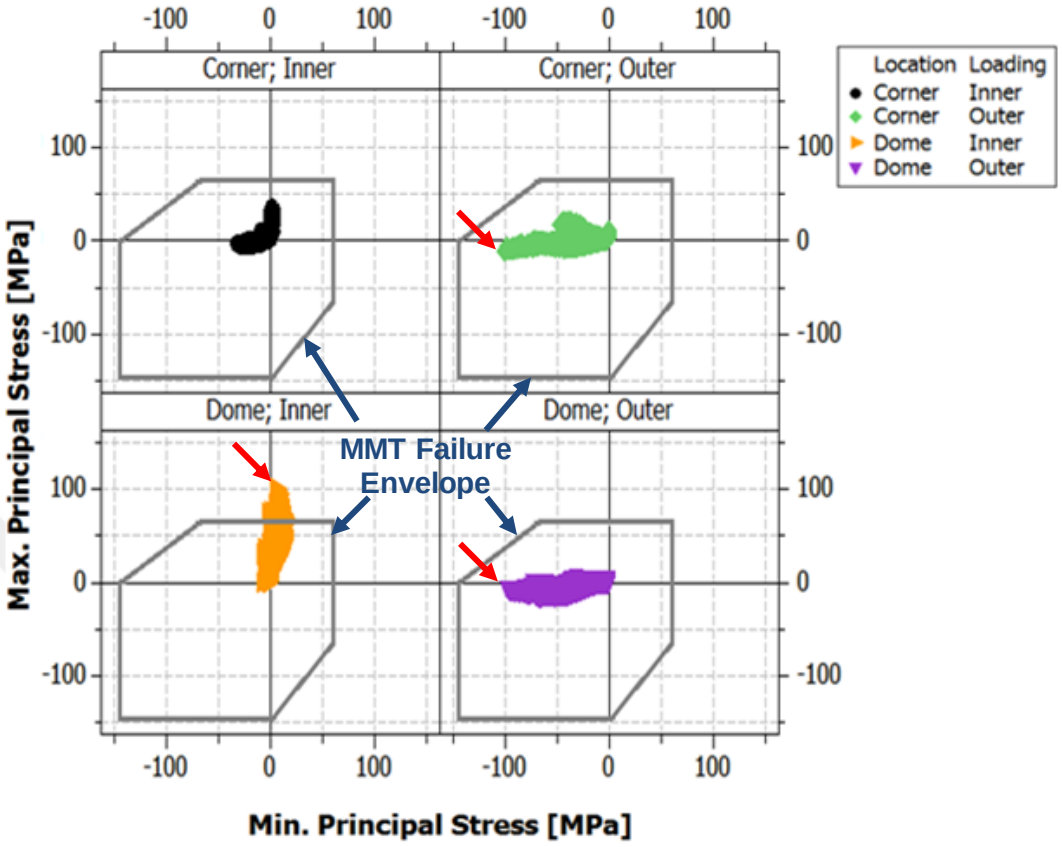

Figure 102: Scatter Plot of Max. and Min. Principal Stresses when 5 P Inner and Outer Pressure is Applied to Model 1

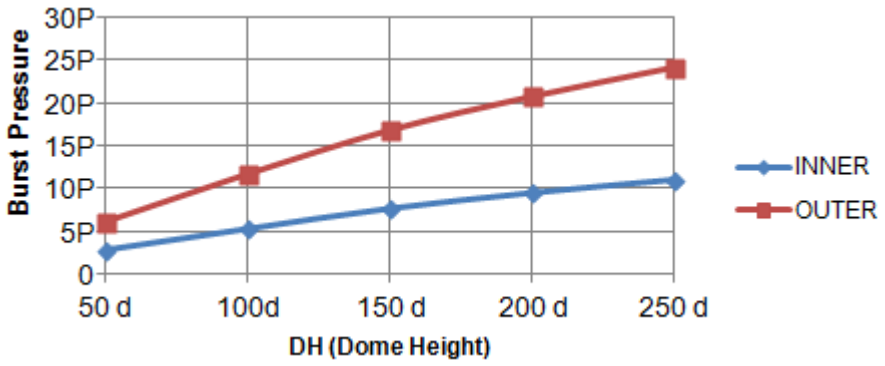

Figure 103: Burst Pressure vs Dome Height (When DT = 11.25 d, NH = 5 d, NL = 225 d, ASY = 375 d)

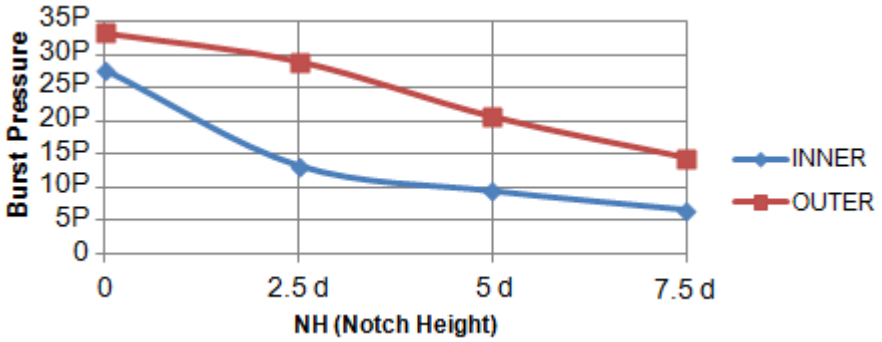

Figure 104: Burst Pressure vs Notch Height (When DH = 200 d, DT = 11.25 d, NL = 225 d, ASY = 375 d)

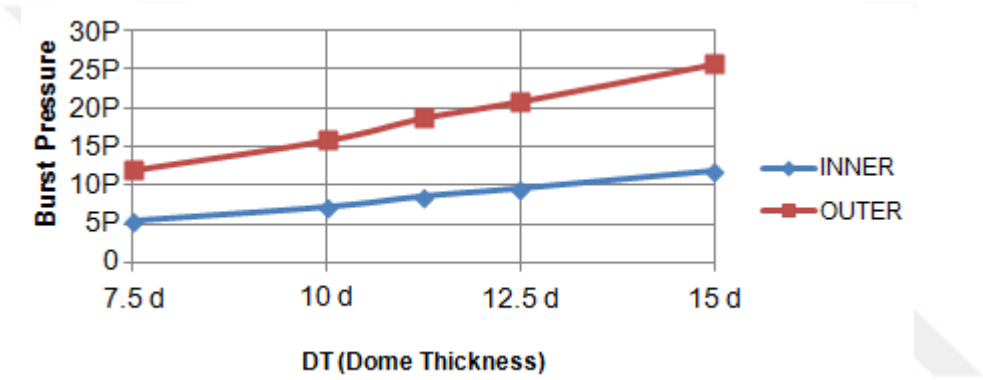

Figure 105: Burst Pressure vs Dome Thickness (When DH = 200 d, NH = 5 d, NL = 225 d, ASY = 375 d)

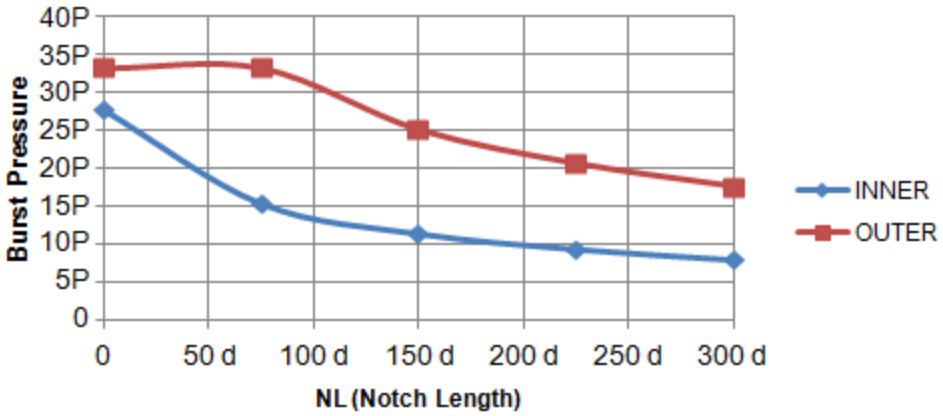

Figure 106: Burst Pressure vs Notch Length (When DH = 200 d, NH = 5 d, DT = 11.25 d, ASY = 375 d)

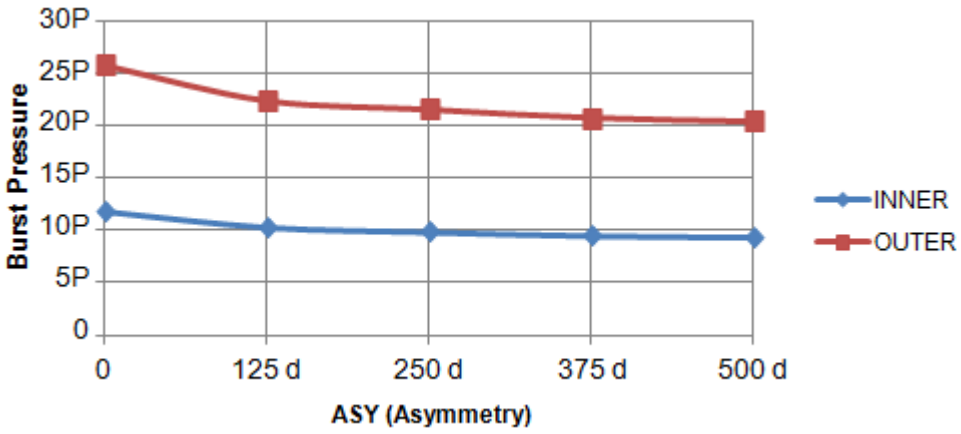

Figure 107: Burst Pressure vs Asymmetry (When DH = 200 d, NH = 5 d, DT = 11.25 d, NL = 225 d)

General summary of burst pressures of the models is given in Table 15.

According to one of the most critical requirements (Opening prior to launch), the inner burst pressure of the cover has to be lower than 12.5 P. In addition, it can be concluded that inner burst pressure and maximum outer pressure are interrelated with each other, and therefore, higher inner burst pressure means higher the maximum outer pressure. Thus, the lowest inner burst pressure cannot be selected because of the probability of failure due to outer pressure.

Another consideration is dome height of the cover. In FloEFD analysis results; it is observed that resultant axial force decreases with the increasing dome height slightly. However, increasing dome height also increases the length of the pod and conflicts with the length requirement of the pod. For this reason, dome height is selected as 200 d and FloEFD analyses are also conducted for 200 d dome height.

Table 15: General Summary of Burst Pressures

MODEL #	DH – DOME HEIGHT	NH – NOTCH HEIGHT	DT – DOME THICKNESS	NL – NOTCH LENGHT	ASYMMETRY	INNER		OUTER	
						BURST PRESSURE	FAILURE LOCATION	BURST PRESSURE	FAILURE LOCATION
1	50 d	5 d	11.25 d	225 d	375 d	2.7 P	Dome	5.95 P	Corner
2	100 d	5 d	11.25 d	225 d	375 d	5.2 P	Dome	11.55 P	Dome
3	150 d	5 d	11.25 d	225 d	375 d	7.6 P	Dome	16.7 P	Dome
4	200 d	5 d	11.25 d	225 d	375 d	9.45 P	Dome	20.65 P	Dome
5	250 d	5 d	11.25 d	225 d	375 d	11 P	Dome	24.05 P	Dome
6	200 d	0	11.25 d	225 d	375 d	27.8 P	Corner	33.25 P	Corner
7	200 d	2.5 d	11.25 d	225 d	375 d	13.3 P	Dome	29 P	Corner
4	200 d	5 d	11.25 d	225 d	375 d	9.45 P	Dome	20.65 P	Dome
8	200 d	7.5 d	11.25 d	225 d	375 d	6.6 P	Dome	14.45 P	Dome
9	200 d	3.75 d	7.5 d	225 d	375 d	5.5 P	Dome	12 P	Dome
10	200 d	5 d	10 d	225 d	375 d	7.25 P	Dome	15.85 P	Dome
11	200 d	2.25 d	11.25 d	225 d	375 d	8.6 P	Dome	18.75 P	Dome
12	200 d	6.25 d	12.5 d	225 d	375 d	9.6 P	Dome	20.9 P	Dome
13	200 d	7.5 d	15 d	225 d	375 d	11.8 P	Dome	25.7 P	Dome
14	200 d	5 d	11.25 d	0	375 d	27.8 P	Corner	33.25 P	Corner
15	200 d	5 d	11.25 d	75 d	375 d	15.45 P	Corner	33.25 P	Corner
16	200 d	5 d	11.25 d	150 d	375 d	11.5 P	Dome	25.1 P	Dome
4	200 d	5 d	11.25 d	225 d	375 d	9.45 P	Dome	20.65 P	Dome
17	200 d	5 d	11.25 d	300 d	375 d	8.05 P	Dome	17.6 P	Dome
18	200 d	5 d	11.25 d	225 d	0	11.75 P	Dome	25.7 P	Corner
19	200 d	5 d	11.25 d	225 d	125 d	10.25 P	Dome	22.3 P	Dome
20	200 d	5 d	11.25 d	225 d	250 d	9.8 P	Dome	21.45 P	Dome
4	200 d	5 d	11.25 d	225 d	375 d	9.45 P	Dome	20.65 P	Dome
21	200 d	5 d	11.25 d	225 d	500 d	9.3 P	Dome	20.3 P	Dome

When production of the cover is considered; notch details in the mold will be used as guidance during fabric lay-up. For this reason, at least 5 d notch height is preferable for convenience. On the other hand, increasing notch height creates thin resin sections at the center of the cover. During release of the cover from the mold, it is exposed to force. Therefore the cover should be thick enough for not to be cracked during mold release. It is assumed that at least 5-6.25 d thickness (DT-NH) is enough.

When the cover without notch (NL=0) and the cover with 75 d notch length are considered, it fails at the corner when inner pressure is applied. Therefore cover

parts cannot be spread away after bursting. On the other hand, when the notch length is increased, the weakened line gets close to the corner. When non-uniform outer pressure which is due to the adjacent rocket is considered; the weak area near the corner is not favorable. These reasons and burst pressures of 150 d, 225 d, and 300 d notch length alternatives are considered and 225 d notch length is chosen.

Increasing asymmetry of the cover increases the ability of cover to be fragmented. On the other hand, flange area is decreased. 500 d asymmetry is limiting value due to bolt holes at the flange. Therefore, to be on the safe side, 375 d asymmetry is chosen.

Arguments about inner and outer burst pressures, constraints due to production, interfaces, and functionality are explained in above paragraphs. It can be concluded that model 4 is suitable to be chosen as a candidate. It has 200 d dome height, 5 d notch height, 11.25 d dome thickness, 225 d notch length and 375 d asymmetry.

In order to check this configuration against a failure due to the adjacent missile, non-uniform pressure profiles are applied to outer surface of the cover. 5 L and 18 L positions are instants with highest axial force. Since the distance between rocket nozzle and the cover is lower at 5 L, force is concentrated to a smaller area (Figure 87).

Contour plots of the maximum and minimum principal stresses of the cover for 5 L instant are given in Figure 108 and Figure 109. The maximum principal stress (tensile) is 51.31 MPa and the minimum principal stress (compressive) is 98.97 MPa. Both the maximum and minimum principal stresses are observed at the corner which is close to rocket exhaust. Tensile stress is observed at the upper surface and compressive stress is observed at the lower surface. This stress distribution is induced by the bending effect of the dome as seen in Figure 110.

When both maximum and minimum principal stresses are considered according to Modified Mohr Theory, as applied to the uniform pressure previously, the cover is expected to resist the pressure of adjacent missile at 5 L instant.

Similarly; contour plots of the maximum and minimum principal stresses of the cover for 18 L instant are given in Figure 111 and Figure 112. Stress levels are 1/10 when compared with results of 5 L instant. Moreover, deflection is not localized in this case (Figure 113). Therefore, it can be concluded that 18 L instant is not critical and it can be negligible.

After investigating non-uniform pressure distributions in the analyses, model 4 is chosen as the candidate. The detailed design of the cover is completed after completing the sizing of the cover. In the next sections, production and testing of the cover are discussed.

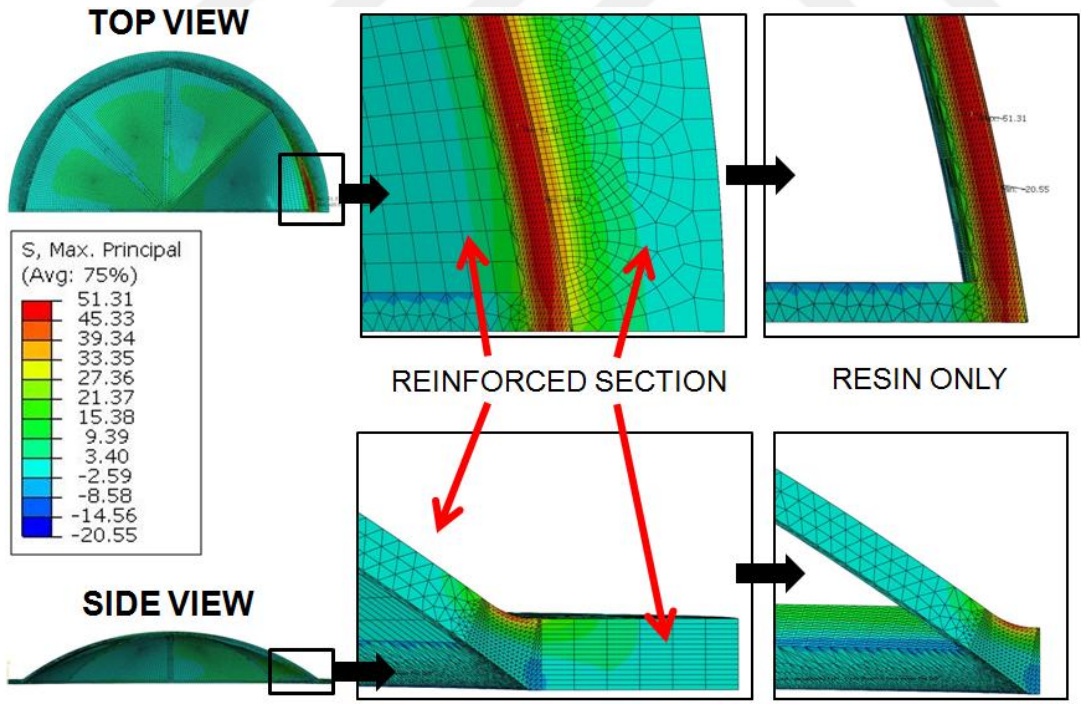

Figure 108: Contour Plot of Maximum Principal Stress at 5 L Instant

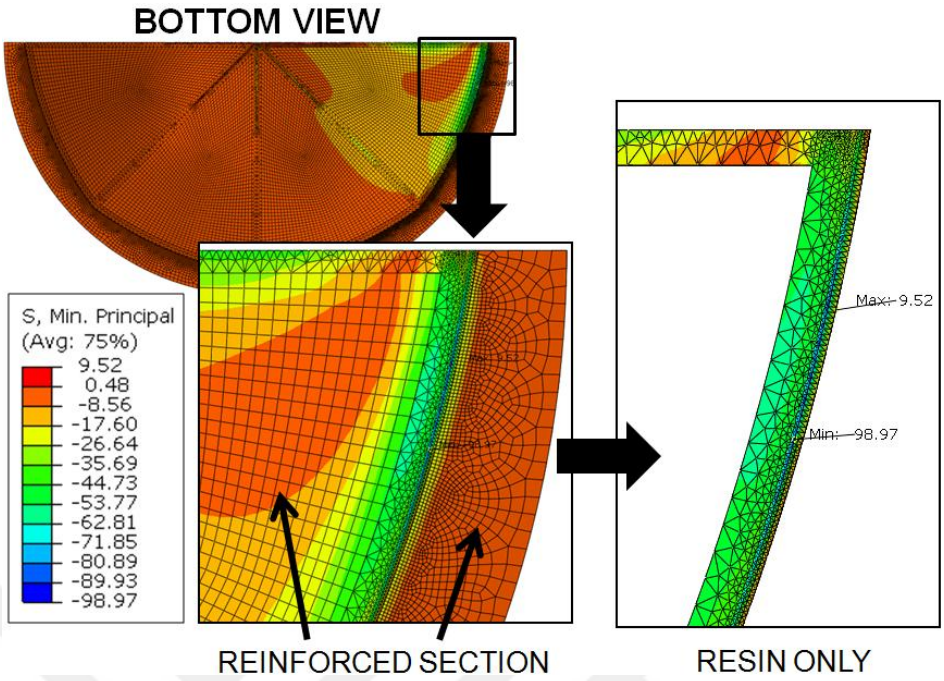

Figure 109: Contour Plot of Minimum Principal Stress at 5 L Instant

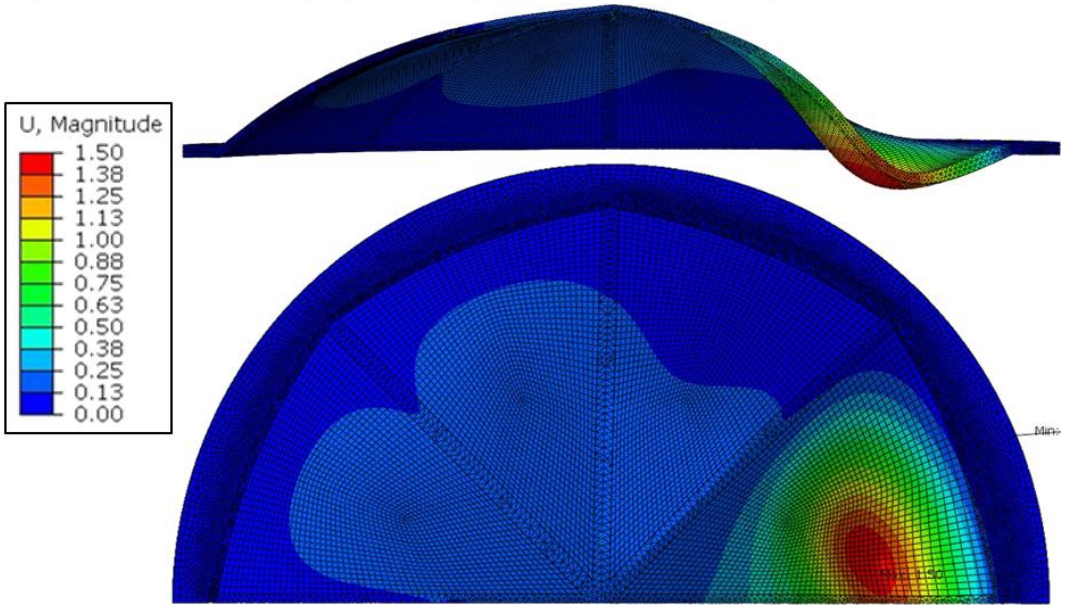

Figure 110: Contour Plot of Displacement [mm] at 5 L Instant

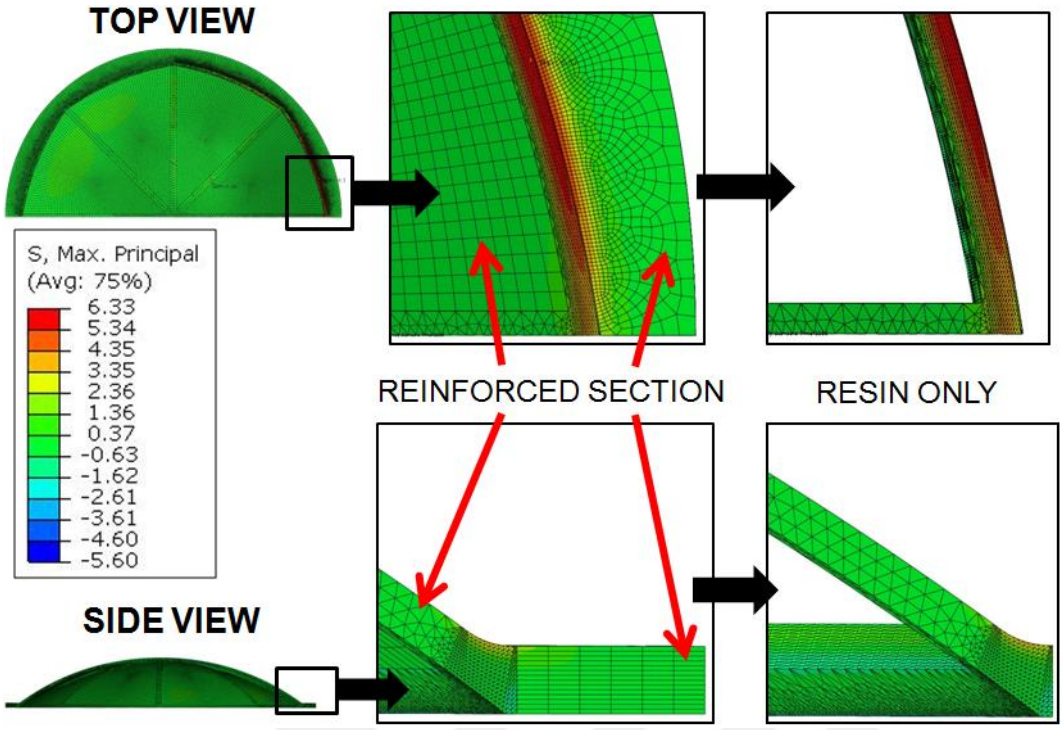

Figure 111: Contour Plot of Maximum Principal Stress at 18 L Instant

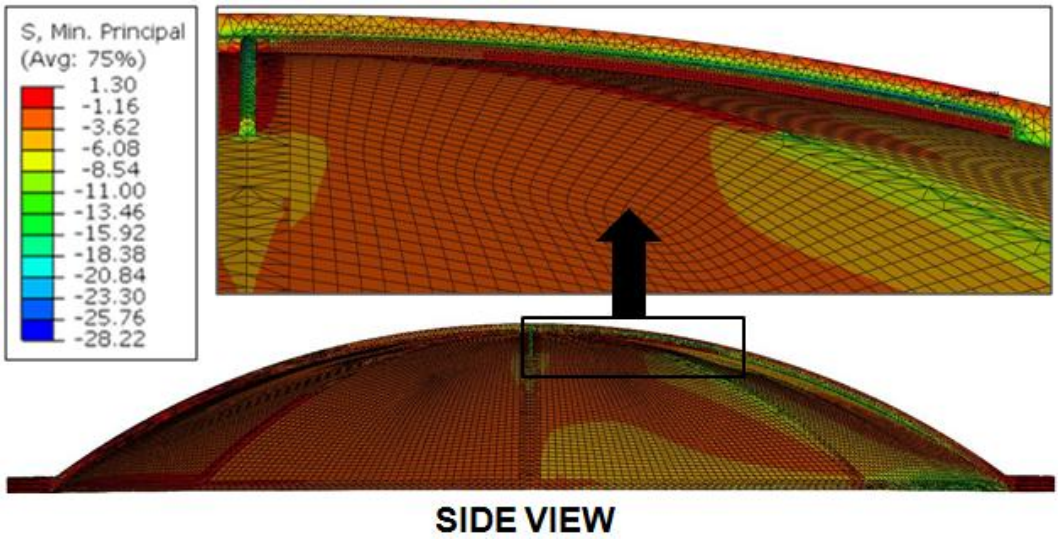

Figure 112: Contour Plot of Minimum Principal Stress at 18 L Instant

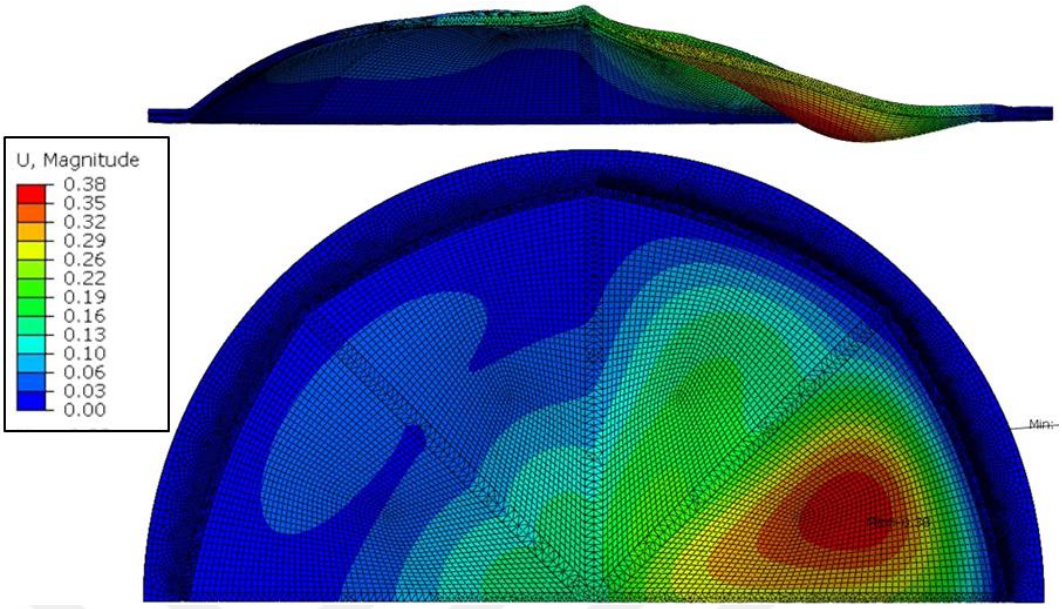

Figure 113: Contour Plot Displacement at 18 L Instant

CHAPTER 6

MANUFACTURING OF COVER

6.1 Materials and Process Parameters

For the resin material, a 3-component epoxy resin system is chosen. The system contains epoxy resin, hardener, and accelerator. It is a hot-curing, low-viscosity impregnating system. This system is widely used in RTM applications and its technical specifications are given in Appendix B.

Recommended viscosity value for RTM is 50-300 mPa.s. Therefore heating the resin and the mold is required [37].

For fabric reinforcement, a multi-axial fiberglass fabric is chosen. Details of the material are given in Appendix B. Two types of reinforcement material are used. Type 1 is used at the dome part of the cover. Type 2 is selected to be used at the flange area of the cover, as it can be cut into smaller pieces.

Another supplementary material is the mold release agent. Properties of the mold release agent are given in Appendix B.

6.2 Mold and Other Equipment

In resin transfer molding process, fiber preform is impregnated with liquid thermoset resin inside a closed mold. Therefore one of the basic element for RTM production is the mold.

If the shape of the geometry is not complex, it is a two-part structure that contains female and male sections. The mold basically has the inner cavity which has the negative shape of the final product as seen in Figure 114.

When the design of the elements of the mold is considered, first of all, the mold has resin inlet port to inject resin into the cavity. Also, it has a vent port for the ejection of the air and excess amount of resin. Moreover, precaution must be taken in order to eliminate leakage of the resin outside to the mold. O-ring is used to provide sealing between two sections of the mold.

Centering pins are used to position mold sections with a required precision. Female and male mold sections must be kept closed during resin injection and curing process. They are generally closed and secured with bolted connection.

When the final product is stuck to the mold surface, the ejector pins are used to push the product out of the mold.

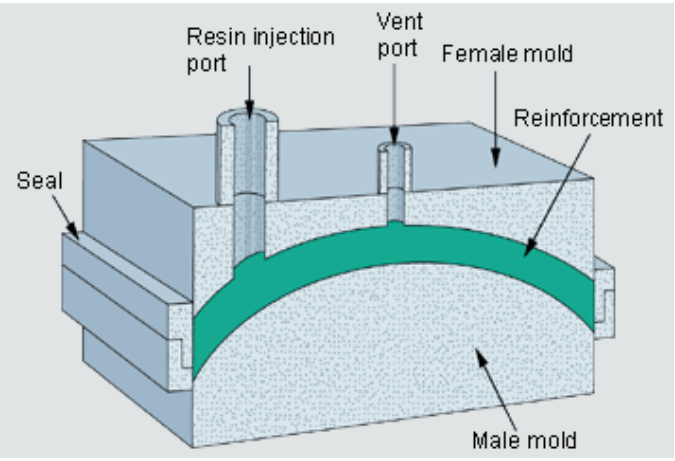

Figure 114: A Typical Mold for Resin Transfer Molding Process [67]

Other important issues that must be considered for easy removal of the part are the draft angle. The shape of the part and mold sections with such angles will provide easy removal.

Another important aspect is the material selection for the mold. Assessments of the materials in order to manufacture the mold for high-temperature composite part are given in Table 16.

Aluminum is chosen for mold material. It is the most widely used tooling material in composite manufacturing. Its cost is relatively low and its lower density makes handling easier. Also, machining of aluminum is relatively easier compared to steel. High thermal conductivity is an advantage to transfer heat to the part during curing. Aluminum can be used up to 200 °C temperature without any thermal limitation. On the other hand, the relatively high coefficient of thermal expansion may cause micro cracks due to the difference of the expansion between composite and aluminum. However, it is not a critical problem if the length and width of the part are in the same order of magnitude. [68]

Table 16: Assessments of Materials for Mold Manufacturing (*CTE: Coefficient of Thermal Expansion) [68]

Tooling Material	**Advantage**	**Disadvantage**
Steel	Good thermal conductivity, Durable	Warpage at high temp. High CTE, High fabrication cost, High density
Invar	Low CTE, High thermal conductivity, Durable	High material cost, High fabrication cost
Titanium	Low CTE, Good thermal conductivity, Durable	High material cost, High fabrication cost
Ceramic	Low CTE, Low-Cost material, Low-cost Fabrication	Low thermal conductivity, Fragile, High Density
Aluminum	Low-cost material, High thermal conductivity	High CTE, Limited strength at high temperatures

After machining process of the mold, the surface of the cavity is polished, in order to prevent adhesion of the part.

Another basic element of composite manufacturing is the heat source. Heat can be applied by oven or internal heat sources integrated to the mold itself. Dimensions of the mold are relatively small, therefore curing can be provided in an oven.

A mold is designed and manufactured on the basis of the information above. Photographs of male and female parts of the mold are in Figure 115 and Figure 116.

In the production of the cover, an RTM system is used to provide impregnation of resin to reinforcement fiber. The resin in a storage tank is injected into the inlet port of the mold.

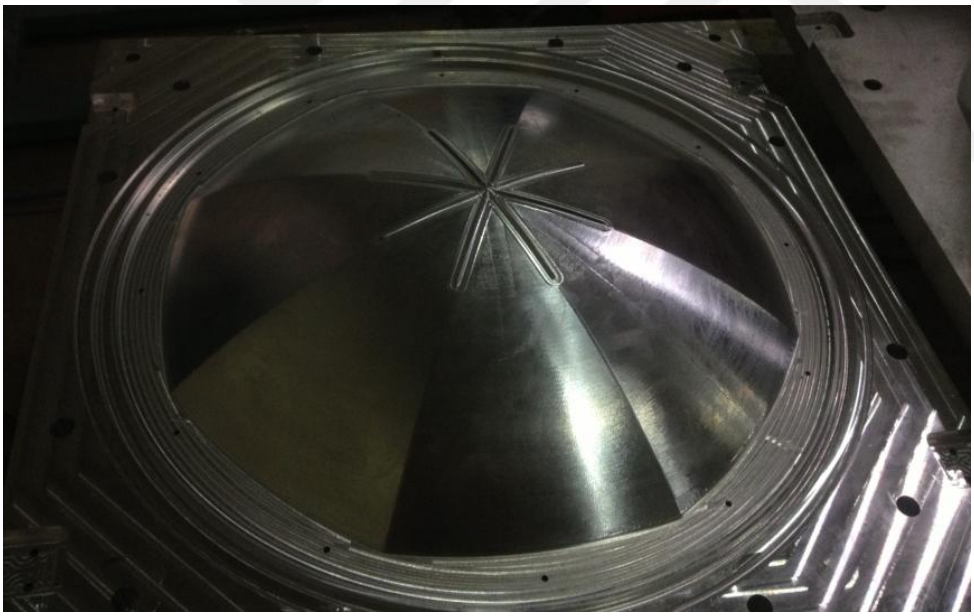

Figure 115: Male Section of the Mold

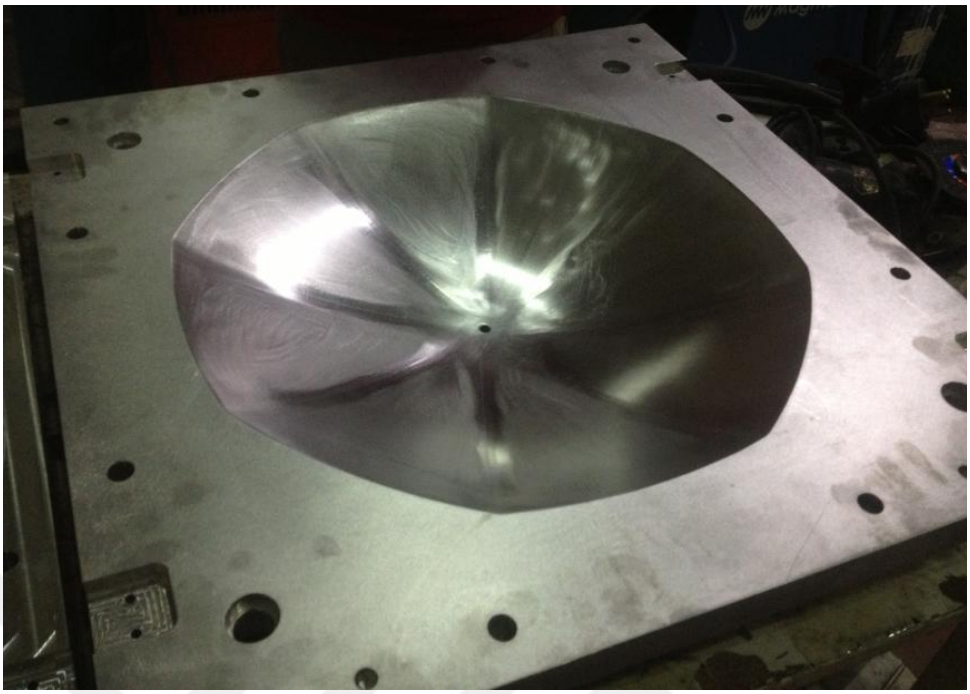

Figure 116: Female Section of the Mold

6.3 Process Steps

After manufacturing of the mold, and supplying mold release agent, reinforcement fabric, resin components to RTM system and using a curing oven; the first prototype of the cover is produced. Production of the cover is explained step-by-step in the following paragraphs.

The mold is preheated to 50 ℃ and mold release agent is applied. Heating provides the release agent to cover and stick itself to the surface better. It also decreases the viscosity of the resin. Therefore, it makes resin impregnation and flows through fabric easier.

A template is prepared according to the mold surface and lay-up configuration. Reinforcement fabric is cut by using the template and fabric slices are laid up to the mold surface (Figure 117).

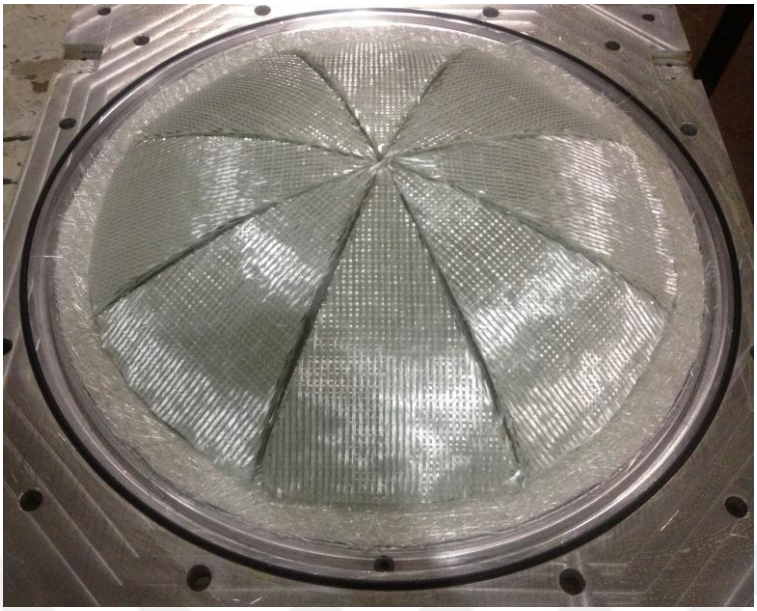

Figure 117: Lay-up of Fabric Slices

Silicon-based O-ring is placed to the groove in the mold, and then the mold sections are closed together (Figure 118). Afterward, bolts are tightened. Resin inlet and outlet ports are prepared and assembled to the mold. They are separated from the mold itself. Because after each production the resin trapped at the port solidifies and stacks the line. Therefore, it must be cleaned prior to each production.

Resin components are precisely weighted and mixed in a pot by using a stick. The pod is closed after mixing, and then vacuum is applied. This process is called "degassing" and during degassing, bubble formation is observed due to the reaction in the resin. An excess amount of gas is released by this application, and therefore bubbles are prevented in the part.

The resin mixture is inserted into the vessel of the RTM system. Resin inlet and outlet ports are connected and the resin is injected into the mold. When the resin impregnated to the reinforcement and fully filled the mold it flows out to the mold, Therefore, the outlet port is closed after the outflow is observed (Figure 119).

Figure 118: Closing Mold Sections

Figure 119: Outlet of Excess Resin

Afterward, the mold is placed into the oven and cure cycle is applied. After completing the cure cycle the mold is opened. Female and male sections are separated (Figure 120). The cover which is stuck to male section of the mold is released by applying force.

Excess resin at the inlet and outlet sections is trimmed. Holes at the outer flange are drilled by using template. Production of the prototype is then completed.

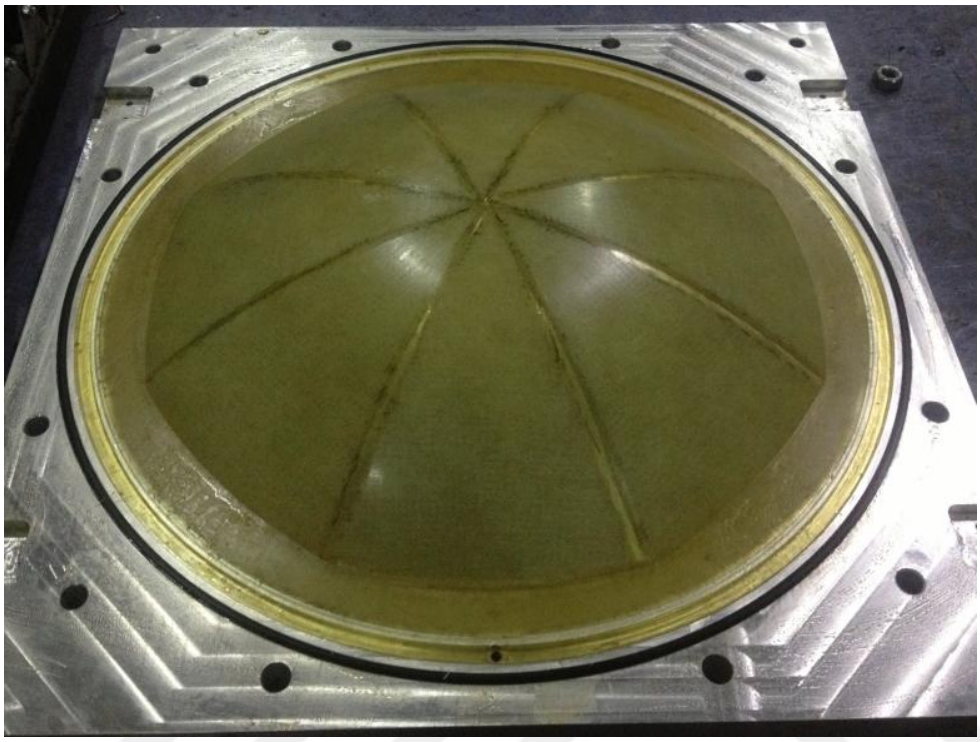

Figure 120: Opening of the Mold

CHAPTER 7

TEST AND VALIDATION OF COVER

7.1 Burst Test

The most determinative and applicable experiment method to investigate the strength of a frangible cover is the burst test.

In the burst test, a test cover is mounted to the test fixture as used in the launch tube. Then, the pressure of the chamber is increased. Liquid (water) is used for safety reasons. The pressure is gradually increased and the pressure value at the instance of the failure of the cover is recorded as the burst pressure.

Burst test is used in order to qualify the design or quality control. Example of its usage can be seen particularly in the area of frangible launch tube covers [69, 70].

In the burst test of the frangible launch tube covers, static pressure is assumed to demonstrate the impulsive pressure that determines the actual time-dependent boundary condition of the cover.

In the study of Wu, Wang and Kam, the test setup which is seen in Figure 121, is used to investigate the burst pressure of the frangible cover [69].

Another example is the study of Yuan. In this study, finite element analysis results are compared with the experimental results and it is stated that the results are conformable [70].

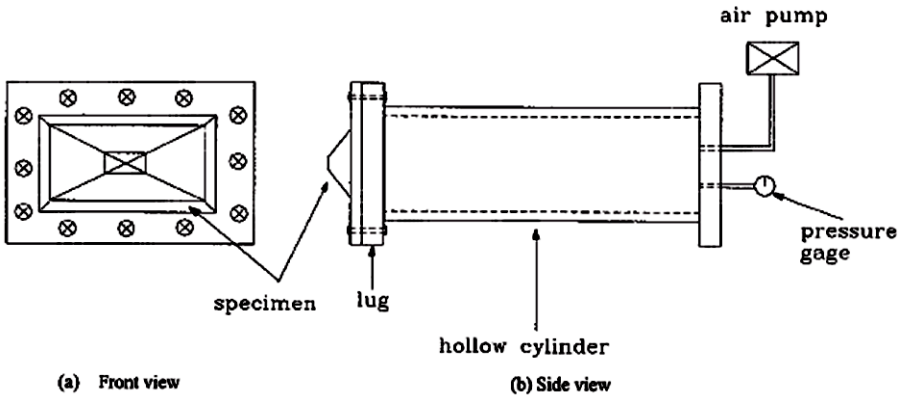

Figure 121: An Illustration of a Sample Burst Test Set-Up [69]

7.1.1 Burst Test Set-Up

The test set-up chamber has a cover mounting interface which represents the front opening of the launch tube. Schematic view of the set-up is seen in Figure 122. A pressure transducer is used to measure the burst pressure. Photograph of the test set-up is also given in Figure 123.

After assembling the cover to the set-up, the chamber is filled with water. Then air inlet is opened and the pressure starts to increase. During pressurizing, the variation of pressure with time inside the chamber is recorded. The maximum pressure is determined when the cover bursts. The test cover can be mounted in two ways. Inner and outer burst pressure can be investigated by turning the cover upside down. The photograph and technical details of the pressure transducer is given in Table 17 and Figure 124.

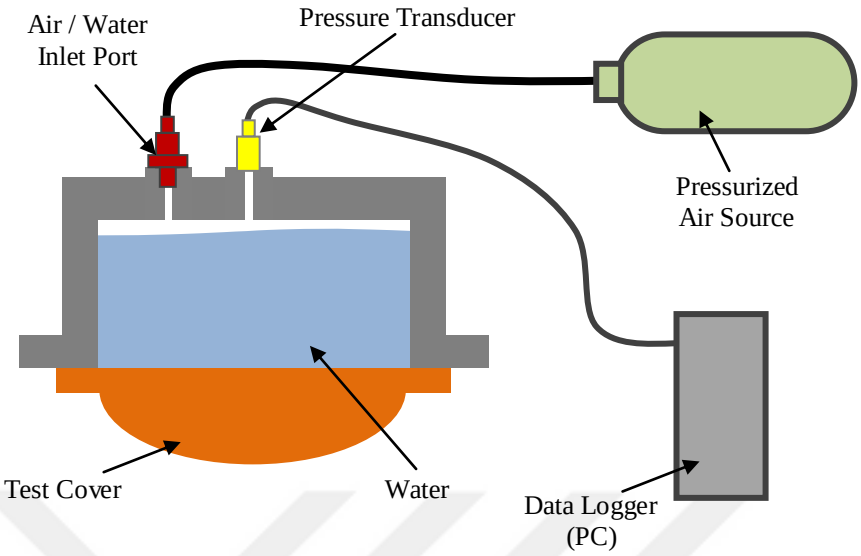

Figure 122: Schematic View of Burst Test Set-Up

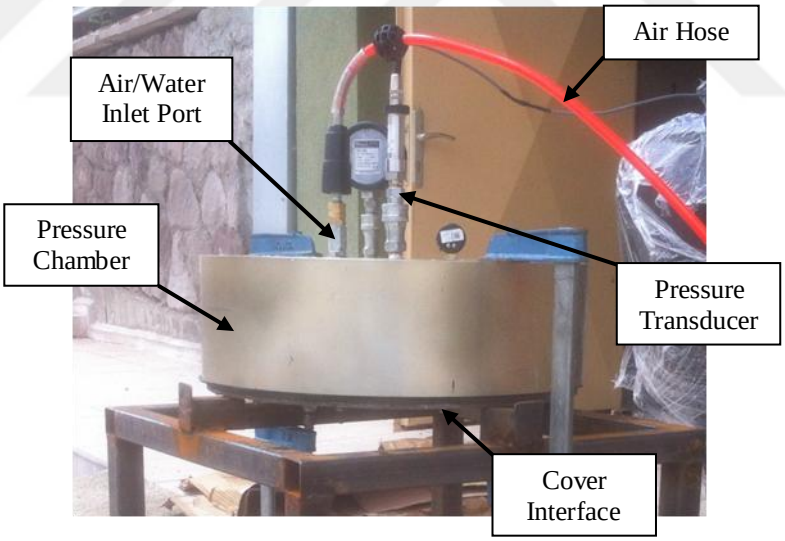

Figure 123: Photograph of the Burst Test Set-up

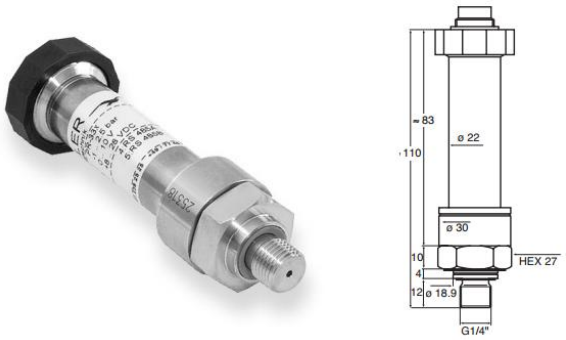

Figure 124: Photograph and Dimensions of Pressure Transducer [71]

Table 17: Properties of Pressure Transducer [71]

Producer Name	KELLER AG für Druckmesstechnik
Model Number	PAA-33X
Measurement Range	0-50 P
Over Pressure	100 P
Precision	5x10^-3 P

7.1.2 Test Results

When the first batch of covers is manufactured, some of them are observed to have cracks. Therefore, these cracked covers are disregarded and not tested. Some tests are conducted for inner burst pressures, some other covers are tested for outer burst pressures. Data of 25 covers is obtained except unsuccessful test trials. Pressure distribution of burst tests is given in Figure 125.

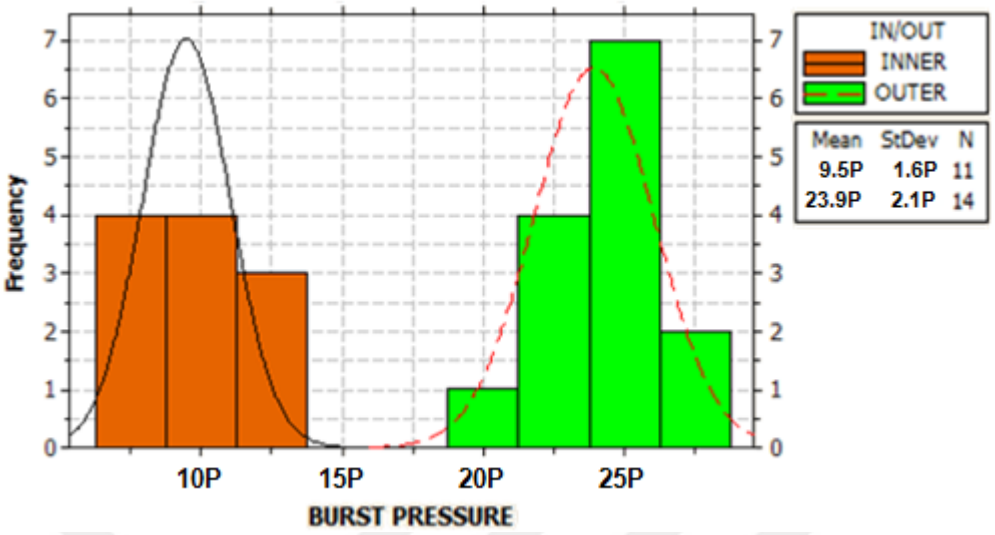

Figure 125: Histogram of Burst Pressures

For the inner burst pressure measurement, 11 covers are used. The mean of the burst pressure is 9.5 P and the standard deviation is 1.6 P. For the outer pressure measurement, 14 covers are tested. The mean of the outer failure pressure is 23.9 P and the standard deviation is 2 P.

7.2 Firing Test

Opening the pod cover with inner pressure is seen in Figure 126. In this figure, high-speed camera images are described schematically. Interaction of the cover with the missile is not observed. It is seen that, when the missile is fired, the cover bursts into pieces before the missile starts the exit from the launch tube. When the missile starts to leave the pod, it exerts exhaust plumes to the adjacent tube covers. These adjacent covers are investigated and no failure is observed.

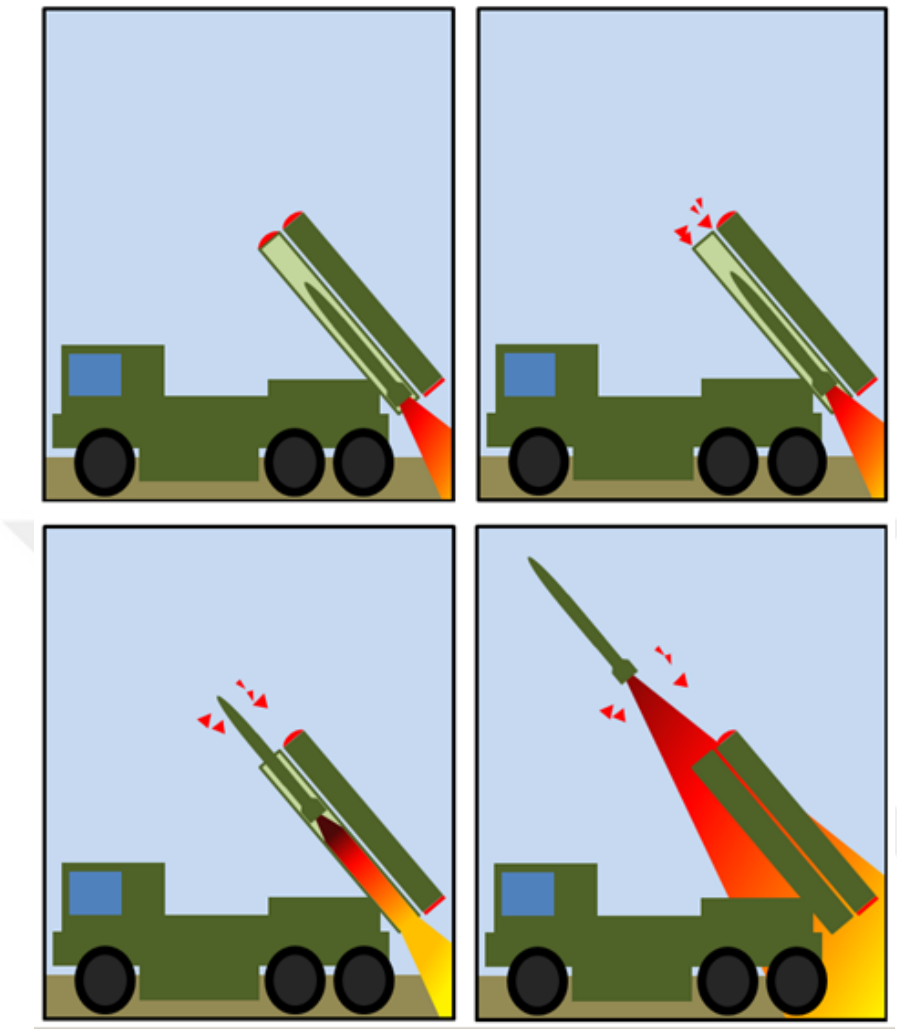

Figure 126: Schematic View of High-Speed Camera Images of Cover Separation During Missile Launch

CHAPTER 8

DISCUSSION AND CONCLUSION

8.1 Summary

The work carried out in this thesis is summarized below in detail.

In the first chapter, motivation and objective of the thesis are explained in detail. Importance of the study is also mentioned. Moreover, detailed information about the necessity of proper design of missile launch tube covers is given. Working principle of the cover is briefly explained.

In the second chapter, literature information is given. Types of launch tube covers and their specifications are mentioned. Cover examples existing in the literature are grouped according to working principles.

The potential use of composite material technologies is investigated since one of the purposes and scopes of the thesis is to use and implement composite materials into the cover design. Types, advantages, and disadvantages of composite materials are mentioned. In addition to material types, composite production methods are also explained and compared with each other. Materials and production method are selected and scope is narrowed accordingly.

Determination of loads on the cover is investigated in the third chapter. Inner and outer load measurement methods and corresponding experiments are mentioned. Moreover, tools and transducers used in measurements are shown. Test results are examined with high-speed camera images. In addition to experiments, a CFD

software is used in order to examine the outer pressure load. Similarly, the effect of cover geometry on outer loads is investigated by using the CFD software.

In Chapter 4, the design of the cover is explained. Firstly, the problem definition is made. After that, design requirements and constraints are derived in accordance with loading conditions, functional requirements, selected material and process method. Technical solutions are developed for requirements which are derived. Functional properties that the cover needs to have in its whole life cycle are examined. Then, the conceptual design process is explained from general to detail, and creative design solution is developed. Design parameters are determined and coupon tests are conducted in order to prove the creative solution concept in the scope of the detailed design process.

In Chapter 5, namely "Numerical Simulation of Cover", the detailed design is finished after completing the sizing of the parameters. Finite element analyses are carried out to find critical stresses. Detailed information about the prepared model, mesh structure, loads, boundary conditions, and material properties is given. Results of analyses are investigated and compared with each other. Then the decision is made for sizing of the cover.

Manufacturing of the cover is explained in Chapter 6. The material properties, process parameters, mold design is described. Moreover, the manufacturing process is explained step-by-step.

Chapter 7 is dedicated to testing and validation of the cover. Burst test set-up is explained and test results are given in this chapter. These inner and outer burst pressures are compared with the numerical results.

8.2 Discussion

In the scope of this study, a pod cover design is conducted. At the beginning of the study, it is decided that the cover should be frangible type and it should be manufactured with composite materials.

Composite material usage enables various production method and material alternatives to be used in the design. This makes composite material usage advantageous in terms of design flexibility. However, in some cases they require molds; thus, prototype production can be more difficult than traditional methods. If the design change requires a mold revision, it is costly to realize that.

Frangible type of covers does not require actuators or complex mechanisms. Their frangible structure makes them open autonomously by fracturing and it is synchronized with the increase of inner pressure of the launch tube due to the firing of the missile. Their simple structure makes their cost relatively low. Also, they do not require maintenance and their risk of malfunction is relatively low when compared with more complex cover types which are actuated by mechanism.

On the other hand, their design and qualification are more difficult than non-autonomous covers. Their inner and outer burst pressures must be arranged such that they have to resist outer pressure and fracture easily when the inner pressure is applied. These two requirements contradict each other and the design parameters need to be optimized in that respect.

Another challenge is to determine loads on the cover. Outer pressure measurement is not achieved during launch test. For this reason, the external force acting on the cover is measured by using load cells. The measured load is compared with the load obtained from CFD software (FloEFD) and it is observed that they are consistent. Inner pressure measurement is achieved by using piezo-resistive pressure transducer.

In this pod covers, the inner pressure during operation is applied uniformly and it is tested with applying uniform pressure by using burst test set-up. On the other hand, it is considered that the weapon system has two adjacent launch tubes on top of each other. For this reason, the outer surface of the cover is exposed to non-uniform pressure distribution and also high-temperature exhaust flow (from adjacent missile). For this reason, it is not possible to simulate outer load by using quasi-static burst test. Nevertheless, this outer burst test is applied to the cover in order to compare and correlate the results with FEA results.

When FEA results and burst tests are compared the same result is obtained for inner burst pressure. For outer burst pressure, the estimated value is lower than the test results by 15%. The failure is based on tensile stress when inner pressure is applied; oppositely it is based on compressive stress when the pressure is applied to the outer surface. Tensile strength of the material (resin) is determined by using coupon level tensile tests and compressive strength is calculated by using tension/compression strength ratio (2.2) which is found in the literature. It is assumed that 15% difference in outer burst pressure is resulted from the ratio assumption. Since estimated (FEA) outer burst pressure is lower than the test results, it is concluded that design and assumption are on the safe side. Since resin material is brittle, Modified Mohr Theory is used as failure criteria and compatible results are obtained.

The maximum axial force (31.4F) is observed at the instant when the distance between the nozzle of the missile and the cover is 5L. At that instant, the maximum pressure of 99.5P occurs on or very near to flange area where the thickness of the cover is large, also there is no notch in that area and therefore there is going to be no stress concentration effect. The maximum value of this pressure exponentially decreases towards the center of the cover (Figure 87). Therefore, it is not a critical issue for the safety of the cover as far as the outer burst pressure is concerned. After this first maximum load, the second local maximum load is observed as 30F at a greater distance than about 11L between

the cover and nozzle of the adjacent missile. At this distance, the maximum pressure drops to around 15P value which is well below the FEA burst pressure results.

8.3 Conclusion

- Internal and external burst pressures are two basic requirements in order to realize a frangible cover design which opens with internal pressure and resists adjacent missile's exhaust plume.
- To achieve this cover design; thickness of the cover, number, and shape of the weak areas achieved by using only resin (for easy fracturing), number of the segmented surfaces with fiber reinforcement, dome height, notch length and depth (control fragmentation), are taken into consideration.
- The internal pressure applied to the cover due to the firing of the missile's engine is found as 12.5P. Any cover to be designed must burst below this pressure.
- The outer pressure which is generated from the adjacent missile's exhaust plume cannot be measured by using available pressure transducers due to high temperature and abrasive particles in the exhaust plume. For outer loading, force is measured instead of pressure by using three load cells. The axial force on the cover due to the outer pressure is recorded. Sudden peak with an approximate value of 28F is observed.
- The application point of resultant external axial force on the cover is at the vicinity of adjacent launch tube at the beginning. This point shifts towards the center of the cover as adjacent missile moves away from its launch tube.
- Outer load on the cover is also investigated by using FloEFD software for different positions of the missile which is launched from the adjacent tube. The maximum axial force (31.4F) is observed at the instant when the distance between the nozzle of the missile and the cover is 5L.

- By using FloEFD software, the effect of the cover geometry on total axial force is also examined. Increasing the dome height of the cover up to its maximum limit of 200d decreases the total force by 6% when the distance between the cover and the missile's nozzle is 5L, and it decreases 12% when the distance reaches to 18L. Due to the dimensional limitations of the total system, the dome height should not exceed 200d.
- After deciding the type of the materials to be used in the cover design, coupon level tensile tests are conducted in order to determine the material properties.
- In order to ease fragmentation with inner pressure, discontinuities are created at the dome of the cover. It is divided into 8 surfaces and umbrella-like shape is obtained. Weak areas consisting only of resin material are created between these surfaces to rupture easily. In addition, groove detail is added to the center of the cover to start fracture from the center of the cover and separate fragments away from the missile's flight path.
- Parametric design alternatives are derived and their burst pressures are determined by using FEA.
- The cover is expected to burst at low inside pressure while it should resist comparatively higher outer pressure acting on it due to the exhaust plume of the adjacent missile. Among these trials, an alternative having 9.5P inner and 20.5P outer burst pressures is selected and manufactured by using resin transfer molding. For optimum design of the cover, the thickness is selected as 11.25d and the notch height and length are determined as 5d and 225d, respectively.
- The optimum configuration needs to be tested for inner and outer burst pressures. For that purpose, a burst test set-up is designed and manufactured. Average inner and outer burst pressures of the cover are determined as 9.5P and 24P, respectively. Inner burst pressures are the same in both test and FEA. As far as the outer burst pressure is concerned,

although, they are different from each other, they are high enough to be on the safe side.

- In real field tests, the cover proves that it works as planned. It is observed that the cover pieces do not interact with missile and also the adjacent cover is not broken with missile's exhaust plume.
- This design is registered as an invention, and a utility model document is obtained. [59]

8.4 Recommendation for Future Work

If the scope of studies in this subject is extended following recommendations can be taken into consideration.

It is important to note that, the solution set of the pod cover design problem is quite large. In this study, one concept is developed as an idea and each step is explained from start to end.

In composites industry, decreasing human factor and dependency of technicians have been studied for a long time. The human factor in cover production can be investigated.

Probabilistic design study can be conducted to investigate the effects of parameters. For example deviation in material properties, loads, dimensions, etc can be considered. Similarly, the reliability of the cover can be examined.

Aging in materials and long-term material properties can be investigated.

Pressure measurement methods can be developed and reliability of this system can be investigated.

Explicit analysis methods can be used and explicit material model can be investigated.

REFERENCES

[1] Ynet News, Israel to Hold Arrow 3 Missile Test Soon, https://www.ynetnews.com/articles/0,7340,L-4197344,00.html, last visited on April 2018.

[2] Harpoon Anti-Ship Missiles, http://www.mdc.idv.tw/mdc/navy/usanavy/E-antisurface-AGM84.htm, last visited on April 2018.

[3] Krol, U. B., "Frangible Cover Assembly for Missile Launchers", U.S. Patent No. 3,742,814, 1973.

[4] Larson, L. R., Teigland, G. L., Anderson, N., Ickstadt, J. M., Voller, V. F., Buehler, J. D., Flakne, A., "Concentric Canister Launcher", U.S. Patent No. 6,230,604, 2001.

[5] Asp, B., Martinsson, J. E., "Device for a Missile", U.S. Patent No. 4,134,328, 1979.

[6] Miao, P. Y., Yuan, Z. F., "Techniques for the Automatic Cover Opening in Concentric Canister Launcher", Transactions of Beijing Institute of Technology, Volume 24, Issue 4, pp. 283-285, April 2004.

[7] Hiroyuki, T., Hiroya, H., "Projectile Launching Device", JP Patent No. 11-201696, 1999.

[8] Williams, M. W., "Break-Away Muzzle Cap Retention Mechanism", U.S. Patent No. 6,336,341, 2002.

[9] Paul, B. R., "Article Comprising a Canister Closure with Pressure Pulse Release", U.S. Patent No. 7,685,920, 2010.

[10] Kennedy, R. E., “Gas Driven Hatch Cover Assembly”, U.S. Patent No. 5,956,901, 1999.

[11] Fleischer, C. A., Chiu, B. S., Heick K., “Rotating and Sliding Hatch Door for a Launcher System”, U.S. Patent No. 8, 087,336, 2012.

[12] Defence.pk, Babur Cruise Missile, http://defence.pk/threads/babur-cruise-missile-database.185609/page-15, last visited on April 2018.

[13] DN - Defence Notes, DSEI 2013: MBDA and Lockheed Test Fire CAMM, https://www.shephardmedia.com/news/defence-notes/dsei-2013-mbda-and-lockheed-test-fire-camm/, last visited on April 2018.

[14] Hunn, D. L., “Device and Method for Sealing a Munition within a Canister Until Munition Launch”, U.S. Patent No. 5,993,921, 1999.

[15] Williams, R. B., Waicukauski, J. A., “Article Comprising a Composite Cover”, U.S. Patent No. 7,520,204, 2009.

[16] Bohs, B. E., Everitt, W. E., “Article Comprising a Missile Canister Cover”, U.S. Patent No. 8,256,340, 2012.

[17] Fumiya, H., Hiroya, H., “Firing Apparatus for Missile”, JP Patent No. 11-183088, 1999.

[18] Encyclopedie des Armes, British Aerospace Sea Skua, http://encyclopedie-des-armes.com/index.php/aviation/air-mer/1360-british-aerospace-sea-skua, last visited on April 2018.

[19] Guide to Military Equipment and Civil Aviation, Marte Mk2/N, http://www.deagel.com/Offensive-Weapons/Marte-Mk2N_a001121002.aspx, last visited on April 2018.

[20] Doane, W. J., “Frangible Fly Through Diaphragm for Missile Launch Canister”, U.S. Patent No. 4,498,368, 1985.

[21] Kuchta, B. J., Gardner, J. L., “Extended Canister Fly-Through Cover”, U.S. Patent No. 6,123,005, 2000.

[22] Seiji, M., Makoto, T., “Firing Apparatus for Missile”, JP Patent No. 11-183090, 1999.

[23] Global Security, Patriot TMD, https://www.globalsecurity.org/space/systems/patriot-pics.htm, last visited on April 2018.

[24] Forris, V. G., Tokiyama, T., “Protective Missile Launch Tube Enclosure”, U.S. Patent No. 6,311,604, 2001.

[25] Naval Weapons, Naval Technology and Naval Reunions, Sea Sparrow AIM-7/RIM-7, http://www.navweaps.com/Weapons/WMUS_Sea_Sparrow_RIM7.php, last visited on April 2018.

[26] Boeglin, P. H., Chigot, C. R., “Plate-Glass Fitted with an Explosion-Cutting Device”, U.S. Patent No. 4,333,381, 1982.

[27] Feiler, A. M., “Missile Container and Launcher”, U.S. Patent No. 3,158,062, 1964.

[28] Mussey, R. A., “Launch Tube Closure”, U.S. Patent No. 4,301,708, 1981.

[29] Shook, R. G., “Shock Wave End Cap Removal Device”, U.S. Patent No. 4,455,917, 1984.

[30] Hombeck, W. D., “Combination Sabot and Launch Seal” U.S. Patent No. 7,506,572, 2009.

[31] Fitzgerald, H., “Weather Proof Canister”, U.K. Patent No. 2,140,898A, 1984.

[32] Zhang, H., “Topology Self-Lock Fragile Water Separation Cover”, CN Patent No. CN 201003934 (Y), 2006.

[33] Zhang, X. L., Yang, Z. H., Zhang, H., Zhang, J., Song, B. C., "Structural Study on a Kind of Directional Fracture Composite", Ordnance Material Science and Engineering, Volume 30, Issue 3, pp. 10-13, 2007.

[34] Wei, F. C., Zhang, X., Yang, Z. H., Zhang, X., Zhang, H., "Design and Experiment for Topological Interlocking Fragile Composites Structure", Journal of Mechanical Strength, Volume 31, Issue 4, pp. 573-577, 2009.

[35] Tegel, M., Wenzel, D., “Cap for a Rocket Exit Opening”, U.S. Patent No. 5,062,345, 1991.

[36] Guide to composites - Gurit, http://www.gurit.com/-/media/Gurit/Datasheets/guide-to-composites.pdf, last visited on April 2018.

[37] Miravete, A., “Processing and Manufacturing”, 2009, http://ftp.ae.metu.edu.tr/~ae469/AM.Manufacturing.pdf, last visited on April 2018.

[38] Floros, M. W., “Elastically Tailored Composite Rotor Blades for Stall Alleviation and Vibration Reduction”, PhD. Thesis, pp. 200-203, The Pennsylvania State University, December, 2000.

[39] Clyne., T. W., Natural Sciences Tripos Part II, Material Science C16: Composite Materials Lecture Notes, https://www.msm.cam.ac.uk/ug-study/part-ii, last visited on January 2017.

[40] CES Edupack, Material and Process Selection Charts - Granta Design, http://www.grantadesign.com/download/pdf/teaching_resource_books/2-Materials-Charts-2009.pdf, last visited on April 2018.

[41] Im, E., Thomson, M., Fang, H., Pearson, J. C., Moore J., Lin, J. K., " Prospects of Large Deployable Reflector Antennas for a New Generation of Geostationary Doppler Weather Radar Satellites", AIAA Space 2007 Conference and Exposition, California, United States, September 18-20, 2007.

[42] BBC, X-47B Stealth Drone Targets New Frontiers, http://www.bbc.com/future/story/20121218-stealth-drone-targets-life-at-sea, last visited on April 2018.

[43] Hoa, S. V., Principles of the Manufacturing of Composite Materials, DEStech Publications Inc., Pennsylvania, 2009.

[44] Pandey, P. C., Web-Based Course: Composite Materials, http://basalt.today/images/Learning-material-composite-material.pdf, last visited on April 2018.

[45] Mallick, P. K., Fiber-Reinforced Composites Materials, Manufacturing and Design, Taylor & Francis Group, LLC, Florida, 2007.

[46] Hancox., N. L., Mayer, R. M., Design Data For Reinforced Plastics, Chapman and Hall, p. 274, London, 1994.

[47] ME 338 - Manufacturing Processes II Lecture Notes, Prof. Ganesh Soni, http://www.me.iitb.ac.in/~ramesh/courses/ME338/comp.pdf, last viewed on April 2018.

[48] AE-ME484 Lecture Note: Applications, Advantages and Challenge of Composites, https://global-

stl.mst.edu/media/extendedlearning/eec/documents/birmansamples/Sample_Introduction_AE-ME484.pdf, last viewed on April 2018.

[49] ASM International, Handbook: Composites, Volume 21, 2001.

[50] Lee, S. J., "Initial Transient Analysis of Missile Launch-Tube Gas Flow and Its Interaction with Structures", AIAA/SAE/ASME/ASEE 29th Joint Propulsion Conference and Exhibit, California, United States, June 28-30, 1993.

[51] Fu, D. B., Yi, J., "Opening Process of Friable Lid of One Missile", 2007.

[52] Sung, H. G., Kim, Y. G., Kim, J. U., Lee, T. H., Kim, B. S., "Numerical and Experimental Studies of Rocket Exhaust Flow in Rocket Launch Tube", AIAA/SAE/ASME/ASEE 28th Joint Propulsion Conference and Exhibit, Tennessee, United States, June 28-30, 1993.

[53] Yagla, J., Anderson, L. J., "Internal Ballistics and Missile Launch Environment for the Vertical Launching System", 3rd Joint Thermophysics, Fluids, Plasma and Heat Transfer Conference, Missouri, United States, June 7-11, 1982.

[54] Marongiu, M. J., "Mechanisms Controlling Non-Steady Plume-Wall Interactions in Rocket Launch-Tubes", PhD. Thesis, pp. 12-17, University of Illinois, July, 1985.

[55] Ma, Y., Jiang, Y., Hao, J., Yan, F., "Simulation of the Influence of Missile Exhaust Plume to the Launching Equipment", 2010 International Conference on Measuring Technology and Mechatronics Automation, Changsha, China, March 13-14, 2010.

[56] PCB Piezotronics, http://www.pcb.com/Products.aspx?m=CA102B03, last viewed on April 2018.

[57] Osterholt, D. J., Knox, D. M., "Measuring Fluctuating Pressure Levels and Vibration Response in a Jet Plume", 26th Aerospace Testing Seminar, California, United States, March 29-31, 2011.

[58] Kulite, Super High Temperature Pressure Transducer, https://www.kulite.com/docs/products/XTEH-10L-190.pdf, last viewed on April 2018.

[59] Akkaş, O., Aydoğmuş, A., Demir, S., "Kırılabilen Pod Kapağı", TR Utiliy Model No. 2014 16286, 2015.

[60] Huntsman Advanced Materials, http://3.imimg.com/data3/FH/QT/MY-9803376/araldite-my740_aradur-hy918_acc-dy062_eur_e.pdf, last viewed on April 2018.

[61] Namie, I. A., Ibrahim, A. A., Hassan M. F., "Study the Mechanical Properties of Epoxy Resin Reinforced With Silica (Quartz) and Alumina Particles", The Iraqi Journal For Mechanical And Material Engineering, Volume 11, Issue 3, pp. 486-506, 2011.

[62] Committee on Assessment of Research Needs for Wind Turbine Rotor Materials Technology, National Research Council, Assessment of Research Needs for Wind Turbine Rotor Materials Technology, National Academy Press, p. 41, Washington D.C., 1991, ISBN: 0-309-58318-7.

[63] Jordan, J. L., Foley, J. R., Siviour, C. R., "Mechanical Properties of Epon 826/DEA Epoxy", Mechanics of Time-Dependent Materials, Volume 12, Issue 3, pp. 249-272, September 2008.

[64] Simth, J. C., "Experimental Values for the Elastic Constants of a Particulate-Filled Glassy Polymer", Journal of Research of the National Bureau of Standards - Physics and Chemistry, Volume 80A, Issue 1, pp. 45-49, February 1976.

[65] Kinloch, A. J., Mohammed, R. D., Taylor, A. C., "The Interlaminar Toughness of Carbon-Fibre Reinforced Plastic Composites using 'Hybrid-Toughened' Matrices", Journal of Materials Science, Volume 41, Issue 15, pp. 5043-5046, May 2006.

[66] Chamis, C. C., "Design Properties of Randomly Reinforced Fiber Composites", NASA Scientific and Technical Publications, Technical Note NASA TN D-6696, March 1972.

[67] Wacker, Resin Transfer Molding (RTM), https://www.wacker.com/cms/en/industries/pl_composites/pl_comp_appl/resintransmould.jsp, last viewed on April 2018

[68] Chun, M., Niu, Y., Composite Airframe Structures: Practical Design Information and Data, Conmilit Press, pp. 132-133, Florida, 1992.

[69] Wu, J. H., Wang, W. T., Kam T. Y., "Failure Analysis of a Frangible Laminated Composite Canister Cover", Proceedings of the Institution of Mechanical Engineers, Part G: Journal of Aerospace Engineering, Volume 213, Issue 3, pp. 187-195, March 1999.

[70] Zhou, G. M., Yuan, Z. W., Wang, X. F., "Study of Design and Experiment for Integrated Frangible Composite Diaphragm Cover", Journal of Astronautics, Volume 28, Issue 3, pp. 707-712, May 2007.

[71] Keller, Highly Precise Pressure Transmitters, http://www.keller-druck.com/picts/pdf/engl/33xe.pdf, last viewed on April 2018

[72] METYX Composite Reinforcements, Technical Datasheet, Metycore-LT600/125pp1/600m

[73] METYX Composite Reinforcements, Technical Datasheet, Metycore-600M/250PP1/600M

[74] Axel Plastics, Xtend 19mdr Datasheet, https://axelplastics.com/wp-content/uploads/2018/03/TD-XTEND-19MDR.pdf, last viewed on April 2018

APPENDIX A

PRESSURE TRANSDUCER

Technical details of Kulite pressure transducer is given in Figure 127 and Table 18.

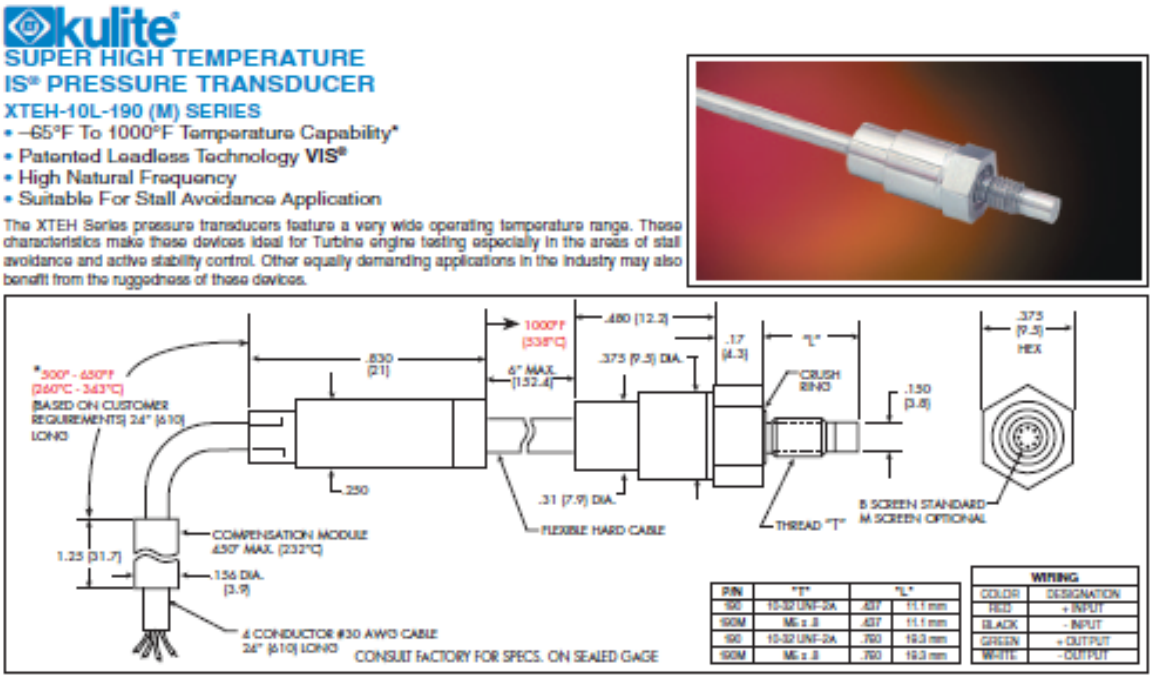

Figure 127: Datasheet of Kulite Pressure Transducer [58]

Table 18: Properties Kulite Pressure Transducer [58]

INPUT	Pressure Range	1.7 25	3.5 50	7 100	14 200	21 300	35 500	70 1000	140 2000	210 BAR 3000 PSI
	Operational Mode	Absolute, Sealed Gage								
	Over Pressure	2 Times Rated Pressure to a Maximum of 5000 PSI (350 BAR)								
	Burst Pressure	3 Times Rated Pressure to a Maximum of 5000 PSI (350 BAR)								
	Pressure Media	Most Liquids and Gases - Please Consult Factory								
	Rated Electrical Excitation	10 VDC								
	Maximum Electrical Excitation	12 VDC								
	Input Impedance	1000 Ohms (Min.)								
OUTPUT	Output Impedance	1000 Ohms (Nom.)								
	Full Scale Output (FSO)	100 mV (Nom.)								
	Residual Unbalance	± 5 mV (Typ.)								
	Combined Non-Linearity, Hysteresis and Repeatability	± 0.1% FSO BFSL (Typ.) ± 0.5% FSO (Max.)								
	Resolution	Infinitesimal								
	Natural Frequency of Sensor Without Screen (KHz) (Typ.)	240	300	380	500	575	700	1000	1400	1650
	Acceleration Sensitivity % FS/g Perpendicular	$5.0x10^{-4}$	$3.0x10^{-4}$	$1.5x10^{-4}$	$1.1x10^{-4}$	$9.0x10^{-5}$	$6.5x10^{-5}$	$4.0x10^{-5}$	$2.5x10^{-5}$	$1.9x10^{-5}$
	Insulation Resistance	100 Megohm Min. @ 50 VDC								
ENVIRONMENTAL	Operating Temperature Range	-65°F to +932°F* (-55°C to +500°C) - (See limits above)								
	Compensated Temperature Range	+80°F to +850°F (+25°C to +454°C)								
	Thermal Zero Shift	± 1.5% FS/100°F (Typ.)								
	Thermal Sensitivity Shift	± 1.5% /100°F (Typ.)								
	Linear Vibration	10-2,000 Hz Sine, 100g. (Max.)								
	Mechanical Shock	20g half Sine Wave 11 msec. Duration								
PHYSICAL	Electrical Connection	4 Conductor 30 AWG Shielded Cable (24" After Module)								
	Weight	8 Grams (Nom.) Excluding Cable								
	Pressure Sensing Principle	Fully Active Four Arm Wheatstone Bridge Dielectrically Isolated Silicon on Silicon Patented Leadless Technology								
	Mounting Torque	15 Inch-Pounds (Max.) 1.7 N-m								

APPENDIX B

MATERIAL PROPERTIES

Properties of resin, fabrics and mold release agent are given in Tables 19-22.

Table 19: Properties of Resin [60]

Manufacturer Company	Huntsman International LLC
Name of the Resin System	Araldite Impregnating Resin System
Name of the Epoxy Resin	Araldite MY 740
Name of the Hardener	Aradur HY 918
Name of the Accelerator	Accelerator DY 062
Mixing Ratio (by weight)	Resin (100), Acc. (1.5), Hard. (85)
Cure Cycle	30 min 20-80 °C 2 h 80 °C 15 min 80-120° C 4 h 120 °C 2.5 h 120-40 °C
Initial Viscosity	950 mPa.s (25 °C) 70 mPa.s (60 °C)
Pot Life	3.5 h (60 °C)
Gel Time	5.6 h (60 °C)

Table 20: Properties of Reinforcement Fabric Type 1 [72]

Manufacturer Company	METYX Composite Reinforcements
Name of the Product	METYCORE-LT600/125PP1/600M
Area Weight (ISO 3374)	1350 g/m^2 (± 3%)
Resin Compatibility	Polyester, Vinylester, Epoxy
Loss on Ignition (ISO 1887)	Max.0.55% by weight
Moisture Content (ISO 3344)	Max.0.20% by weight

Table 21: Properties of Reinforcement Fabric Type 2 [73]

Manufacturer Company	METYX Composite Reinforcements
Name of the Product	METYCORE-600M/250PP1/600M
Area Weight (ISO 3374)	1475 g/m^2 (± 3%)
Resin Compatibility	Polyester, Vinylester, Epoxy
Loss on Ignition (ISO 1887)	Max.0.55% by weight
Moisture Content (ISO 3344)	Max.0.20% by weight

Table 22: Properties of Mold Release Agent [74]

Manufacturer Company	Axel Plastics Research Laboratories Inc.
Name of the Product	Xtend 19 MDR
Application Temperature	38 – 66 ℃
Max. Process Temperature	204 ℃